12-5-2023

Resolution of the *Tetrabothrius jagerskioeldi* Cryptic Species Complex among Holarctic Alcidae (Charadriiformes): Cestodes among Fraterculinae—Exploring Marine Diversity, Host Range, and Dynamic Oceanography in the Greater North Pacific

Eric P. Hoberg
University of New Mexico, geocolonizer@gmail.com

Kaylen Marie Soudachanh
University of New Mexico

Svetlana K. Bondarenko
Nature Research Centre, Vilnius

MANTER: Journal of Parasite Biodiversity (ISSN 2470-8224)
Occasional Papers, Number 34, December 5, 2023
doi: 10.32873/unl.dc.manter34
https://digitalcommons.unl.edu/manter

MANTER: Journal of Parasite Biodiversity

Resolution of the *Tetrabothrius jagerskioeldi* Cryptic Species Complex among Holarctic Alcidae (Charadriiformes): Cestodes among Fraterculinae—Exploring Marine Diversity, Host Range, and Dynamic Oceanography in the Greater North Pacific

Eric P. Hoberg,[1] Kaylen Marie Soudachanh,[1] and Svetlana K. Bondarenko[2]

1 Museum of Southwestern Biology, Department of Biology, University of New Mexico, Albuquerque, NM, 87131 USA
2 Institute of Ecology, Nature Research Centre, Akademijos 2, Vilnius 08412, Lithuania

Corresponding author – Eric P. Hoberg, Museum of Southwestern Biology, Department of Biology, University of New Mexico, Albuquerque, NM, 87131 USA, email geocolonizer@gmail.com

Abstract

In the biosphere, limits for diversity among species, communities, and biomes are revealed through intensive and extensive field-based inventory and assembly of voucher specimens and associated informatics examined in a phylogenetic, historical, ecological, and biogeographic arena. Archival resources for specimens and information contribute to a cumulative view of faunal structure and assembly under a comparative umbrella. Ultimately, species definitions, and inclusive partitions among populations and lineages, are fundamental in articulating hypotheses that examine interactions about evolution, the nature of organisms, and the condition of environments across space and time. We conclude our proposals establishing species limits for tapeworms of the cryptic complex historically accommodated in *Tetrabothrius jagerskioeldi* Nybelin, 1916 among Alcidae seabirds (Charadriiformes). Explorations of this facet of marine diversity summarize inventory data for species of *Tetrabothrius* Rudolphi, 1819 from field collections among 1,976 seabirds of 41 species representing 3 avian orders (Charadriiformes, Suliformes, Procellariiformes) examined across 58 oceanic/geographic localities from the greater North Pacific basin between 1949 and 2019, or over the past 70 years. Cestodes of the complex including *T. jagerskioeldi* sensu stricto, *T. alcae* Hoberg and Soudachanh, 2021, and *T. sinistralis* Hoberg and Soudachanh, 2021, along with 2 previously unrecognized taxa, are documented, occurring in 128 of 1976 seabirds examined (6%) and 17 of 41 marine avian species from 23 insular, coastal, and pelagic sites spanning the North Pacific. In completing an evaluation of this assemblage, we focus on those cestodes among 8 species of medium- to small-bodied alcids, subfamily Fraterculinae. Specimens designated as *Tetrabothrius fraterculus* n. sp. were observed among puffins (2 species of *Fraterculus* and *Cerorhinca*), whereas *Tetrabothrius aithuia* n. sp. is proposed for tapeworms in auklets (4 species of *Aethia* and *Ptychoramphus*) and a puffin (*Cerorhinca*); both cestodes are currently unknown among the Alcinae species of *Cepphus*, *Uria*, *Brachyramphus*, and *Synthliboramphus* based on the North Pacific inventory collections. These large-bodied cestodes, typical of the 5 species in the complex, are characterized

among 46 currently valid species of *Tetrabothrius* in avian hosts, based on unique configurations of the genital atrium; male and female genital papillae; terminal genital ducts; numbers of testes; and the structure, position, and dimensions of the vaginal and atrial seminal receptacles. Ancillary characters contributing to differentiation include attributes of the scolex, structure, dimensions, and position of the vitelline gland and relative position of the dorsal and ventral osmoregulatory canals. A suite of complex attributes unequivocally separates 5 respective species that had historically been relegated to a single geographically widespread and morphologically variable taxon under *T. jagerskioeldi* sensu lato. Host range for respective cryptic species of the *T. jagerskioeldi*–complex reveal an intricate view of ecological isolation and connectivity across the greater North Pacific basin. Seabirds, marine mammals, and parasites are indicators of changing conditions over space and time. Oceanic regime shifts, prey cascades, and diversity for birds and parasites serve as proxies for revealing accelerating perturbation in marine foodwebs under climate forcing.

Keywords: *Tetrabothrius* spp., cestodes, species complex, Alcidae, Fraterculinae, puffins and auklets, Stockholm Paradigm, ecological fitting, host range, North Pacific basin marine ecology

Introduction

We now complete resolution within the cryptic complex circumscribed by *Tetrabothrius jagerskioeldi* Nybelin, 1916 and probe the extent of our current taxonomic and ecological understanding of this assemblage of marine cestodes. Definitions of diversity linked directly to field-based and archived specimens are essential in recognizing historical associations of parasites and hosts, ecological and evolutionary drivers for diversification, assembly and structure of complex faunas, and articulation of baselines against which accelerating and dynamic change in the biosphere can be assessed across space and time (e.g., Brooks and Hoberg, 2000; Brooks and McLennan, 2002; Hoberg and Brooks, 2008; Dunnum et al., 2017; Brooks et al., 2014, 2019; Hoberg and Soudachanh, 2020, 2021; Hoberg et al., 2023, and references therein).

Explorations of this facet of marine diversity summarize inventory data for species of *Tetrabothrius* Rudolphi, 1819 from field collections among 1976 seabirds of 41 species representing 3 avian orders (Charadriiformes, Suliformes, Procellariiformes) examined across 58 oceanic/geographical localities from the greater North Pacific basin between 1949 and 2019, or over the past 70 years (Hoberg and Soudachanh, 2020, 2021; Supplementary Data Tables 1 and 2). Within a temporally deep and spatially broad series of field inventories we assembled specimens and historical data for diversity, prevalence, and occurrence of *Tetrabothrius* among Alcidae and a diverse assemblage of seabirds. A multispecies assemblage of *Tetrabothrius* tapeworms was revealed among 453 hosts of 1,976 (23%) seabirds examined, including 34 of 41 avian species across 34 of 58 sites.

Nominal species attributed to the cryptic complex are distributed as parasites among medium and large alcids of the Subfamily Alcinae (according to Smith, 2011) and infrequently among a broader assemblage of alcid, larid, and phalacrocoracid seabirds (Hoberg and Soudachanh, 2020, 2021). *Tetrabothrius jagerskioeldi* s. str. and *T. sinistralis* occur principally among guillemots (Tribe Cepphini), species of *Cepphus* Pallas, 1769 across insular seas of the Holarctic. *Tetrabothrius alcae* occurs primarily among murres (Alcini), species of *Uria* Brisson, 1760, minimally across the greater North Pacific. Archived specimens with provenance for host(s) from localities across the Arctic Basin and North Atlantic are not available to identify a more extensive oceanic range for *T. alcae*. Further, specimens necessary to evaluate limits for diversity of a *Tetrabothrius* fauna among other Alcini [including the razorbill, *Alca torda* Linnaeus, 1758, and dovekie, *Alle alle* (Linnaeus, 1758)] and murrelets among Brachyramphini (3 species of *Brachyramphus* Brandt, 1837) and Synthliboramphini (5 species of *Synthliboramphus* Brandt, 1837) are not available in global collections (Hoberg and Soudachanh, 2020, 2021).

Cestodes of the complex including *T. jagerskioeldi* sensu stricto, *T. alcae* Hoberg and Soudachanh, 2021, and *T. sinistralis* Hoberg and Soudachanh, 2021, along with 2 additional taxa characterized here, are documented, occurring in 128 of 1,976 seabirds examined (6%) and 17 of 41 marine avian species from 23 of 58 localities (Hoberg and Soudachanh, 2020, 2021). Among genera and species of Alcidae, cestodes of the complex are rare and with spatially heterogeneous distributions, having been revealed in 113 hosts of 1,347 (8%) of these seabirds across 15 species from 21 of 45 insular, coastal and pelagic localities; 17 of 21 regularly occurring species from the North Pacific were examined. Additional and limited voucher specimens

held in museum repositories from 3 host species (razorbill, black guillemot, and common murre) from the greater North Atlantic basin were also examined (Hoberg and Soudachanh, 2020).

In completing an evaluation of this assemblage, now with 5 species, we focus on elucidation of 2 previously unrecognized cestodes attributed to the *T. jagerskioeldi*–complex that are distributed among puffins and auklets, subfamily Fraterculinae (as diagnosed by Smith, 2011), based on the North Pacific inventory (Hoberg and Soudachanh, 2020). Host ranges for these respective species of tapeworms are apparently limited: (1) in puffins (tribe Fraterculini) [3 known host species: *Fratercula corniculata* (Naumann, 1821), *F. cirrhata* (Pallas, 1769), and *Cerorhinca monocerata* (Pallas, 1811)] and (2) in auklets (tribe Aethiini) and a puffin [6 known host species: *Aethia cristatella* (Pallas, 1769), *A. psittacula* (Pallas, 1769), *A. pusilla* (Pallas, 1811), *A. pygmaea* (Gmelin, 1789), *Ptychoramphus aleuticus* (Cassin, 1811), and *C. monocerata*]. Overall, these cestodes occur in 8 species of medium to small alcids and are currently unknown among the Alcinae—species of *Cepphus*, *Uria*, *Brachyramphus*, and *Synthliboramphus* based on the North Pacific collections (Hoberg and Soudachanh, 2020). Further, identity of specimens designated as *T. jagerskioleldi* s. lato in rhinoceros auklets and tufted puffins from the Western Pacific and Russian Far East (Temirova and Skrjabin, 1978; Smetanina and Leonov, 1984), in common puffins from the Arctic Basin (Barents Sea) and Northwestern Atlantic (Belopol'skaia, 1952; Threlfall, 1971) and in parasitic jaegers from the Barents Sea and Chukotka (Belopol'skaia, 1952; Temirova and Skrjabin, 1978) cannot be corroborated and may be among species attributed to the cryptic complex or among other species of *Tetrabothrius* (Hoberg and Soudachanh, 2020, 2021).

Materials and Methods

Specimens Examined

We update and incorporate complete field data into summaries outlined in Hoberg and Soudachanh (2020, 2021) for marine bird diversity, oceanic/geographic localities, and host range for an assemblage of *Tetrabothrius* cestodes, with a focus on 5 species attributed to the *Tetrabothrius jagerskioeldi*–complex (Supplementary Data Tables 1, 2, and 3). Data outlined here are inclusive during a 70-year time frame, from 1949 through 2019, for a geographically extensive inventory, with archived specimens, across the greater North Pacific basin and adjacent sub-Arctic and Arctic seas. Data and observations supersede prior cumulative summaries defining this tetrabothriid fauna. Host taxonomic nomenclature follows Chesser et al. (2020) for species of Charadriiformes (Alcidae, Laridae, Stercorariidae), and genera and species of Procellariiformes, whereas Kennedy and Spencer (2014) are authorities for Suliformes (Phalacrocoracidae—shags and cormorants).

Cestode specimens were originally examined in the course of a comprehensive redescription of *T. jagerskioeldi* as a basis for establishing morphological and taxonomic limits within the putative species complex (Hoberg and Soudachanh, 2020). Initial taxonomic dimensions of the complex were revealed in descriptions of *T. alcae* and *T. sinistralis* among medium to large alcids (Hoberg and Soudachanh, 2021). Primary data for field collections and specimens, including a synoptic listing of avian species, georeferenced localities, and host occurrence denoting prevalence and intensity of infection (Supplementary Data Tables 1, 2, 3), are held in the Arctos data platform (http://arctos.database.museum).

Specimens now designated in the type and voucher series for 2 additional cryptic species within the complex, described in our current study, are archived as MSB:PARA in the Parasitology Division, Museum of Southwestern Biology, University of New Mexico, Albuquerque (Supplementary Data Table 4). An additional strobilate specimen of this series is archived in the Helminthological Collection of the Institute of Ecology, Lithuanian Academy of Sciences, Vilnius, Lithuania, as EKOI-HELMI. A series of voucher specimens from alcid hosts, including other identified and unidentified species of *Tetrabothrius* cestodes, are also archived and catalogued in the MSB (Supplementary Data Table 5). The distribution and prevalence of ancillary *Tetrabothrius* cestodes in larids, stercorariids, and procellariiforms, unequivocally excluded from the *T. jagerskioeldi*–complex (Hoberg and Soudachanh, 2021), are also documented; these specimens are archived in the MSB and remain uncatalogued without complete taxonomic evaluation (Supplementary Data Table 3).

Specimen Preparation

Cestode specimens from inventory collections of seabirds between the years 1975 and 2019 were usually fixed in buffered 10% formalin or preserved in 70% ethanol; specimens collected by other field biologists prior to 1975 were fixed in 10% formalin. *Tetrabothrius* specimens in shearwaters during 2019 were collected from dead or beached birds during an ongoing mortality event in the Bering Strait (G. Shugart, Slater Museum, University of Puget Sound, pers. comm., 2019); hosts were collected in the field, frozen, and later examined with preservation of tapeworms in ethanol. Generally, in historically recent collections by EPH, prior to fixation, live cestodes were immediately recovered from avian specimens and allowed to relax for an

extended period of time in water at ambient temperature. Cestodes were heat-killed in either H_2O or in fixative. Avian specimens from Grays Marine Canyon in 1982, 1985, and 1987 were examined during shipboard necropsies immediately following collection; entire organ systems and the gastrointesitinal tracts of all seabirds were frozen with dry ice for later dissection in the laboratory. Strobilate specimens were prepared as whole mounts stained in Semichon's acetic carmine, destained in 70% ethanol and HCl, dehydrated through a series of ethanol, cleared in terpineol or xylene, and mounted in Permount or Canada balsam. Tegument was stripped from the strobila of some series of specimens at the time of clearing to facilitate examination of internal anatomy in whole mounts. Hand-cut thick sections were generally prepared from each strobila coincidental with clearing. Transverse sections were prepared in reference to ontogeny of the male and female reproductive systems to view the progressive development of the genital atrium, male and female genital ducts and uterus, and to confirm the position of the genital ducts and transverse uterus relative to the poral osmoregulatory canals. A single specimen in an auklet from Talan Island, Sea of Okhotsk, in 1997, by SBK, was preserved in 70% ethanol and later stained with Ehrlich's hematoxylin and mounted on a microscope slide in Canada balsam.

Diagnostic Criteria in Species of Tetrabothrius *and Tetrabothriidea*

A suite of integrated morphological and meristic attributes is essential in establishing putative limits among species of *Tetrabothrius* and also more broadly for genera and species among the Tetrabothriidea (e.g., Hoberg and Soudachanh, 2020). Comparative morphology remains the gateway to species-level identification and can establish a foundation to assess and interpret molecular-based and genomic data as such become increasingly available. The structure and dimensions of the scolex (configuration of bothridia, auricular appendages, and apical region) provide insights about taxonomic diversity. Consistent with Baer (1954) and Murav'eva (1975), the genital atrium and length of the male atrial canal and positions of the male and female atrial canals remain among the primary diagnostic characters. The structural complexity and position of associated male and female papillae, genital ducts of the male system, and distal vagina (atrial and vaginal seminal receptacles) had seldom been considered in descriptions and redescriptions. It remains necessary to assess the genital atrium in transverse sections and in whole mounts (e.g., Baer, 1954). Interspecific variation in the position and numbers of testes have definable limits and can contribute to differentiation. Attributes and position of the vitelline gland and ovary, especially placement in relation to the midline of the segment, provide adjunct character support. Structure and dimensions of egg capsules, embryophores, and oncospheres can vary across species, but absence of standardized measurements in the taxonomic literature may limit robust diagnostic comparisons (e.g., Temirova and Skrjabin, 1978; Ryzhikov et al., 1985). Further, there is a history of applying counts of longitudinal muscle bundles (inner and outer layers in dorsal and ventral fields, determined in transverse section) in species discrimination (Temirova and Skrjabin, 1978; Ryzhikov et al., 1985). Variation in the numbers of muscle bundles, however, is demonstrated among conspecific specimens (with identity confirmed by the genital atrium) and is revealed for relative age and progressive development of proglottids within a single strobila, suggesting such data may not be reliable in establishing species limits either directly or as an adjunct (Hoberg and Soudachanh, 2021; and current observations outlined in the following).

As suggested by Murav'eva and Popov (1976), and later Hoberg (1987) and Hoberg et al. (1991), ontogenetic markers or bench points are necessary to describe the outcomes of progressive development, including changes in dimensions and function of organ systems, that are considered or have been established as diagnostic for species identification. Structural changes during ontogeny require context, or they may be misinterpreted and can otherwise be misleading with respect to identification of morphologically similar species. Benchmarks define progressive development of proglottids and relatively specific regions of the strobila: (1) *Early Mature*—testes, ovary, vitelline gland, cirrus sac, and genital atrium are differentiated and have functional ducts. (2) *Mature*—initial expansion of the vaginal seminal receptacle, ovary, and vitelline gland; narrow transverse uterine stem visible and extending toward proglottid margins. Complete development of genital atrium, with male and female papillae (when present) and atrial genital ducts associated respectively with the cirrus sac and vagina. Diameter of cirrus sac and genital atrium, along with length of the respective male and female atrial ducts often continue to increase through stages of maturity, pregravid and gravid proglottids. (3) *Late Mature/Postmature*—maximum dimensions in female organ systems, saccate expansion of uterine stem, and later in post-mature initial dissolution of female organs (ovary and vitelline gland) and testes. (4) *Pregravid*—lobate uterine expansion with initial presence of developing eggs and initial development of median dorsal uterine pore. (5) *Gravid*—complete expansion of the uterus, with fully developed capsules containing embryophore and oncosphere with hooks; dorsal uterine pore patent. Substantial structural changes occur during ontogeny,

thus characterization at specific stages of development reveals the extent of intraspecific variation and is the basis for establishing interspecific limits. Data from original descriptions and subsequent redescriptions among species of the complex are summarized as a basis for comparisons (Hoberg and Soudachanh, 2020, 2021). These data are augmented by new observations and series of measurements completed during the current study. All measurements are reported in micrometers unless otherwise indicated. Mensural data are given as n = (number examined) followed by the range with the mean in parentheses.

A limited or narrow range of measurements and observations from small samples of specimens and limited, unspecified regions of the strobila are insufficient for robust or complete descriptions and redescriptions that circumscribe ontogenetic variation in fully developed cestodes (e.g., Baer, 1954; Temirova and Skrjabin, 1978; Ryzhikov et al., 1985). Specimens that encompass the range of multiple host species and widespread geographic localities are suggested, when possible. All specimens from designated type series and associated vouchers should be permanently archived and databased in collections of a recognized natural history museum (e.g., Hoberg et al., 2022). The Parasite Division of the Museum of Southwestern Biology, University of New Mexico, Albuquerque, currently holds all specimens from the North Pacific inventories.

Results

Inventory data summarize collections among species of *Tetrabothrius* in 1,976 seabirds of 41 species representing 3 avian orders (Charadriiformes, Suliformes, Procellariiformes) across 58 oceanic/geographical localities from the greater North Pacific basin between the years 1949 and 2019 (Hoberg and Soudachanh, 2020, 2021). Overall, a multispecies assemblage of *Tetrabothrius* occurred in 453 hosts among 1,976 seabirds (23%) and 34 of 41 avian species from 34 of 58 localities, including 349 of 1,801 Charadriiformes (19%), with 140 hosts (16 of 17 species examined) among 1,347 Alcidae (10%), 206 hosts (8 of 10 species) among 417 Laridae (49%), and 3 hosts (2 of 3 species) among 37 Stercorariidae (8%); Suliformes with 1 host (single species of 3 examined) among 72 Phalacrocoracidae (1%); and Procellariiformes with approximately 90%–100% prevalence among 103 hosts (7 species examined). Localities, host range, prevalence, intensity, and diversity reflected for the *T. jagerskioeldi*–complex, other identified species and unidentifiable immature specimens of *Tetrabothrius* among Alcidae and other marine birds presented in the current manuscript (Supplementary Data Tables 1, 2, 3, 4, and 5) supersede those reported previously for this assemblage (Hoberg and Soudachanh, 2020, 2021). Additional unidentifiable immature, incomplete, and fragmented specimens in alcid hosts have not been archived nor cataloged (Supplementary Data Table 3).

Specific prevalence data for *Tetrabothrius* spp., based on survey of avian species within Procellariiformes from the North Pacific presented by Hoberg and Soudachanh (2021) are now incorporated in the current paper (Supplementary Data Table 3). These latter survey data for species of *Tetrabothrius* are included here with regard to the total numbers of avian species and specimens examined, along with specific geographic localities across the North Pacific basin between 1949 and 2019 (Supplementary Data Tables 1, 2, and 3). Definitive taxonomic evaluations for faunas associated with Laridae, Stercorariidae, and Procellariiformes, held in ethanol or mounted on slides, remain incomplete, although morphologically these cestodes are unequivocally excluded from the *T. jagerskioeldi*–complex; these series of specimens are archived and remain to be cataloged in the collections of the Museum of Southwestern Biology.

Cestodes of the complex, including *T. jagerskioeldi* s. str., *T. alcae*, *T. sinistralis*, and 2 additional nominal species are documented, based on inventory, in 128 of 1976 (6%) seabird specimens of 17 species examined from 23 of 58 localities and among 114 of 1,347 alcids (8%) of 15 species (encompassing 17 of 25 extant alcid species) from 21 of 45 localities. Species of the *T. jagerskioeldi*–complex appear to have ecologically restricted host distributions limited principally to avian species among the Alcidae. Based on current inventory, cestodes of the assemblage, *T. jagerskioeldi* s. str., have also been recognized in single host species [*Larus glaucescens* (Naumann, 1840) and *Urile pelagicus* (Pallas, 1811)], respectively, among the Laridae (Charadriiformes) and Phalacrocoracidae (Suliformes) but not among the Stercorariidae (Charadriiformes). Cestodes attributable to the complex have not been revealed among genera and species of Procellariiformes across the greater North Pacific basin (Hoberg and Soudachanh, 2020, 2021) (Table 2; Supplementary Data Table 3).

Expanding Diversity in the T. jagerskioeldi*–complex, Cestodes in Puffins*

A previously unrecognized species of *Tetrabothrius*, a component of the *T. jagerskioeldi*–complex, occurred in 3 species of Alcidae among 17 examined, and from 7 of 58 localities across the greater North Pacific basin (encompassing the region from Grays Marine Canyon in the eastern North Pacific, Gulf of Alaska, Aleutian Islands, to the northern Sea of Okhotsk, Russia in the west) representing inventory between 1949 and 2019 (Table 2; Supplementary Data Table 3).

Cestodes we attribute to *Tetrabothrius fraterculus* n. sp. were found as parasites in 21 hosts of 3 species among 1,347 (< 2%) alcids examined. These cestodes were observed only in puffins, alcids of medium body size, and among 21 of 474 of these seabirds irrespective of species, age, or breeding status (prevalence 4%) from 7 of 20 localities (35%) where these 3 species were examined as summarized in Supplementary Data Table 3. Among horned puffins, *T. fraterculus* occurred in 7 of 149 birds (5%; intensity = 1–19 cestodes per host) across 4 of 17 localities where this avian species was collected, including 5 of 114 (4%) breeding adult birds, 1 of 7 subadults, and 1 of 28 chicks at fledging. Among tufted puffins, cestodes were found in 6 of 286 examined (2%; intensity = 1–16) across 3 of 14 sites, including 5 of 230 adults (2%), 1 of 23 subadults (4%), and none of 33 chicks at fledging. Among rhinoceros auklets, cestodes were revealed in 8 of 39 examined at 3 of 6 sites (20.5%; intensity = 1–19), including 6 of 37 adults (16%) and 2 of 2 subadults. Specimens of *T. fraterculus* were observed in multiple species of puffins in sympatry from pelagic waters south of the Aleutian Islands (*F. corniculata*, *F. cirrhata*, *C. monocerata*) and from Talan Island, Sea of Okhotsk (*F. corniculata*, *F. cirrhata*). *Tetrabothrius fraterculus* was not observed among other species of Alcidae nor a broader assemblage of marine birds occurring in sympatry across the greater North Pacific basin (Supplementary Data Table 3; Hoberg and Soudachanh, 2020, 2021).

Primary materials representing *T. fraterculus* include specimens in 21 alcid hosts (*F. corniculata*, 7; *F. cirrhata*, 6; *C. monocerata*, 8) across 7 localities. In the type series, there are 28 cestodes on 62 slides upon which the description is based (Supplementary Data Table 4). Additionally, there are 30 stained and mounted vouchers, primarily postlarval or immature specimens, excluded from the description, on 22 slides, across 4 localities, identified based on the configuration and structure of the scolex and numbers of testes. Unmounted specimens from the type and voucher series are held in vials in 70% or greater ethanol.

Description—*Tetrabothrius fraterculus* n. sp.

Figures 1–26.

General Description: Large, robust, tetrabothriids; maximum length of strobila (n = 5 strobilae) 120–248 mm × 4,275–7,500 in width, with (n = 5 strobilae) 473–642 proglottids in gravid specimens. Segments wider than long throughout strobila; 375–450 long × 2,425–3,125 wide in immature to early mature proglottids; 425–750 × 3,125–3,925 in mature; 350–1,000 × 4,175–6,025 in postmature to pregravid; 575–1,125 × 3,525–7,500 in gravid; maximum width most often attained in pregravid proglottids. Length-to-width ratio 1:4.62–8.8 in early mature; 1:4.63–7.68 in mature; 1:5.0–10.43 in pregravid; 1:3.13–8.69 in gravid. Scolex rectangular, flat, longer than wide (n = 22) 500–700 (570) long × 500–626 (567) wide; auricles and apical complex relatively prominent. Bothridia well developed, (n = 45) 380–577 (464) long × 194–380 (286) wide, with muscular margins. Apical region hypertrophied, domelike, expanded anterior to auricles. Neck, as measured from base of scolex to first indication of internal segmentation, relatively short, (n = 14) 320–600 (437) long × 450–601 (512) wide. Ventral osmoregulatory canals (OSM) 50–130 in diameter, increasing in width throughout development, maximum in gravid segments; transverse canal 5–15, without multiple anastomoses; dorsal canals 10–50, maximum in gravid condition. Dorsal OSM shifted mediad relative to ventral canals. Genital pores unilateral, dextral in dorsal view, situated marginally in middle to anterior third of proglottid; suckerlike, prominent, in late mature to pregravid proglottids. Male and female genital ducts passing between extensions of transverse uterus passing ventrally, to poral OSM at all stages of development.

Longitudinal Musculature: Musculature prominent in transverse sections of proglottids; inner and outer bundles arranged in single layers. Inner bundles large in diameter; (n = 4 strobilae) 133–193 (163) in number; (n = 25) 3–20 (10) fibers per bundle. Outer bundles relatively small in diameter; (n = 4) 166–307 (251) in number; (n = 35) 1–6 (3) fibers per bundle. Numbers of muscle bundles demonstrate variation in single strobila, maximum in mature proglottids, diminishing in number with development posteriad in postmature and gravid segments.

Male Genitalia: *Genital anlagen* visible immediately posterior to neck, protandrous; first testes observed in 250th–300th segment; mature in 380th–407th segment. Testes positioned dorsally in 1–2 layers, (n = 58) 50–110 (70) in diameter; completely overlapping ovary in confluent antiporal field beyond midline; testes surround female organs, without gap anterior to vitelline gland and ovary. Testes (n = 135 segments from 15 strobilae in 11 hosts) 50–96 (67) in number in immature to early mature segments, decreasing posteriad in number with maturation of male and female organs; testes seldom < 60–70 in number. Vas deferens prominent, highly convoluted, distended adjacent to poral OSM. Cirrus sac ovoid, situated in dorsal aspect of genital atrium; (n = 35) 68–95 (80) in diameter through early maturity; increasing in diameter posteriad in strobila, attaining maximum dimensions in late maturity to pregravid condition (n = 205 from 22 strobilae in 11 hosts) 70–130 (101); muscular wall thickened, 5–20 in early mature to mature, 7–25 in pregravid, 15–25 in gravid.

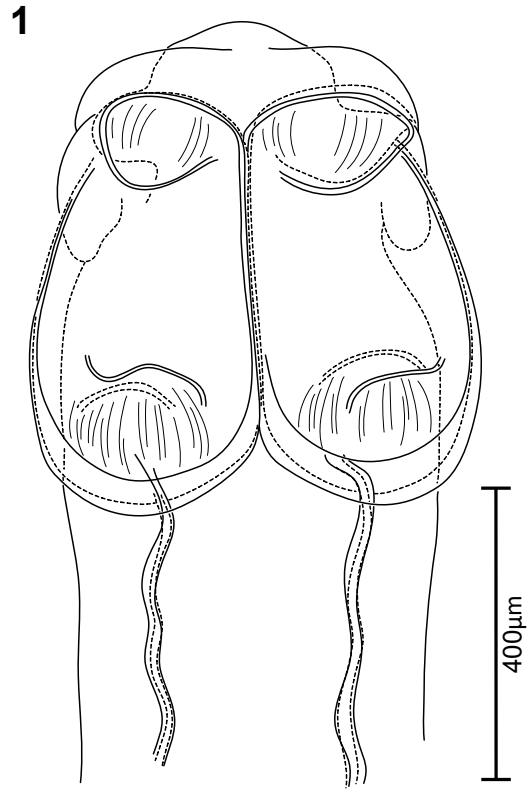

Figure 1. *Tetrabothrius fraterculus* n. sp. scolex in dorsoventral view from holotype specimen (2783-1A) in *Fratercula corniculata* from Talan Island, Sea of Okhotsk. Shown is structure in gravid specimen (scale bar in micrometers).

Figures 2–3. *Tetrabothrius fraterculus* n. sp. showing details of proglottids in ventral view from holotype (2783-1A) in *Fratercula corniculata* from Talan Island, Sea of Okhotsk (scale bars in micrometers). **Fig. 2.** Proglottid, complete, in ventral view in early maturity showing distribution of testes relative to female organs, developing structure of the marginal genital atrium and position of the transverse uterine stem. **Fig. 3.** Proglottid, near maturity (without expansion of atrial and vaginal seminal receptacles), showing detail in poral half, with genital ducts between the ventral and dorsal osmoregulatory canals; uterus ventral to the canals. Note muscular genital atrium with strongly bilobed male papillae dorsally and single, triangular, female papilla situated ventrally.

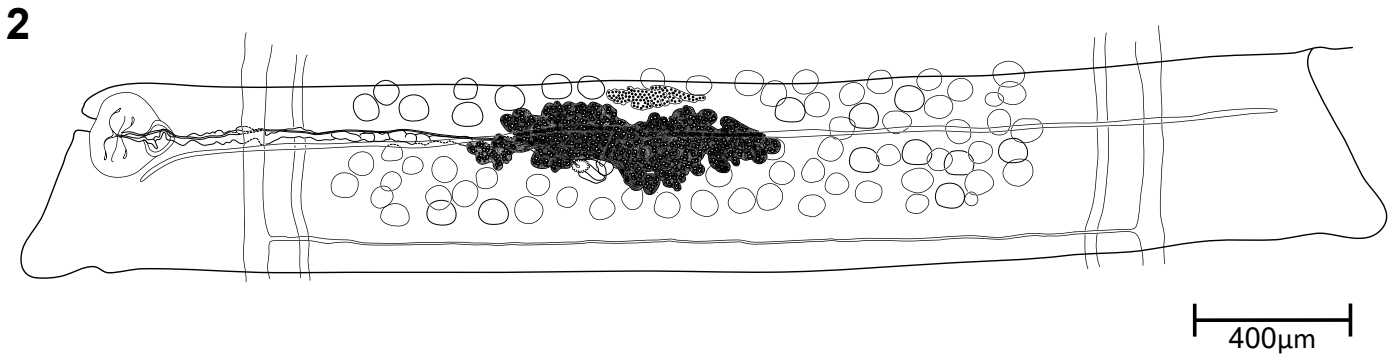

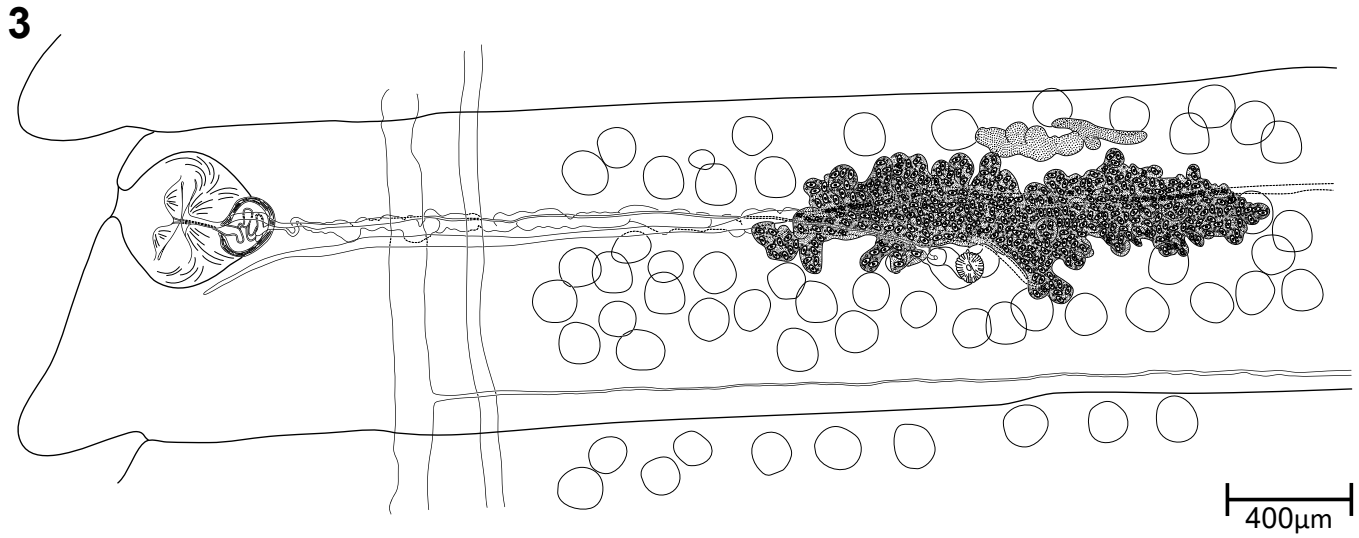

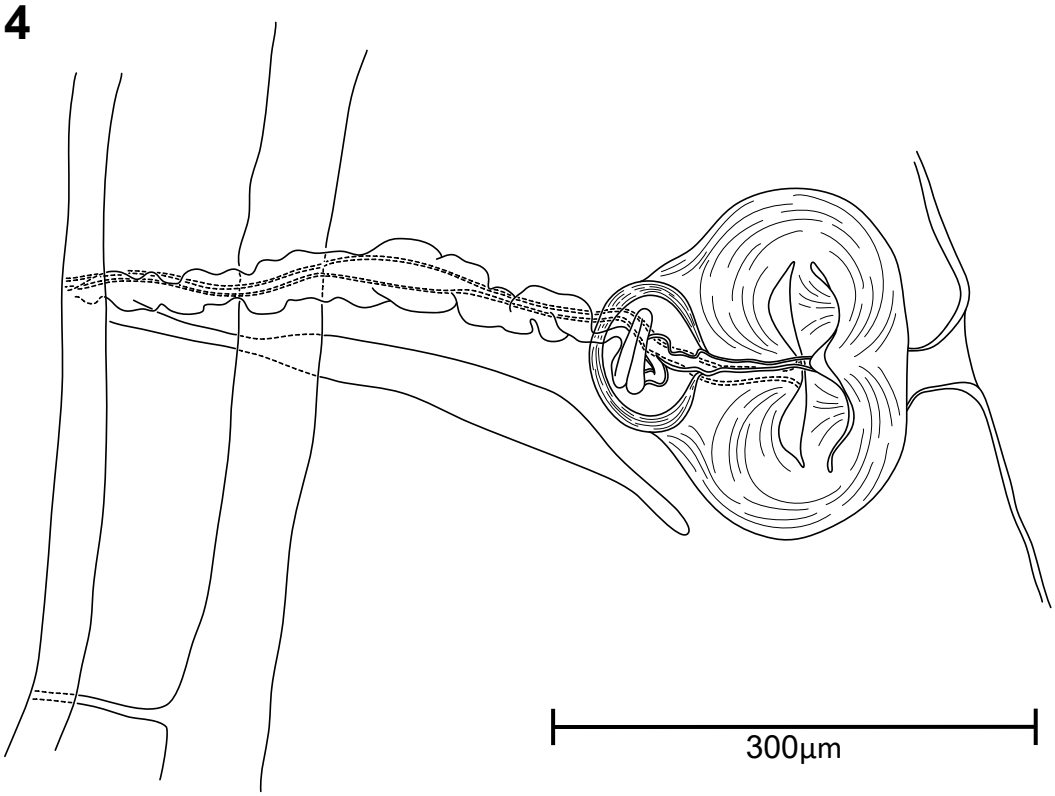

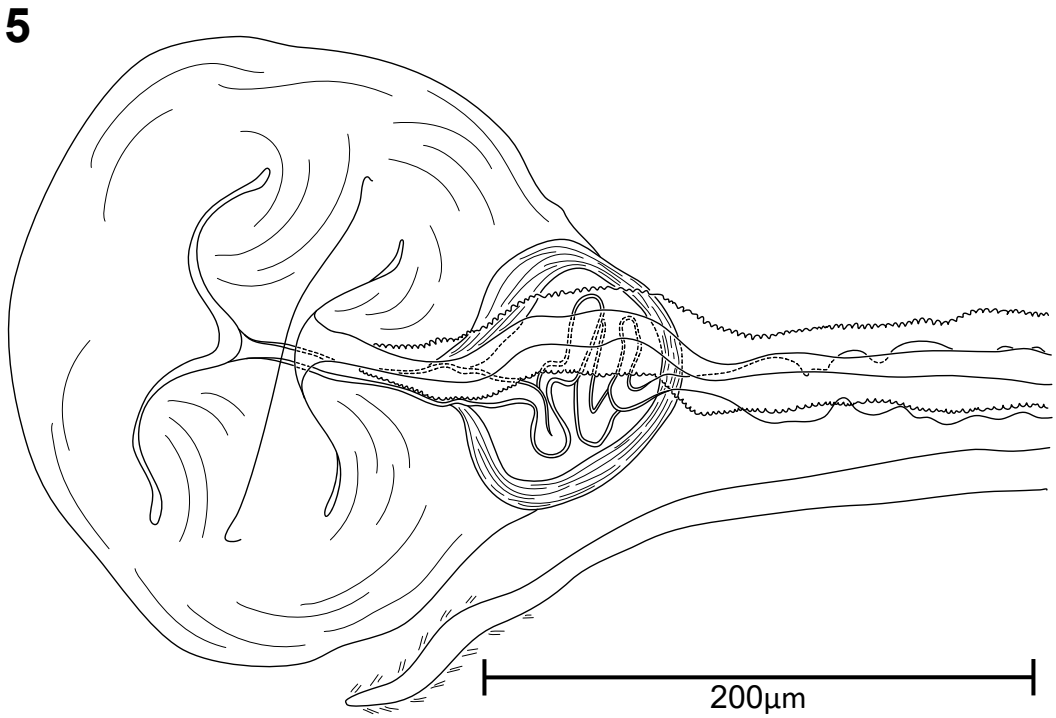

Figures 4–5. *Tetrabothrius fraterculus* n. sp. with details of the genital atrium and terminal genital ducts in progressive stages of ontogeny from the holotype (2783) in *Fratercula corniculata* from Talan Island, Sea of Okhotsk (scale bars in micrometers). **Fig. 4.** Genital atrium in dorsal orientation (2783-1B) in maturity from whole mount, showing aperture of male canal between bilobed genital papillae, aperture of female canal ventral and on prominent papilla, nascent expansion of vaginal seminal receptacle, genital ducts between and extension of transverse uterine stem ventral to osmoregulatory canals, and a median shift of the dorsal osmoregulatory canal. **Fig. 5.** Genital atrium in ventral orientation (2783-1A) in maturity from whole mount.

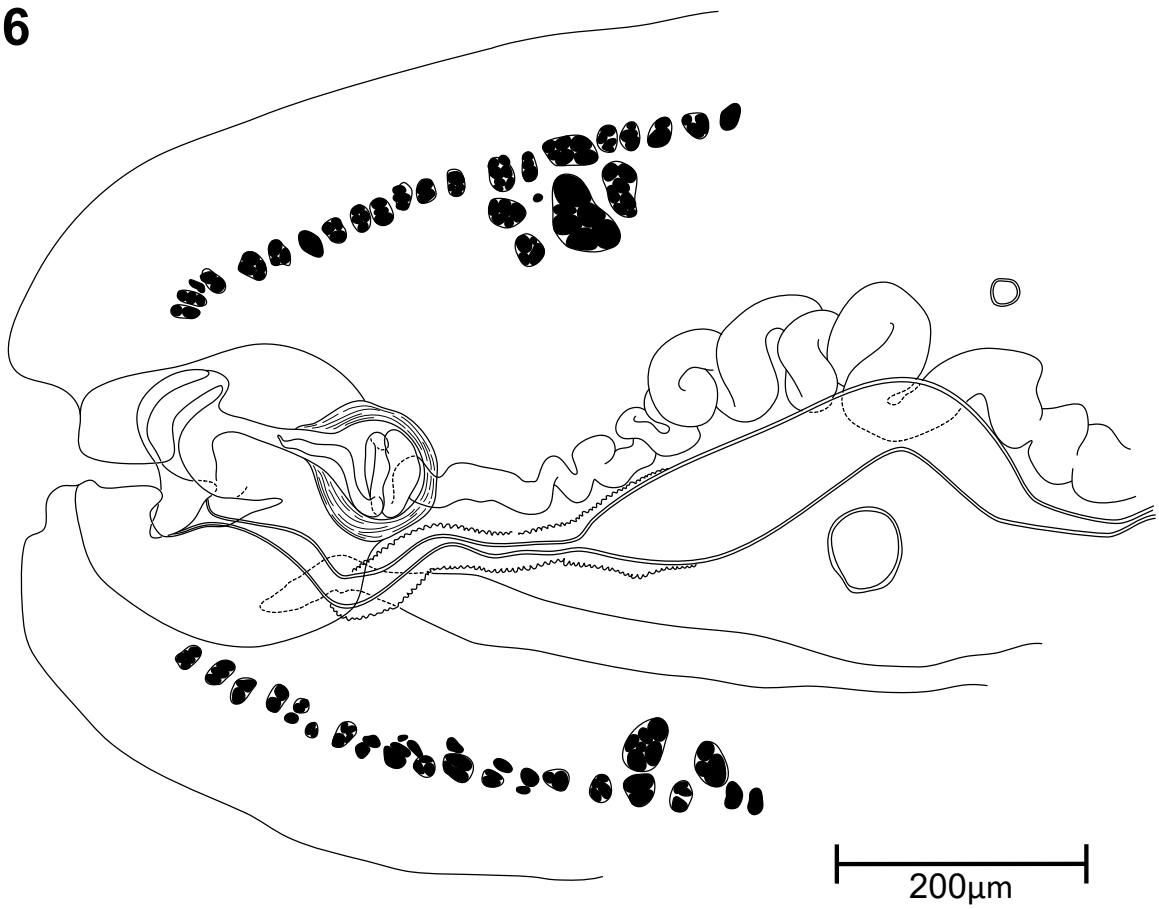

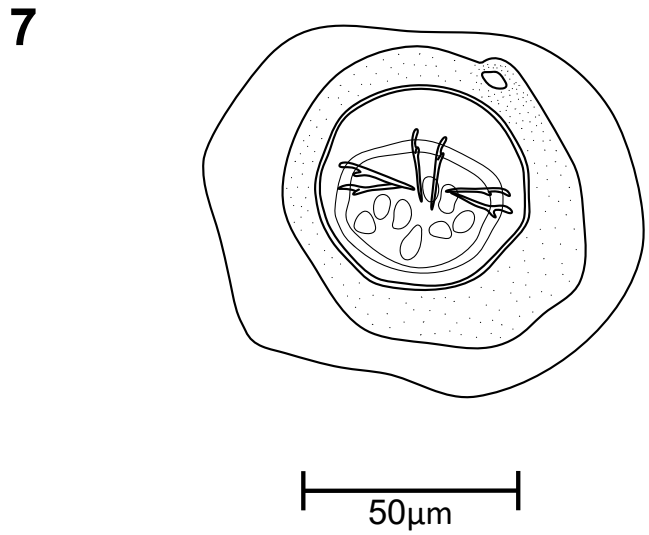

Figures 6–7. *Tetrabothrius fraterculus* details of the terminal genital complex and the egg from the holotype (2783) (scale bars in micrometers). **Fig. 6.** Genital atrium and associated genital ducts in transverse section (view from anterior) (2783-1D) in late mature/pregravid condition, dorsal to top. Note, paired, symmetrical male genital papillae and dorsally deflected male canal, single ventral female genital papilla, expanding vaginal and atrial seminal receptacles between osmoregulatory canals, expanding transverse uterine stem situated ventrally, and position of inner and outer muscle bundles. **Fig. 7.** Oncosphere, embryophore, and egg envelopes (2783-1F).

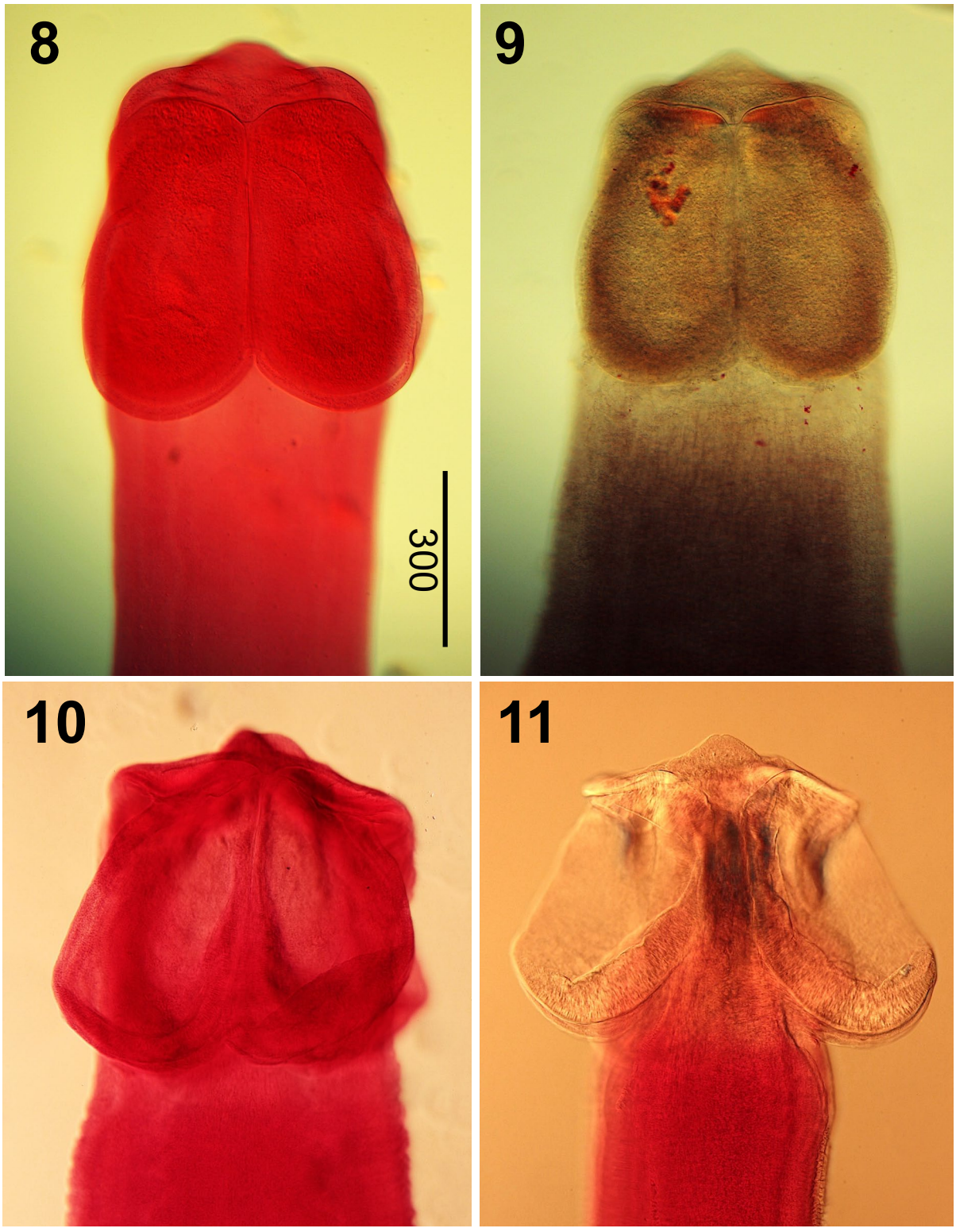

Figures 8–11. *Tetrabothrius fraterculus* n. sp., showing structure of adult scolex in dorsoventral and lateral views (scale bars in micrometers; all same scale). **Fig. 8.** Scolex, dorsoventral, showing elongate dimensions consistently longer than wide, with well-developed auricular appendages and rounded apical region from holotype specimen (2783-1A) in *Fratercula corniculata* from Talan Island, Sea of Okhotsk. **Fig. 9.** Scolex in paratype specimen (042-F) in *F. corniculata* from Buldir Island, Western Aleutian Islands. **Fig. 10.** Scolex in paratype specimen (1929) in *F. cirrhata* from pelagic zone, south of Western Aleutian Islands. **Fig. 11.** Scolex, lateral orientation, in paratype specimen (2457-5A) in *Cerorhinca monocerata* from Grays Marine Canyon.

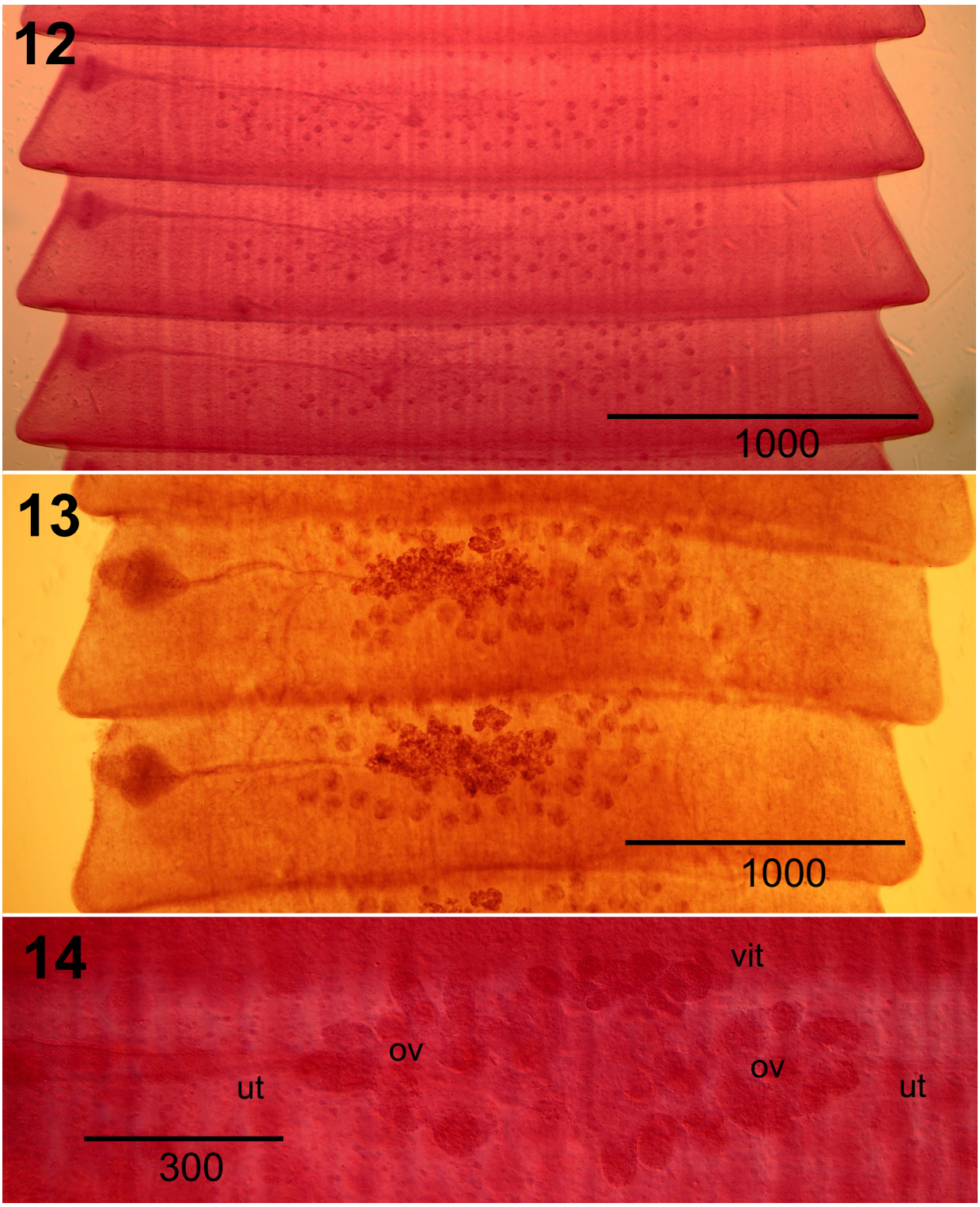

Figures 12–14. *Tetrabothrius fraterculus* n. sp., showing structure of developing proglottids and distribution of male and female organ systems (scale bars in micrometers). **Fig. 12.** Immature proglottids in ventral view in holotype specimen (2783-1A) showing number and arrangement of testes relative to initial development of ovary and vitelline gland; note position of the female organs shifted porad of the midline; dextral, marginal genital pore. **Fig. 13.** Early mature proglottids in ventral view in paratype specimen (042-F) showing distribution of testes completely surrounding female organs; globular, compact vitelline gland shifted toward antiporal wing of multilobate ovary. **Fig. 14.** Mature proglottid, ventral view, in holotype specimen (2783-1A) showing structure of multilobate ovary (ov), compact vitelline gland (vit), and developing transverse uterine stem (ut).

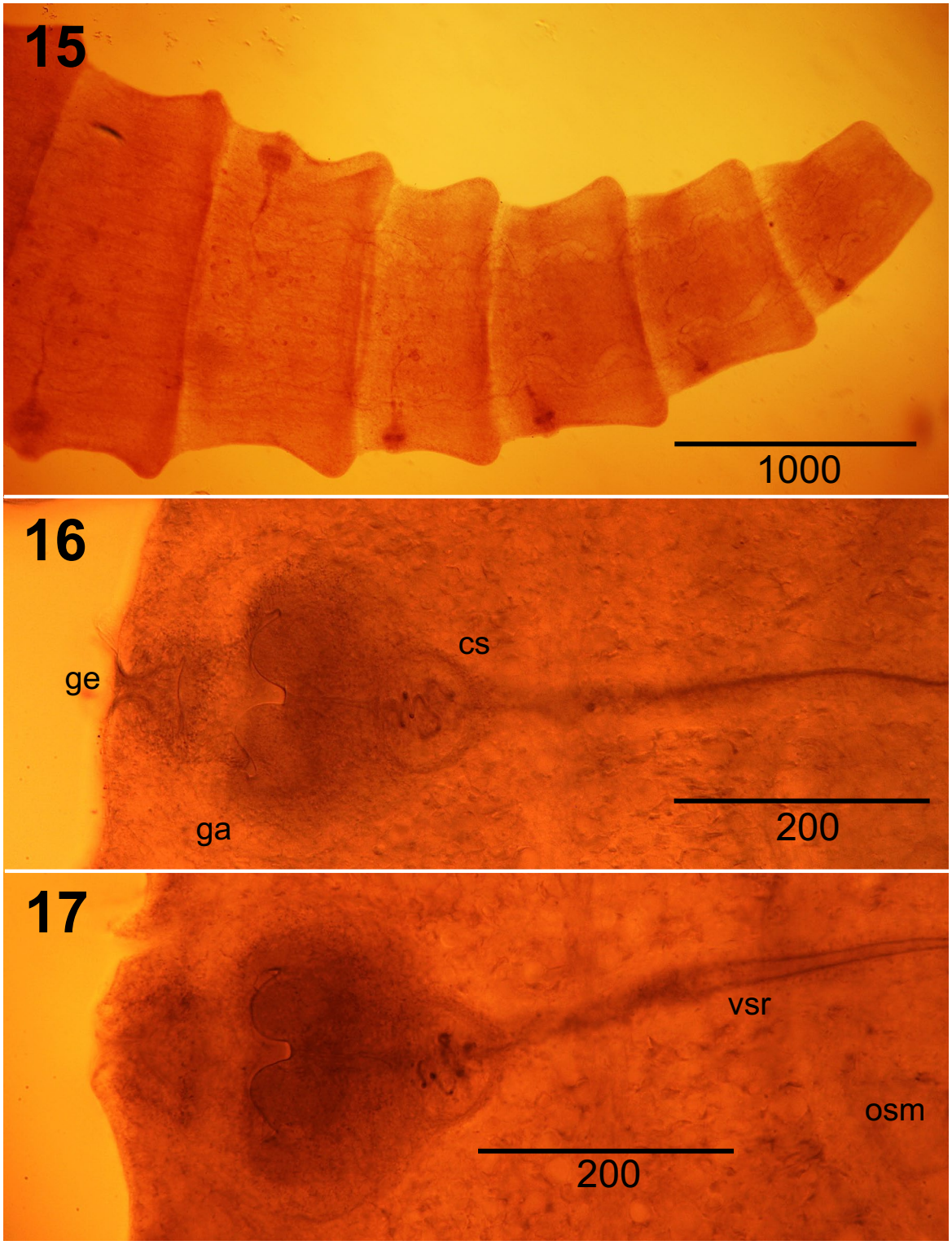

Figures 15–17. *Tetrabothrius fraterculus* n. sp., showing structure of terminal primary proglottids and configuration of marginal genital pore and atrium (scale bars in micrometers). **Fig. 15.** Primary proglottids in paratype specimen (042-F) in *Fratercula corniculata* from Buldir Island, in ventral view. Note tapering primary terminal segments and irregular alternation of genital pore to left. **Fig. 16.** Marginal dextral genital pore (ge), genital atrium (ga), and cirrus sac (cs) in maturity in ventral view of paratype specimen (042-F); note strongly bilobed and divergent male genital papillae and subspherical cirrus sac. **Fig. 17.** Marginal genital atrium and cirrus sac in late maturity in ventral view from paratype (042-F); note expansion of elongate vaginal seminal receptacle (vsr) crossing poral osmoregulatory canals (osm).

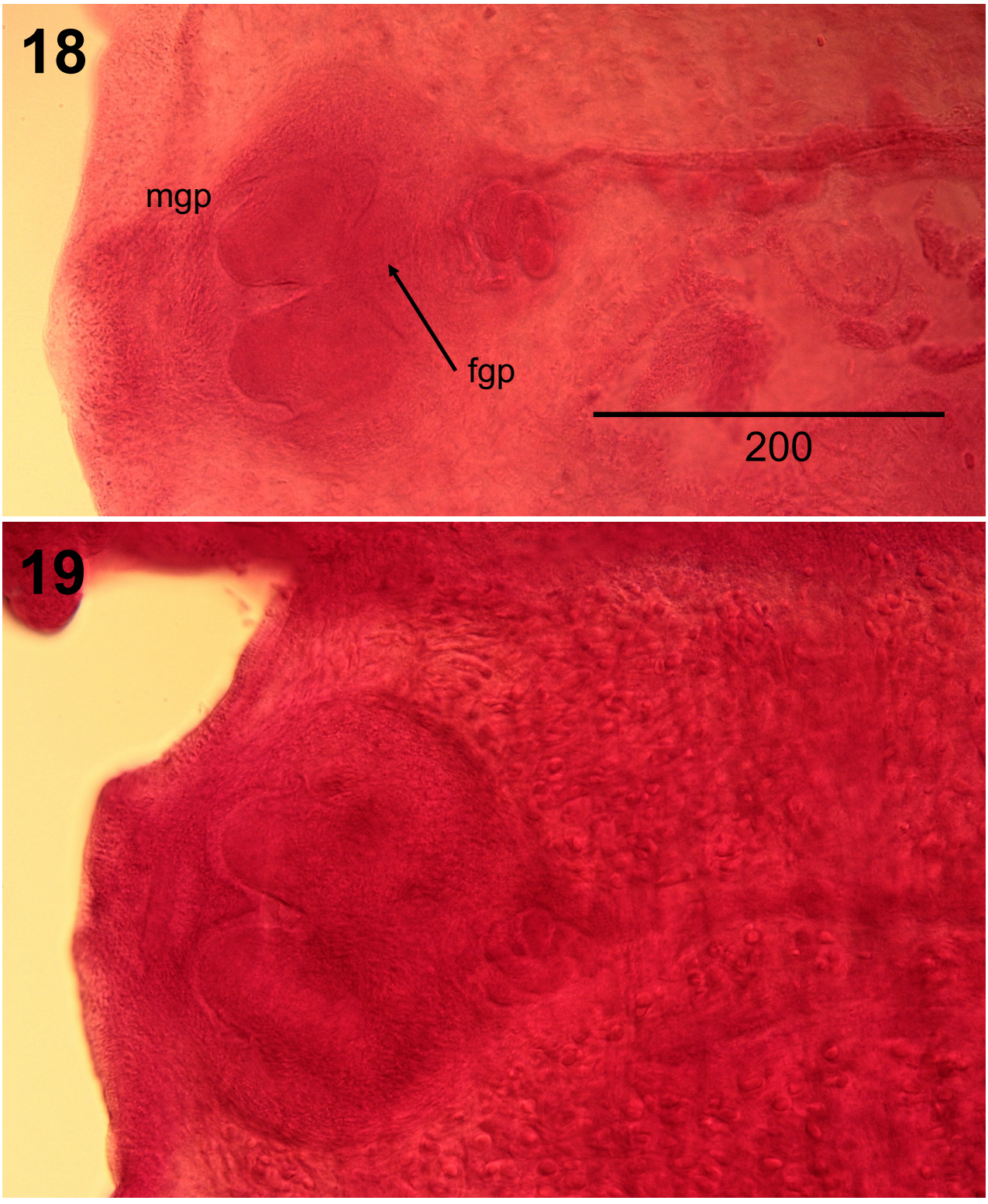

Figures 18–19. *Tetrabothrius fraterculus* n. sp., poral region, ventral view showing genital atrium, genital papillae, and cirrus sac in proglottids representing specimens in different host species (scale bar in micrometers). **Fig. 18.** Pregravid proglottid from paratype (1929) in *Fratercula cirrhata* from pelagic zone south of western Aleutian Islands showing triangular female papilla (fgp) ventral to paired, divergent male papillae (mgp). **Fig 19.** Late mature proglottid from paratype (1142-2B) in *Cerorhinca monocerata* from pelagic zone, south of western Aleutian Islands.

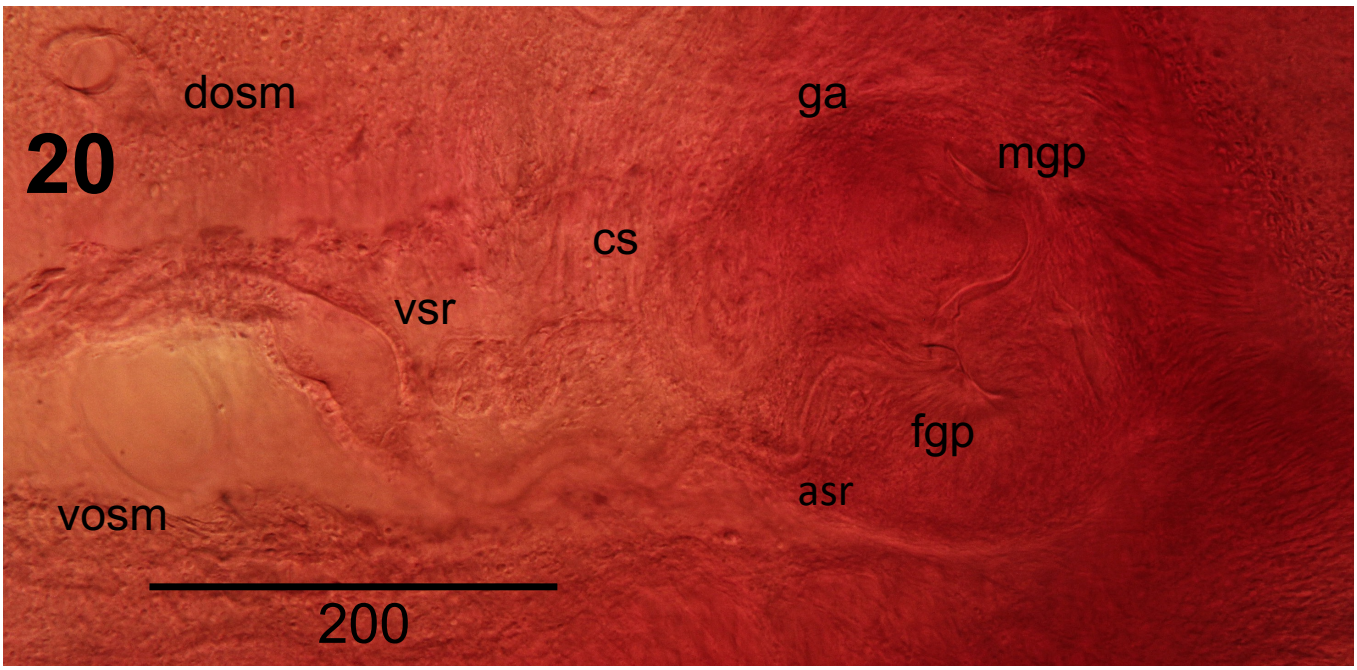

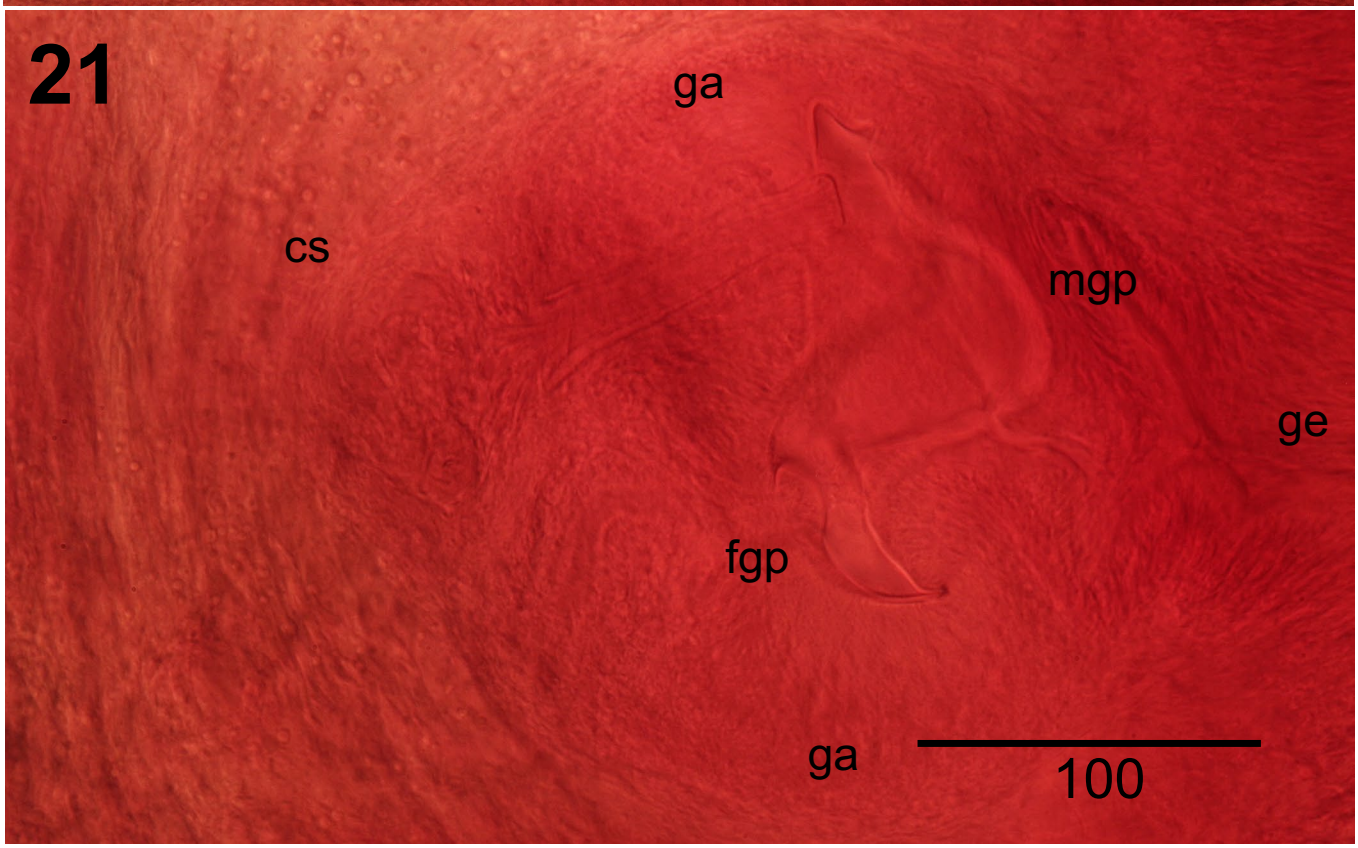

Figures 20–21. *Tetrabothrius fraterculus* n. sp., poral region of proglottid showing genital atrium with male and female papillae in maturity, viewed from posterior, in transverse section of paratype (30066-1c) in *Fratercula corniculata* from Amukta Island, east-central Aleutian Islands (scale bars in micrometers). **Fig. 20.** Genital atrium (ga), showing positions of symmetrical male (mgp) papillae and single female (fgp) papilla, cirrus sac (cs), nascent atrial seminal receptacle (asr) and expanding vaginal seminal receptacle (vsr) passing between dorsal (dosm) and ventral (vosm) osmoregulatory canals. **Fig. 21.** Genital pore (ge), genital atrium (ga), cirrus sac (cs), dorsally deflected male canal with extended cirrus, symmetrical male genital papillae (mgp), and female genital papilla and orifice of atrial vagina (fgp).

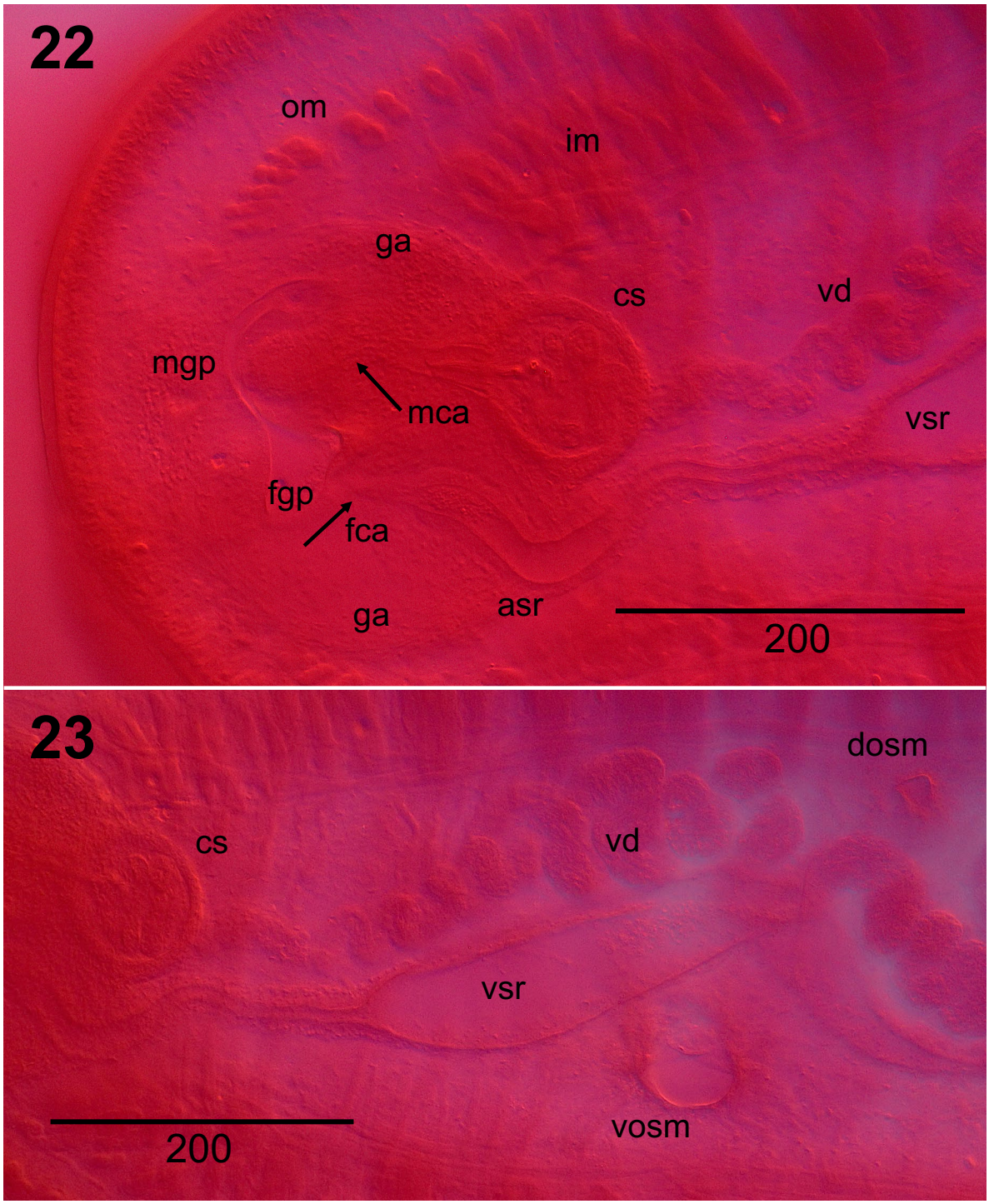

Figures 22–23. *Tetrabothrius fraterculus* n. sp., showing structure of genital atrium, genital ducts, and relative positions of osmoregulatory canals in transverse section of late mature proglottid, viewed from anterior, dorsal to top, in holotype specimen (2783-1D) (scale bars in micrometers). **Fig. 22.** Structure of genital atrium (ga), cirrus sac (cs), and positions of male and female genital canals, and positions of the apertures of the male (mca) and female canals (fca) (*arrows*) relative to the prominent, paired, male genital papillae (mgp) and single female papilla (fgp); note 90° turn in terminal vagina entering wall of genital atrium and expansion of atrial seminal receptacle (asr). A prominent, convoluted vas deferens (vd), expansion of the vaginal seminal receptacle (vsr), and distribution of outer (om) and inner (im) longitudinal muscle bundles are indicated. **Fig. 23.** Poral region of proglottid, showing relative position of the cirrus sac (cs), with convoluted vas deferens (vd) and elongate, spindle-shaped vaginal seminal receptacle (vsr) passing between the dorsal (dosm) and ventral (vosm) osmoregulatory canals; position of transverse uterine stem not visible.

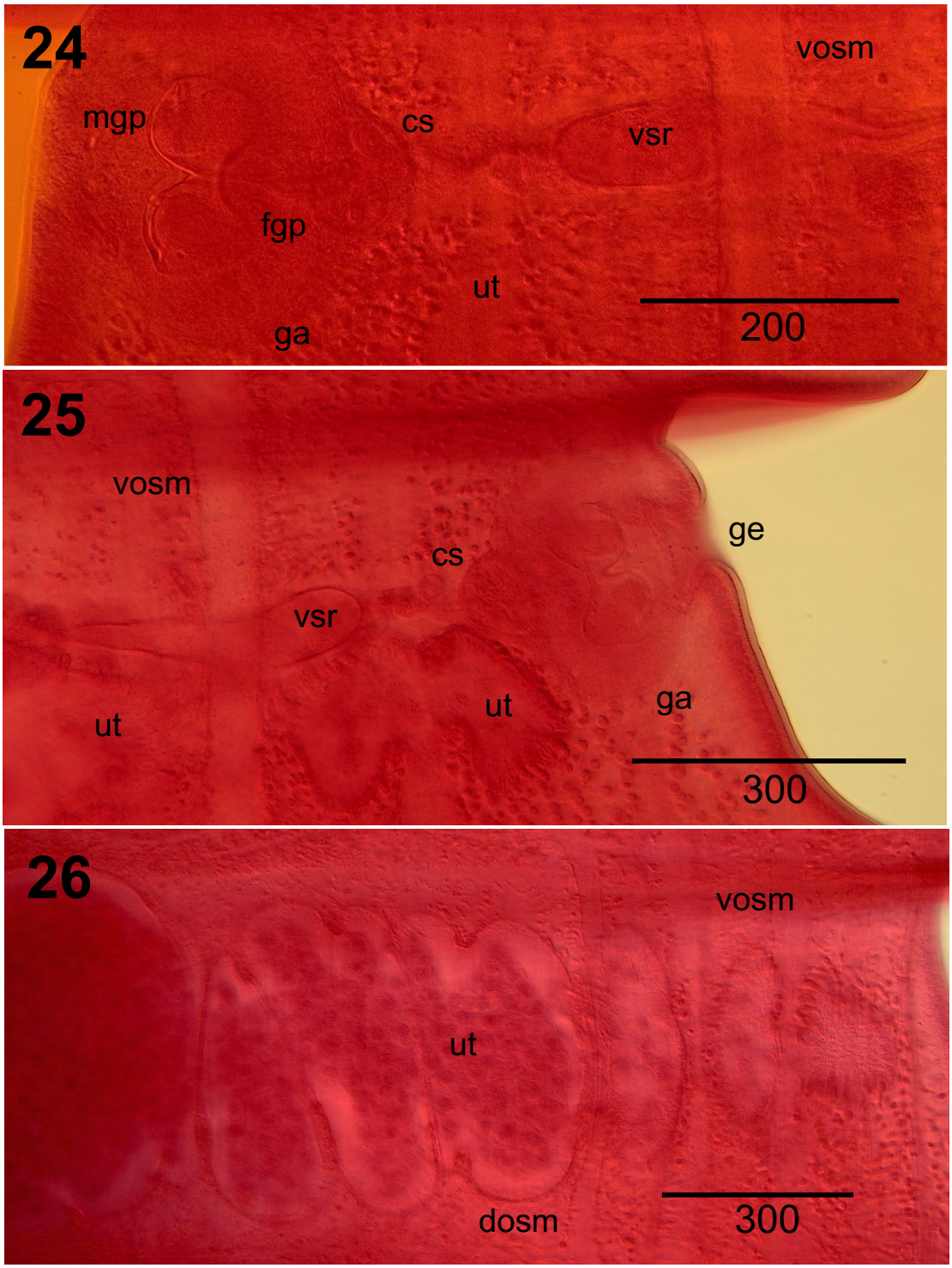

Figures 24–26. *Tetrabothrius fraterculus* n. sp. proglottids, mature pregravid and gravid development, showing structure of genital atrium; position of genital pore; vaginal seminal receptacle; and expanding, lobate uterus (scale bars in micrometers). **Fig. 24.** Margin of mature proglottid, ventral view, in holotype (2783-1A), showing genital atrium (ga), divergent male papillae (mgp), triangular (rounded) female papilla (fgp), cirrus sac (cs), vaginal seminal receptacle (vsr), ventral osmoregulatory canal (vosm), and narrow transverse uterine stem (ut). **Fig. 25.** Margin of pregravid proglottid, dorsal view, in holotype (2783-1F) showing dextral genital pore (ge), structure of genital atrium (ga), cirrus sac (cs), spindle to pyriform-shaped vaginal seminal receptacle (vsr), developing and expanding lobate uterus (ut), and position of the ventral osmoregulatory canal (vosm). **Fig. 26.** Margin of gravid proglottid, antiporal, ventral view, in holotype (2783-1F), showing structure of lobate transverse uterus (ut) extending ventrally and beyond ventral (vosm) and dorsal (dosm) osmoregulatory canals; note mediad shift of dorsal canal.

Cirrus sac contains extension of convoluted vas deferens. Genital atrium ovoid, highly muscularized (n = 33) diameter in early mature, 140–225 (183); attaining maximum dimensions in late maturity through gravid proglottids, (n = 170 from 22 strobilae) 185–300 (238). Male genital papillae massive, paired, strongly divergent in dorsoventral view, symmetrical in transverse section; diameter of respective anterior and posterior papillae in dorsoventral orientation (n = 35) 50–75 (59) in early mature, (n = 260) 55–75 (67) in mature to gravid proglottids. Male genital canal straight, extending from cirrus sac through genital atrium wall, directed with slight dorsal deflection, opening on dorsal aspect between massive paired genital papillae; increasing in length through ontogeny, in early mature (n = 28) 45–73 (69) long, in mature to gravid proglottids (n = 138 in 14 strobilae and 11 hosts) 58–95 (74).

Female Genitalia: Ovary multilobate, with 2 prominent wings, initially visible in 270th to 330th segment, fully developed, not dendritic, in 380th to 407th segment; (n = 36) 644–1,520 (881) wide in early maturity; (n = 91) 880–1,700 in mature and postmature segments; situated in anterior 2/3 of segment with center of female organs shifted porad of midline; not extending to OSM. Vitelline gland, compact to weakly follicular (n = 30) in early maturity, 35–110 (68) long × 110–415 (259) wide; maximum dimensions in mature to late mature segments (n = 95) 60–200 (101) long × 131–465 (267) wide; situated anteroventral to ovary, with center of organ shifted under antiporal wing of ovary; single, broad common vitelline duct passing ventrally to ovary. Vitelline gland and ovary becoming diffuse in postmature to pregravid proglottids coincidental with expansion of uterus. Common vitelline duct extends posteriad becoming confluent with common vaginal and ovarian duct to ventrally enter prominent Mehlis' gland, (n = 42) 40–80 (62) in diameter; nascent ascending, convoluted, uterine stem extends dorsally from Mehlis' gland. Proximal vagina terminates with expansion as thin-walled, ellipsoidal inner seminal receptacle (ISR), (n = 21) 75–140 (97) in diameter at complete expansion; receiving broad ovarian duct slightly dorsolateral to Mehlis' gland. Vagina extends porad from ISR as thin tube enveloped in thickened epithelium, dorsal to ovary, ventral to testes. Vaginal seminal receptacle (VSR) present, as voluminous, elongate, spindle-shaped to pyriform dilatation of vagina, initially with thickened epithelium, wall becoming membranous with expansion. VSR extending between poral OSM; expansion defines onset of maturity; maximum diameter attained at level of OSM in mature to gravid proglottids, (n = 75) 175–500 (285) long × 15–105 (62) wide; not attaining ovarian margin, becoming variable, diminishing in dimensions in pregravid to gravid proglottids. Distal vagina with prominent expansion of atrial seminal receptacle (ASR) in pregravid to gravid proglottids, entering genital atrium in sinuous curve, ascending at about 90° ventral to cirrus sac. Female genital canal opening ventrally in central region of atrium through apex of massive, domelike, triangular papilla, separate from aperture of male canal, at base of paired male genital papillae in dorsoventral and transverse view. Orifice of female canal ventral to aperture of male canal, not immediately adjacent; expanded distally as well-developed ASR as viewed in transverse sections and whole mounts. Ascending uterus extends anteriad from dorsal aspect of Mehlis' gland; transverse tubular uterine stem initially visible coinciding with ovarian development, dorsal to ovary, ventral to testes. Mature uterus, a broad sacculate structure lined with prominent epithelium, situated dorsally in proglottid, extending ventrally beyond OSM; gravid by 460th to 600th segment. Uterus extends to level of cirrus sac and genital atrium and beyond antiporal OSM when fully gravid. Uterine pore median, dorsal, patent in pregravid strobilae; segments anapolytic. Mature eggs contained within capsule with granular membrane, (n = 50) 40–73 (54) in diameter. Hyaline embryophore (n = 50) 35–45 (38) wide × 25–37.5 (29) long, containing oncosphere (n = 50) 25–37.5 (29) wide × 20–27.5 (22) long. Embryonic hooks (n = 40) 15–17.5 (15.4) in length for medial pairs, (n = 50) 17.5–20 (18) for lateral groups.

Taxonomic Summary

Hosts: Type host—horned puffin, *Fratercula corniculata* (Naumann, 1821). Other known hosts—tufted puffin, *Fratercula cirrhata* (Pallas, 1769) and rhinoceros auklet, *Cerorhinca monocerata* (Pallas, 1811); currently unknown in Atlantic puffin, *Fratercula arctica* (Linnaeus, 1758), other species of Alcidae, and an assemblage of northern pelagic seabirds.

Localities: Type locality—Talan Island, northern Sea of Okhotsk, Russia, ca. 59°19′N, 149°06′E in type host, a chick at fledging, on 11 September 1988. Other known localities—Buldir Island, western Aleutian Islands, AK; Amukta Island, Islands of the Four Mountains, east-central Aleutian Islands, AK; pelagic waters south and adjacent to western Aleutian Islands, AK; Sitkalidak Island, Kodiak Island Region, Gulf of Alaska, AK; pelagic waters over Grays Marine Canyon, eastern North Pacific Ocean, WA; Destruction Island, Washington Outer Coast, eastern North Pacific Ocean, WA. Consult Supplementary Data Table 2 for georeferenced locality information and Supplementary Data Table 3 for host and geographic range based on inventory collections.

Specimens: Holotype—in type host, from type locality collected by E.P. Hoberg, A.Ya. Kondratiev, L. Kondratieva, and S.K. Bondarenko (field number 2783-1A through

2783-1F, single specimen on 6 slides including scolex, strobila, and hand-cut thick sections); identification by EPH. Museum of Southwestern Biology, MSB Collection No. 29177. Paratype series and vouchers in puffin hosts with complete georeferenced data for collection and MSB catalog numbers are listed in Supplementary Data Table 3 and Supplementary Data Table 4.

Zoobank Name Registration for *Tetrabothrius fraterculus*: LSID urn:zoobank.org:act:BCBF9CAD-D97A-41C1-AA41-7EB65603FA8C

Symbiotype: Host specimens or tissues not generally retained and archived. Some specimens of *Cerorhinca monocerata* and *Fratercula cirrhata* are held in avian collections of the Burke Memorial Washington State Museum among an assemblage of seabirds from Grays Marine Canyon, eastern North Pacific during 1982, 1985, and 1987 (Supplementary Data Tables 3 and 4).

Etymology: *Tetrabothrius fraterculus* n. sp. is based on Medieval Latin *fratercula* for "little brother," proposed as the 4th species recognized in the *T. jagerskioeldi*–complex, and for the tribe Fraterculini and generic name for 3 species of puffins, *Fratercula* Brisson, 1760, including the type host *F. corniculata*.

Remarks and Diagnosis

Tetrabothrius fraterculus n. sp. is the 4th cestode attributed to the *T. jagerskioeldi*–complex. Morphologically, specimens attributed to *T. fraterculus* are most similar to those of *T. jagerskioeldi*, *T. alcae*, and *T. sinistralis*, all cestodes in alcid seabirds (Table 1). Avian hosts are typical for 45 species of *Tetrabothrius* with inclusion of *T. fraterculus*. Comparisons involve attributes defined in the redescription and recognition of *T. jagerskioeldi* s. str. as outlined by Hoberg and Soudachanh (2020, 2021).

Similar to congeners in the *T. jagerskioeldi*–complex, specimens of *T. fraterculus* are characterized by large, robust strobilae when gravid. A suite of complex attributes (Figures 1–26), however, unequivocally separates *T. fraterculus* from respective species that had historically been relegated to a single geographically widespread and morphologically variable taxon (Hoberg and Soudachanh, 2020, 2021). Further, among cestodes of the complex, overall dimensions of fully developed gravid strobilae in *T. fraterculus* substantially exceed those documented for other species.

Among specimens of *T. fraterculus*, the structure of the muscular genital atrium, associated terminal ducts, and genitalia for male and female systems are diagnostic (Table 1). Prominent genital papillae are characteristic, assessed in dorsoventral view of whole-mounted specimens and in transverse sections of proglottids (from mature through gravid) (Figures 4–6, 16, 17, 20–22, 24). In the male system, genital papillae are paired, massive, and laterally divergent in dorsoventral view and symmetrical in anterior-posterior orientation, positioned in the dorsal aspect of the atrial lumen. The male canal is straight, with a slight dorsal deflection through the atrial wall (from the cirrus sac), opening on the dorsal aspect of the atrial lumen between the male papillae; a curved male atrial canal distinguishes *T. alcae* and *T. sinistralis* from *T. fraterculus*. In the female system of *T. fraterculus*, there is a single strongly developed, rounded, domelike, triangular papilla situated ventrally in the lumen, at the base of the male papillae. The terminal female duct opens through the apex of the single papilla, and the apertures of the male and female ducts are distant, not adjacent (Figures 4, 5, 8, 20). Further, the female atrial canal is sinuous, passing through the wall of the genital atrium in a 90° turn (similar to *T. alcae* and *T. sinistralis* but contrasting with *T. jagerskioeldi*), expanding as an ASR (in transverse view). Similar morphology and overall configurations for the genital atrium and respective genital papillae are not observed among congeners in the *T. jagerskioeldi*–complex (Table 1), nor among other nominal species in the genus (e.g., Baer, 1954; Temirova and Skrjabin, 1978; Ryzhikov et al., 1985).

Ancillary characters of the scolex, osmoregulatory system and male and female organ systems further distinguish specimens of *T. fraterculus* within this assemblage (Table 1). The scolex with well-developed bothridia, auricular appendages, and quadrilobate apical complex is substantially greater in dimensions and longer than wide (Figures 1, 8–11), contrasting with *T. alcae*, *T. jagerskioeldi*, and *T. sinistralis*, where the holdfast is consistently wider than long. The dorsal OSM are shifted mediad relative to the broad ventral canals (Figures 2, 6, 23), similar to specimens of *T. alcae* and dissimilar to *T. jagerskioeldi* and *T. sinistralis*; genital ducts pass between the poral OSM, a position observed in specimens of *T. jagerskioeldi* and *T. sinistralis* but not *T. alcae*. Among specimens of *T. fraterculus*, the genital pore is often prominent and suckerlike; further, the pore and atrium are dextral in dorsal view, contrasting with *T. sinistralis*.

Organization of the testes in *T. fraterculus*, completely surrounding the female organs without a gap anterior to the vitelline gland and ovary (Figures 2, 3, 12, 13), is similar to *T. jagerskioeldi* but distinct from *T. alcae* and *T. sinistralis*. Testes are rarely < 60–70 in number with a maximum of 96 in *T. fraterculus*, overlapping only with *T. alcae* (seldom < 75, with a maximum of 134) and are consistently greater than *T. jagerskioeldi* (seldom > 60, maximum 70) and *T sinistralis* (seldom < 50, maximum 70).

In specimens of *T. fraterculus*, the center of the female organ systems, in early mature to postmature proglottids, is

Table 1. Morphological Data, Hosts, and Geographic Localities for Differentiation of *Tetrabothrius jagerskioeldi* Nybelin, 1916; *T. alcae* Hoberg and Soudachanh, 2021; *T. sinistralis* Hoberg and Soudachanh, 2021; *T. fraterculus* n. sp.; and *T. aithuia* n. sp. among Alcidae

Character	*Tetrabothrius jagerskioeldi* s. str.[1,2]	*Tetrabothrius jagerskioeldi* s. str.[3]	*Tetrabothrius alcae*[4]	*Tetrabothrius sinistralis*[5]	*T. fraterculus* n. sp.[6]	*T. aithuia* n. sp.[7]
Host(s) species	*Cepphus grylle* (type host)	*Brachyramphus marmoratus*, *Cepphus grylle*, *Cepphus carbo*, *Cepphus columba*, *Cerorhinca monocerata*, *Uria aalge*, *Larus glaucescens*, *Urile pelagicus*	*Uria aalge* (type host), *Uria lomvia*, *Cepphus columba*, *Synthliboramphus antiquus*, *Aethia psittacula*	*Cepphus columba* (type host), *Cepphus grylle*	*Fratercula corniculata* (type host), *Fratercula cirrhata*, *Cerorhinca monocerata*	*Aethia cristatella* (type host), *Aethia pusilla*, *Aethia pygmaea*, *Aethia psittacula*, *Ptychoramphus aleuticus*, *Cerorhinca monocerata*
Geograhic locality	Kristineberg, Sweden (type); Väderöarna, Sweden (*)	North Pacific Basin, Gulf of Alaska, Bering Sea, Aleutian Islands, Sea of Okhotsk	Talan Island, Sea of Okhotsk (type); Cape Thompson, Eastern Chukchi Sea; Cape Lisburne, eastern Chukchi Sea; St. Lawrence Island, Bering Sea; St. Matthew Island, Bering Sea; Buldir Island, Aleutian Islands; western Aleutian Islands, pelagic zone; Kodiak Island, Gulf of Alaska; Ugaiushak Island, Gulf of Alaska; Humboldt Bay, eastern North Pacific Ocean; Grays Marine Canyon, pelagic zone, eastern North Pacific	St. Matthew Island, Bering Sea (type); Kangerluk, (Diskofjord) West Greenland	Talan Island, Sea of Okhotsk (type); Buldir Island, western Aleutian Islands; western Aleutian Islands, pelagic zone; Amukta Island, east-central Aleutian Islands; Sitkalidak Island, Gulf of Alaska; Destruction Island, eastern North Pacific; Grays Marine Canyon, pelagic zone, eastern North Pacific	Talan Island, Sea of Okhotsk (type); St. Lawrence Island, Bering Sea; St. Matthew Island, Bering Sea; St. Paul Island, Bering Sea; Buldir Island, western Aleutian Islands; Amchitka Island, central Aleutian Islands; Grays Marine Canyon, pelagic zone, eastern North Pacific

Character	*Tetrabothrius jagerskioeldi* s. str.[1,2]	*Tetrabothrius jagerskioeldi* s. str.[3]	*Tetrabothrius alcae*[4]	*Tetrabothrius sinistralis*[5]	*T. fraterculus* n. sp.[6]	*T. aithuia* n. sp.[7]
Strobila (L × W, maximum, in mm)	90 × 4.0	85–203 × 3.9	127–210 × 4.35–6.16	111–180 × 3.5–4.47	120–248 × 4.275–7.5	62–132 × 2.35–4.62
Muscle bundles, outer (#)	202–221 (*)	185–237 (204)	183–235 (217)	213–238 (226)	166–307 (251)	184–242 (213)
Fibers/bundle outer (#)	3–12 (*)	3–11 (7)	2–15 (7)	1–5 (3)	1–6 (3)	1–6 (4)
Muscle bundles, inner (#)	118–125 (*)	99–146 (114)	95–177 (139)	111–119 (115)	133–193 (163)	105–142 (123)
Fibers/bundle, inner (#)	5–53 (*)	6–37 (19)	9–72 (35)	5–20 (11)	3–20 (10)	3–22 (10)
Scolex (L)	510 (original); 325 (*)	350–580 (489)	190–392 (297)	355–420 (388)	500–700 (570)	350–470 (389)
Scolex (W)	560 (original); 430 (*)	490–700 (580)	201–422 (359)	376–490 (421)	500–626 (567)	310–450 (374)
Bothridia (L)	285–300 (*)	240–500 (406)	152–255 (212)	240–340 (298)	380–577 (464)	195–350 (280)
Bothridia (W)	195–215 (*)	235–370 (277)	103–198 (168)	209–240 (225)	194–380 (286)	113–230 (181)
Neck (L)	Short (*)	Short	500–1,550 (843)	200–480	320–600 (437)	210–350 (291)
Genital pore (position)	Dextral in dorsal view (*)	Dextral in dorsal view	Dextral in dorsal view	Sinistral in dorsal view	Dextral in dorsal view	Dextral in dorsal view
Genital ducts (relation to osmo-regulatory canals)	Between (*)	Between	Ventral to poral osmoregulatory canals	Between	Between	Between
Osmoregulatory canals	—	Dorsal/ventral canals laterally concordant	Dorsal canals shifted mediad	Dorsal/ventral canals laterally concordant	Dorsal canals shifted mediad	Dorsal canals shifted mediad
Cirrus pouch (diameter)	100–111 (original); 70–114 (*) (mature to gravid)	65–110 (88) (mature); 75–130 (94) (pregravid); 78–152 (107) (gravid)	80–137 (107), increasing in diameter through ontogeny, maximum in late mature	71–120 (92), increasing in diameter through ontogeny, maximum in pregravid to gravid	70–130 (101), increasing in diameter through ontogeny, maximum in pregravid to gravid	62.5–110 (89), increasing in diameter through ontogeny, maximum pregravid to gravid

Character	*Tetrabothrius jagerskioeldi* s. str.[1,2]	*Tetrabothrius jagerskioeldi* s. str.[3]	*Tetrabothrius alcae*[4]	*Tetrabothrius sinistralis*[5]	*T. fraterculus* n. sp.[6]	*T. aithuia* n. sp.[7]
Genital atrium (diameter)	117–169 (*) (mature to gravid)	125–190 (154) (mature); 112–230 (169) (pregravid); 142–205 (176) (gravid)	140–304 (218), maximum diameter in late mature to pregravid	138–230 (178), increasing in diameter through ontogeny, maximum in pregravid to gravid	85–300 (238), in diameter through increasing ontogeny, maximum in pregravid to gravid	120–200 (152), increasing in diameter through ontogeny, attains maximum in mature proglottids
Structure male papilla	Single, triangular (*)	Single, triangular	Single, weakly bilobed (dorsoventral view)	Single, weakly bilobed (dorsoventral view)	Paired, strongly bilobed, divergent (dorsoventral view); single papillae, 55–75 (67) in width (mature to gravid)	Paired, weakly bilobed, in apposition (dorsoventral view); single papillae, 20–30 (25.5) in width (mature to gravid)
Genital ducts (position in genital atrium)	Male, female canals straight; opening center of papilla (male); female at base, ventral (*)	*Male*—straight, opening through center of triangular papilla; *female*—curved through atrial wall, straight, opening ventrally base of male papilla	*Male*—weakly curved ventrally, opening through weakly bilobed papilla; *female*—sinuous curve, passing through ventral atrial wall at 90° to cirrus sac, opening ventral to male canal	*Male*—strongly decurved, opening near ventral apex of prominent, bulbous, weakly bilobed papilla; *female*—passing through atrial wall in 90° curve parallel to male canal, opening ventral to papilla/aperature of male canal	*Male*—straight, deflected dorsally, male canal opening on dorsal aspect between paired, massive divergent papillae; *female*—passing through atrial wall in 90° curve ventral to cirrus sac, opening ventrally on prominent, rounded, triangular papilla in atrial lumen	*Male*—straight, male canal opening between apices of prominent, paired papillae in apposition; *female*—passing through atrial wall in 90° curve ventral to cirrus sac, opening ventral/basal to paired male papillae, strongly expanded as atrial seminal receptacle
Male canal (L)	39–57 (*) (mature); 44–49 (*) (gravid)	41–50 (45) (mature); 37–62 (47) (late mature to pregravid)	44–68 (55) (early maturity); 65–94 (77) (late mature to pregravid); 44–94 (72) (all stages of ontogeny)	70–100 (91), maximum in late mature; 75–88 (81), decreasing in pregravid to gravid	45–73 (61) (early mature); 58–95 (77) (mature to gravid); 45–95 (74) (all stages of ontogeny)	52.5–70 (61), maximum in late mature; relatively constant throughout progressive stages of ontogeny

Character	*Tetrabothrius jagerskioeldi* s. str.[1,2]	*Tetrabothrius jagerskioeldi* s. str.[3]	*Tetrabothrius alcae*[4]	*Tetrabothrius sinistralis*[5]	*T. fraterculus* n. sp.[6]	*T. aithuia* n. sp.[7]
Testes (#)	58–62 (original); 46–58 (*)	40–70 (54); seldom > 60 testes in number; surround female organs	75–134 (100) (immature); 66–111 (87) (late mature); seldom < 75 testes in number; gap anterior to vitelline gland and ovary	47–70 (58), (immature to early mature); seldom < 50 testes in number; gap anterior to vitelline gland and ovary	50–96 (67) (immature to early mature); seldom < 60–70 testes in number; surround female organs	40–74 (51), (immature to early mature); seldom < 45 testes in number; gap anterior to vitelline gland and ovary
Center female organs	Midline	Midline	Shifted porad of midline	Midline	Shifted porad of midline	Midline
Ovary (W)	410–600 (mature) (*)	420–980 (694) (maximum, mature to pregravid)	892–1,820 (1,396) (maximum, early mature to late mature)	559–1,310 (915) (maximum, mature to late mature)	880–1,700 (1,082) (maximum, mature to late mature)	465–700 (566) (early mature); 675–1,400 (981) (maximum, mature to late mature proglottids)
Vitelline gland (W × L)	101–192 × 44–120 (*) (mature)	120–400 (204) × 48–170 (107) (mature to pregravid)	301–1,018 (556) × 52–156 (104) (mature to pregravid)	157–460 (268) × 50–177 (102) (mature to pregravid)	131–465 (267) × 60–200 (101) (mature to late mature)	105–200 (135) × 55–115 (74) (early mature); 105–335 (220) × 65–155 (113) (mature to late mature)
Vitelline gland (structure)	Compact, globular (*)	Compact, globular	Follicular, highly elongate	Compact to weakly follicular	Compact to weakly follicular	Compact, globular
Vitelline duct	Single (*)	Single	Multiple, reticulate	Single	Single	Single
Vaginal seminal receptacle (L × W)	Spindle-shaped; level of osmoregulatory canals (*)	100–170 (132) length in mature; spindle-shaped, short; with thickened epithelium; crossing between osmoregulatory canals	520–1,350 (869) × 36–110 (77) in mature to pregravid; cylindrical to weakly pyriform, highly elongate, thin-walled; tapering porad, crossing poral osmoregulatory canals	78–470 (305) × 40–90 (64); spindle-shaped, elongate, thin-walled; attaining, seldom crossing poral osmoregulatory canals	175–500 (285) × 15–105 (62); spindle-shaped to pyriform, elongate, thin-walled; crossing between poral osmoregulatory canals	140–350 (197) × 25–105 (58); spindle-shaped, elongate, thin-walled; crossing between poral osmoregulatory canals

Character	*Tetrabothrius jagerskioeldi* s. str.[1,2]	*Tetrabothrius jagerskioeldi* s. str.[3]	*Tetrabothrius alcae*[4]	*Tetrabothrius sinistralis*[5]	*T. fraterculus* n. sp.[6]	*T. aithuia* n. sp.[7]
Uterus position (relative to osmoregulatory canals)	Between (*)	Between	Ventral to poral and antiporal osmoregulatory canals	Ventral to poral and antiporal osmoregulatory canals	Ventral to poral and antiporal osmoregulatory canals	Ventral to poral and antiporal osmoregulatory canals
Embryophore (L × W)	Not observed	28–35 (30) × 34–43 (39)	25–46 (34) × 36–56 (44)	37.5–45 (40) × 50–57.5 (52)	25–37.5 (29) × 35–45 (38)	30–42.5 (35.6) × 32.5–45 (41)
Oncosphere (L × W)	Not observed	20–26 (23) × 28–39 (32)	21–34 (26) × 28–45 (36)	27.5–35 (30.5) × 35–45 (39)	20–27.5 (22) × 25–37.5 (29)	22.5–27.5 (24.5) × 25–37.5 (30)

Notes:

[1] Nybelin (1916) from orginal description; asterisk (*) indicates new observations from type and voucher specimens summarized by Hoberg and Soudachanh (2020); throughout the table, all measurements are reported in micrometers unless specified otherwise, with the range followed by the mean in parentheses when available.

[2] Data reported in the literature for *T. jagerskioeldi* s. lato by Baer (1954), Temirova and Skrjabin (1978), and Ryzhikov et al. (1985) and for the synonym *T. intrepidus* Baylis, 1919 in detail by Hoberg and Soudachanh (2020), the latter of which are not repeated in the current study.

[3] North Pacific specimens of *T. jagerskioeldi* in Alcidae hosts. Confirmed based on direct comparisons to type specimens, reported and summarized by Hoberg and Soudachanh (2020). Morphological and meristic data for specimens in Laridae and Phalacrocoracidae are not outlined here but are reported in Hoberg and Soudachanh (2020).

[4] Original comparative data for *T. alcae* from Hoberg and Soudachanh (2021).

[5] Original comparative data for *T. sinistralis* from Hoberg and Soudachanh (2021).

[6] Original comparative data for *T. fraterculus* n. sp.

[7] Original comparative data for *T. aithuia* n. sp.

shifted porad of the midline (Figures 2, 3, 12–14). A similar configuration is typical in *T. alcae* and contrasts with *T. jagerskioeldi* and *T. sinistralis*, where the center of the Mehlis' gland, vitelline gland, and ovary are at the midline. The ovary is lobate and not dendritic in early development in *T. fraterculus*, similar to *T. jagerskioeldi* and *T. sinistralis*, but distinct from *T. alcae*. The weakly follicular vitelline gland is similar to *T. sinistralis*, whereas it contrasts with *T. jagerskioeldi* (compact) and *T. alcae* (follicular-elongate). Further, although the center of the female organs is porad of the midline in *T. fraterculus*, the body of the vitelline gland is shifted under the antiporal wing of the ovary, an attribute shared with *T. alcae* but not *T. jagerskioeldi* and *T. sinistralis* in which it is centered relative to the ovarian wings. The VSR in *T. fraterculus* is well developed, with a thin epithelium in early development, becoming thin-walled, elongate, spindle shaped to pyriform and crossing between the OSM (Figures 4, 6, 23, 24). The VSR is distinct in form and dimensions but similar in position relative to *T. jagerskioeldi* and similar in form, (thin walled) but distinct in shape, and position relative to *T. alcae* and *T. sinistralis*. In *T. fraterculus*, the transverse uterine stem passes ventrally to the OSM, differing from *T. jagerskioeldi* but similar to *T. alcae* and *T. sinistralis*.

Identification of Immature Specimens

Identification of immature specimens designated as vouchers for *T. fraterculus* was based on the structure and configuration of the scolex, particularly the overall length-to-width dimensions of the scolex and bothridia, with an elongate scolex compared to *T. jagerskioeldi*, *T. alcae*, and *T. sinistralis* (e.g., Hoberg and Soudachanh, 2020, 2021). Further, the numbers and distribution of testes (gaps and continuity anterior to the vitelline gland) could be determined in the transition to early maturity.

Testes number is influenced by ontogeny and relative age of proglottids and the strobila of individual cestodes. In recently established cestodes, the numbers of testes appear to be lower, relative to values seen in infections of longer duration, or in complete specimens where the gravid condition has been attained. Maximum numbers of testes are usually observed in immature and early mature proglottids, with diminishing numbers posteriad through maturity into late mature and post-mature proglottids. Although testes are most simply counted prior to maturity, it is necessary to document where counts have been completed, and whether in whole mounted specimens (preferred) or in transverse sections. The overall distribution of testes, relative to the female organ systems, is best assessed in early maturity where gaps or continuity can be unequivocally assessed.

Diversity in the T. jagerskioeldi*–complex, Cestodes in Auklets*

A previously unrecognized species of *Tetrabothrius*, a component of the *T. jagerskioeldi*–complex, occurred in 6 species of Alcidae among 17 examined, and from 7 of 58 localities across the greater North Pacific basin (encompassing a trans-Pacific range across marine domains from the eastern North Pacific, Bering Sea, and Aleutian Islands to the northern Sea of Okhotsk), representing inventory between 1949 and 2019 (Table 2; Supplementary Data Table 3).

Cestodes we attribute to *Tetrabothrius aithuia* n. sp. were found as parasites in 24 hosts of 6 species among 1,347 alcids examined (prevalence < 2%). These cestodes were observed primarily in auklets [species of *Aethia* Merrem, 1788 and the monotypic *Ptychoramphus aleuticus* (Cassin, 1811)] and among 24 of 345 (7%) of these small-bodied alcids from 7 of 11 localities (63%), where these 5 species were examined as outlined in Supplementary Data Table 3. Among crested auklets, *T. aithuia* occurred in 11 of 192 birds (6%, intensity= 1–3 cestodes per host) from 4 localities, including 7 of 82 adults (8%) and 2 of 33 fledglings (6%) at Talan Island. Among least auklets and whiskered auklets, respectively, cestodes were collected in 1 of 63 (2%, intensity= 1) and 1 of 18 (6%, intensity = 1) at single sites. Among parakeet auklets, cestodes occurred in 2 of 56 birds (4%, intensity = 1) at 2 localities, including 1 of 27 adults (4%) and none among 4 fledglings at Talan Island. Infections in Cassin's auklets, 8 of 16 (50%, intensity= 1–2), occurred over multiple years at a single pelagic locality. Cestodes were also collected from a single rhinoceros auklet, 1 of 39 (2.5%, intensity = 1); 1 of 8 adults (12%) and none in a single subadult examined from Grays Marine Canyon in August 1987. Specimens of *T. aithuia* were observed in multiple species of auklets and a puffin in sympatry (but not synchronic) from St. Lawrence Island (*A. cristatella* and *A. psittacula*), Talan Island (*A. cristatella* and *A. psittacula*), and pelagic habitats over Grays Marine Canyon (*P. aleuticus* and *C. monocerata*). Specimens of *Tetrabothrius aithuia* were not observed among other species of Alcidae nor a broader assemblage of marine birds occurring in sympatry across the greater North Pacific basin (Supplementary Data Table 3; Hoberg and Soudachanh, 2020, 2021).

Primary materials representing *T. aithuia* include specimens in 24 alcid hosts (11 *A. cristatella*, 8 *P. aleuticus*, 2 *A. psittacula*, single *A. pusilla*, *A. pygmaea*, and *C monocerata*) with 22 cestodes on 44 slides in the type series in 5 host species on which the description is based (Supplementary Data Table 4). Additionally, there are 8 stained and mounted vouchers, primarily postlarval or immature specimens, excluded from the description, on 8 slides in 3 host species (*A. pygmaea*, *A. cristatella*, and *P. aleuticus*), identified based

on the characteristic configuration and structure of the scolex and numbers of testes. Unmounted specimens from the type and voucher series are held in vials in 70% or greater ethanol.

Description—*Tetrabothrius aithuia* n. sp.

Figures 27–53.

General Description: Medium, robust tetrabothriids; maximum length of strobila (n = 11 strobilae) 61.6–131.6 mm × 2,350–4,620 in width, with (n = 8 strobilae) 165–402 proglottids in gravid specimens. Segments wider than long throughout strobila; 230–400 long × 1,330–3,000 wide in immature to early mature proglottids; 350–550 × 2,000–3,325 in mature; 400–575 × 2,275–3,650 in postmature to pregravid; 425–1,025 × 2,000–4,620 in gravid. Length-to-width ratio 1:5.3–12.5 in immature; 1:4.17–9.5 in mature; 1:4.13–8.1 in pregravid; 1:2.43–7.4 in gravid. Scolex rectangular, flat, longer than wide (n = 10) 350–470 (389) long × 310–450 (374) wide; auricles prominent. Bothridia well developed, (n = 32) 195–350 (280) long × 113–230 (181) wide, with muscular margins. Apical region hypertrophied, domelike, expanded anterior to auricles. Neck, as measured from base of scolex to first indication of internal segmentation, relatively short, (n = 8) 210–350 (291) long × 300–420 (351) wide. Ventral OSM 45–100 in diameter, increasing in width throughout development; transverse canal 10–20, occasionally with multiple anastomoses; dorsal canals 15–20 through maturity, narrowing to 5–7.5 in gravid proglottids. Dorsal OSM shifted slightly mediad relative to ventral canals. Genital pores unilateral, dextral in dorsal view, situated marginally in middle to anterior third of proglottid. Male and female genital ducts passing between, extensions of transverse uterus passing ventrally to, poral OSM at all stages of development.

Longitudinal Musculature: Musculature prominent in transverse sections of proglottids; inner and outer bundles arranged in single layers. Inner bundles large in diameter; (n = 9 strobilae) 105–142 (123) in number; (n = 30) 3–22 (10) fibers per bundle. Outer bundles relatively small in diameter; (n = 9) 184–242 (213) in number; (n = 20) 1–6 (4) fibers per bundle. Number of muscle bundles maximum in mature proglottids, diminishing in number posteriad in postmature and gravid segments.

Male Genitalia: *Genital anlagen* visible immediately posterior to neck, protandrous; first testes observed in 65th–105th segment; mature in 135th–210th segment. Testes positioned dorsally in 1–2 layers, (n = 80) 45–105 (68) in diameter; completely overlapping ovary in confluent antiporal field beyond midline; prominent anterior gap defined by vitelline gland with few testes, 3–7, occasionally 0, anterior to ovary and transverse uterine stem in poral field. Testes (n = 123 segments from 17 strobilae in 14 hosts) 40–74 (51) in number in immature to early mature segments, decreasing posteriad in number with maturation of male and female organs; seldom < 45 testes in number. Vas deferens prominent, highly convoluted, distended adjacent to poral OSM. Cirrus sac ovoid, situated in dorsal aspect of genital atrium; (n = 31) 60–100 (79) in diameter through early maturity; increasing in diameter posteriad in strobila, attaining maximum dimensions in late maturity to pregravid condition (n = 188 in 14 strobilae) 62.5–110 (89); muscular wall thickened, 10–20 thick in mature, 15–20 in pregravid, 5–10 in gravid. Cirrus sac contains extension of convoluted vas deferens. Genital atrium ovoid, highly muscularized (n = 26) diameter in early mature, 92.5–150 (122); attaining maximum dimensions in late maturity through gravid proglottids, (n = 178 in 14 strobilae) 120–200 (154). Male genital canal, dorsal, extending through wall of atrium, straight, without deflection, opening between apices of prominent, paired genital papillae in apposition, overall appearing as weakly bilobed male genital papilla in dorsoventral view; asymmetrical in anterior-posterior view in transverse section; diameter of anterior and posterior papillae in dorsoventral orientation, (n = 166) 20–30 (25.5). Length of male genital canal relatively constant at progressive stages of development (mature, late mature, pregravid) for genital atrium and age of proglottid as determined in hand-cut transverse sections; (n = 52 in 12 strobilae) 52.5–70 (61) long.

Female Genitalia: Ovary multilobate, with 2 prominent wings, initially visible in 90th–100th segment; fully developed in 135th–210th segment; (n = 20) 465–700 (566) wide in early maturity; (n = 75) 675–1,400 (981) in mature and postmature segments; situated in anterior 2/3 of segment with center of female organs positioned on midline; not extending to OSM. Vitelline gland globular, compact, (n = 25) in early maturity, 55–115 (74) long × 105–200 (135) wide; maximum dimensions in mature to late mature segments (n = 96) 65–155 (113) long × 105–335 (220) wide; situated anteroventral to ovary, with center of organ on midline; single, broad common vitelline duct passing ventral to ovary. Vitelline gland and ovary becoming diffuse in pregravid proglottids coincidental with expansion of uterus. Common vitelline duct extends posteriad becoming confluent with common vaginal and ovarian duct to ventrally enter prominent Mehlis' gland, (n = 40) 45–80 (61) in diameter; nascent ascending, convoluted, uterine stem extends dorsally from Mehlis' gland. Proximal vagina terminates with expansion as thin-walled, ellipsoidal ISR, (n = 30) 60–130 (94) in diameter at complete expansion; receiving broad

Table 2. Records of Host and Geographic Occurrence for *Tetrabothrius jagerskioeldi* Nybelin, 1916; *T. alcae* Hoberg and Soudachanh, 2021; *T. sinistralis* Hoberg and Soudachanh, 2021; *T. fraterculus* n. sp.; and *T. aithuia* n. sp. among Alcidae Seabirds

Avian species	*Tetrabothrius jagerskioeldi*	*Tetrabothrius alcae*	*Tetrabothrius sinistralis*	*Tetrabothrius fraterculus* n. sp.	*Tetrabothrius aithuia* n. sp.
Tribe Alcini					
Alca torda Linnaeus, 1758	Seven Islands Reserve, Barents Sea (Belopol'skaia, 1952) ▲	Cannot be determined: no specimens are available	Cannot be determined: no specimens are available	Cannot be determined: no specimens are available	Cannot be determined: no specimens are available
Alle alle (Linnaeus, 1758)	Northwestern North Atlantic (Threlfall, 1971) ?▲	Cannot be determined: no specimens are available	Cannot be determined: no specimens are available	Cannot be determined: no specimens are available	Cannot be determined: no specimens are available
Uria aalge (Pontoppidan, 1763)	Seven Islands Reserve, Barents Sea (Belopol'skaia, 1952) ▲ Northwestern Atlantic (Threlfall, 1971) ▲ Big Bay, Shuyak Island, Gulf of Alaska ❋★	Chiniak Bay, Kodiak Island, Gulf of Alaska ❋ St. Matthew Island, Bering Sea ❋ Cape Lisburne, Chukchi Sea ❋ Talan Island, Sea of Okhotsk ❋ Grays Marine Canyon, eastern North Pacific ❋ Humboldt Bay, eastern North Pacific ❋	No current specimens nor records	No current specimens nor records	No current specimens nor records
Uria lomvia (Linnaeus, 1758)	Northwestern Atlantic (Threlfall, 1971) ▲ Peter the Great Bay, Russian Far East (Semtanina, 1979, 1981) ▲	Ugaiushak Island, Gulf of Alaska ❋ Buldir Island, western Aleutian Islands ❋ western Aleutian Islands (pelagic) ❋ St. Lawrence Island, Bering Sea ❋ St. Matthew Island, Bering Sea ❋ Cape Thompson, Chukchi Sea ❋ Talan Island, Sea of Okhotsk ❋	No current specimens nor records	No current specimens nor records	No current specimens nor records
† *Pinguinus impennis* (Linnaeus, 1758)	Host specimen(s) examined: *T. jagerskioeldi* not discovered	Host specimen(s) examined: *T. jagerskioeldi*–complex not discovered	Host specimen(s) examined: *T. jagerskioeldi*–complex not discovered	Host specimen(s) examined: *T. jagerskioeldi*–complex not discovered	Host specimen(s) examined: *T. jagerskioeldi*–complex not discovered

Avian species	*Tetrabothrius jagerskioeldi*	*Tetrabothrius alcae*	*Tetrabothrius sinistralis*	*Tetrabothrius fraterculus* n. sp.	*Tetrabothrius aithuia* n. sp.
Tribe Cepphini					
Cepphus carbo Pallas, 1811	Sudzukhinsky Reserve, Russian Far East (Belopol'skaia, 1963a, 1963b) ▲ Peter the Great Bay, Russian Far East (Smetanina, 1979, 1981) ▲ Northern Sea of Okhotsk ❋★	No current specimens nor records	No current specimens nor records	No current specimens nor records	No current specimens nor records
Cepphus columba Pallas, 1811	St. Lawrence Island, Bering Sea ❋✪★ Uganik Bay, Kodiak Island, Gulf of Alaska ❋✪★ Uyak Bay, Kodiak Island, Gulf of Alaska ❋✪★ St. Matthew Island, Bering Sea ❋✪★ Sledge Island, Bering Sea ❋✪★ Ugaiushak Island, Gulf of Alaska ❋ ✪★	St. Lawrence Island, Bering Sea ❋	St. Matthew Island, Bering Sea ❋	No current specimens nor records	No current specimens nor records
Cepphus grylle (Linnaeus, 1758)	Kristineberg, Sweden (Nybelin, 1916) ❋ Väderöarna, Sweden ❋ Barents Sea (Baylis, 1918) ❋ Seven Islands Reserve, Barents Sea (Belopol'skaia, 1952) ▲ Seven Islands Reserve, Barents Sea (Kuklin and Kuklina, 2005) ▲ Reykjavik, Iceland ❋★ Boxer Bay, St. Lawrence Island, Bering Sea ❋★	No current specimens nor records	Kangerluk, West Greenland (Baer, 1956) ❋	No current specimens nor records	No current specimens nor records

Notes:

◎ Species of Alcidae lacking parasitological data and which apparently have not been examined for parasites

▲ Historical record not supported by archival specimens.

❋ Record substantiated by permanent archived specimens held in an international museum collection; specimens examined during the current study.

✪ New host record.

★ New geographic record.

Table 2. Records of Host and Geographic Occurrence for *Tetrabothrius jagerskioeldi* Nybelin, 1916; *T. alcae* Hoberg and Soudachanh, 2021; *T. sinistralis* Hoberg and Soudachanh, 2021; *T. fraterculus* n. sp.; and *T. aithuia* n. sp. among Alcidae Seabirds *(continued)*

Avian species	*Tetrabothrius jagerskioeldi*	*Tetrabothrius alcae*	*Tetrabothrius sinistralis*	*Tetrabothrius fraterculus* n. sp.	*Tetrabothrius aithuia* n. sp.
Tribe Brachyramphini					
Brachyramphus marmoratus (Gmelin, 1789)	Chiniak Bay, Kodiak Island, Gulf of Alaska ❋✪★	No current specimens nor records	No current specimens nor records	No current specimens nor records	No current specimens nor records
Brachyramphus brevirostris (Vigors, 1829)	Host specimen(s) examined: *T. jagerskioeldi* not discovered	No current specimens nor records	No current specimens nor records	No current specimens nor records	No current specimens nor records
Brachyramphus perdix (Pallas, 1811) ◎					
Tribe Synthliboramphini					
Synthliboramphus antiquus (Gmelin, 1789)	Sudzukhinsky Reserve, Russian Far East (Belopol'skaia, 1963a, 1963b) ▲ Peter the Great Bay, Russian Far East (Smetanina, 1979, 1981) ▲	Western Aleutian Islands (pelagic) ❋ St. Lawrence Island, Bering Sea ❋	No current specimens nor records	No current specimens nor records	No current specimens nor records
Synthliboramphus craveri (Salvadori, 1865) ◎					
Synthlibramphus hypoleucus (Xantus de Vesey, 1860) ◎					
Synthliboramphus scrippsi (Green and Arnold, 1939)	Host specimen(s) examined: *T. jagerskioeldi* not discovered		No current specimens nor records		No current specimens nor
records	No current specimens nor records		No current specimens nor records		
Synthliboramphus wumizuzume Temminck, 1836 ◎					
Tribe Aethiini					
Ptychoramphus aleuticus (Pallas, 1811)	Host specimen(s) examined: *T. jagerskioeldi* not discovered	No current specimens nor records	No current specimens nor records	No current specimens nor records	Grays Marine Canyon, eastern North Pacific ❋
Aethia psittacula	Host specimen(s) examined:	Talan Island,	No current specimens	No current specimens	Talan Island,

(Pallas, 1769)	*T. jagerskioeldi* not discovered	Sea of Okhotsk ❋	nor records	nor records	Sea of Okhotsk ❋
Aethia cristatella (Pallas, 1769)	Host specimen(s) examined: *T. jagerskioeldi* not discovered	No current specimens nor records	No current specimens nor records	No current specimens nor records	Talan Island, Sea of Okhotsk ❋ Amchitka Island, Central Aleutian Islands ❋ St. Lawrence Island, Bering Sea ❋ St. Paul Island (Pribilof Islands) Bering Sea ❋
Aethia pygmaea (Gmelin, 1789)	Host specimen(s) examined: *T. jagerskioeldi* not discovered	No current specimens nor records	No current specimens nor records	No current specimens nor records	Buldir Island, western Aleutian Islands ❋
Aethia pusilla (Pallas, 1811)	Host specimen(s) examined: *T. jagerskioeldi* not discovered	No current specimens nor records	No current specimens nor records	No current specimens nor records	St. Matthew Island, Bering Sea ❋

Notes:

◎ Species of Alcidae lacking parasitological data and which apparently have not been examined for parasites.

▲ Historical record not supported by archival specimens.

❋ Record substantiated by permanent archived specimens held in an international museum collection; specimens examined during the current study.

✪ New host record.

★ New geographic record.

Table 2. Records of Host and Geographic Occurrence for *Tetrabothrius jagerskioeldi* Nybelin, 1916; *T. alcae* Hoberg and Soudachanh, 2021; *T. sinistralis* Hoberg and Soudachanh, 2021; *T. fraterculus* n. sp.; and *T. aithuia* n. sp. among Alcidae Seabirds *(continued)*

Avian species	*Tetrabothrius jagerskioeldi*	*Tetrabothrius alcae*	*Tetrabothrius sinistralis*	*Tetrabothrius fraterculus* n. sp.	*Tetrabothrius aithuia* n. sp.
Tribe Fraterculini					
Fratercula arctica (Linnaeus, 1758)	Seven Islands Reserve, Barents Sea (Belopol'skaia, 1952) ▲ Northwestern Atlantic (Threlfall, 1971) ▲	Cannot be determined: no specimens are available	Cannot be determined: no specimens are available	Cannot be determined: no specimens are available	Cannot be determined: no specimens are available
Fratercula cirrhata (Pallas, 1769)	Russian Far East or Kurile Islands (?) (Temirova and Skrjabin, 1978) ▲	No current specimens nor records	No current specimens nor records	Sitkalidak Island (Kodiak Island Region), Gulf of Alaska ❋ Western Aleutian Islands (pelagic) ❋ Talan Island, Sea of Okhotsk ❋	No current specimens nor records
Fratercula corniculata (Naumann, 1821)	Host specimen(s) examined: *T. jagerskioeldi* not discovered	No current specimens nor records	No current specimens nor records	Buldir Island, western Aleutian Islands ❋ Western Aleutian Islands (pelagic) ❋ Amukta Island, western Aleutian Islands ❋ Talan Island, Sea of Okhotsk ❋	No current specimens nor records
Cerorhinca monocerata (Pallas, 1811)	Shikotan Island, Kurile Islands (Smetanina and Leonov, 1984) ▲ Western Aleutian Islands (pelagic) ❋★	No current specimens nor records	No current specimens nor records	Grays Marine Canyon, eastern North Pacific ❋ Destruction Island, Outer Washington Coast, eastern North Pacific ❋ Western Aleutian Islands (pelagic) ❋	Grays Marine Canyon, eastern North Pacific ❋
Other Seabird Species—Laridae, Stercorariidae, Phalacrocoracidae					

Larus glaucescens Naumann, 1840	Central Island, Gulf of Alaska (Hoberg and Soudachanh, 2020) ❋ Puffin Island, Gulf of Alaska (Hoberg and Soudachanh, 2020) ❋	No current specimens nor records	No current specimens nor records	No current specimens nor records	No current specimens nor records
Stercorarius parasiticus (Linnaeus, 1758)	Seven Islands Reserve, Barents Sea (Belopol'skaka, 1952) ▲ Enurmino, Chukotka (Temirova and Skrjabin, 1978) ▲	No current specimens nor records	No current specimens nor records	No current specimens nor records	No current specimens nor records
Urile pelagicus (Pallas, 1811)	Buldir Island, western Aleutian Islands (Hoberg and Soudachanh, 2020) ❋	No current specimens nor records	No current specimens nor records	No current specimens nor records	No current specimens nor records

Notes:

◎ Species of Alcidae lacking parasitological data and which apparently have not been examined for parasites.

▲ Historical record not supported by archival specimens.

❋ Record substantiated by permanent archived specimens held in an international museum collection; specimens examined during the current study.

✪ New host record.

★ New geographic record.

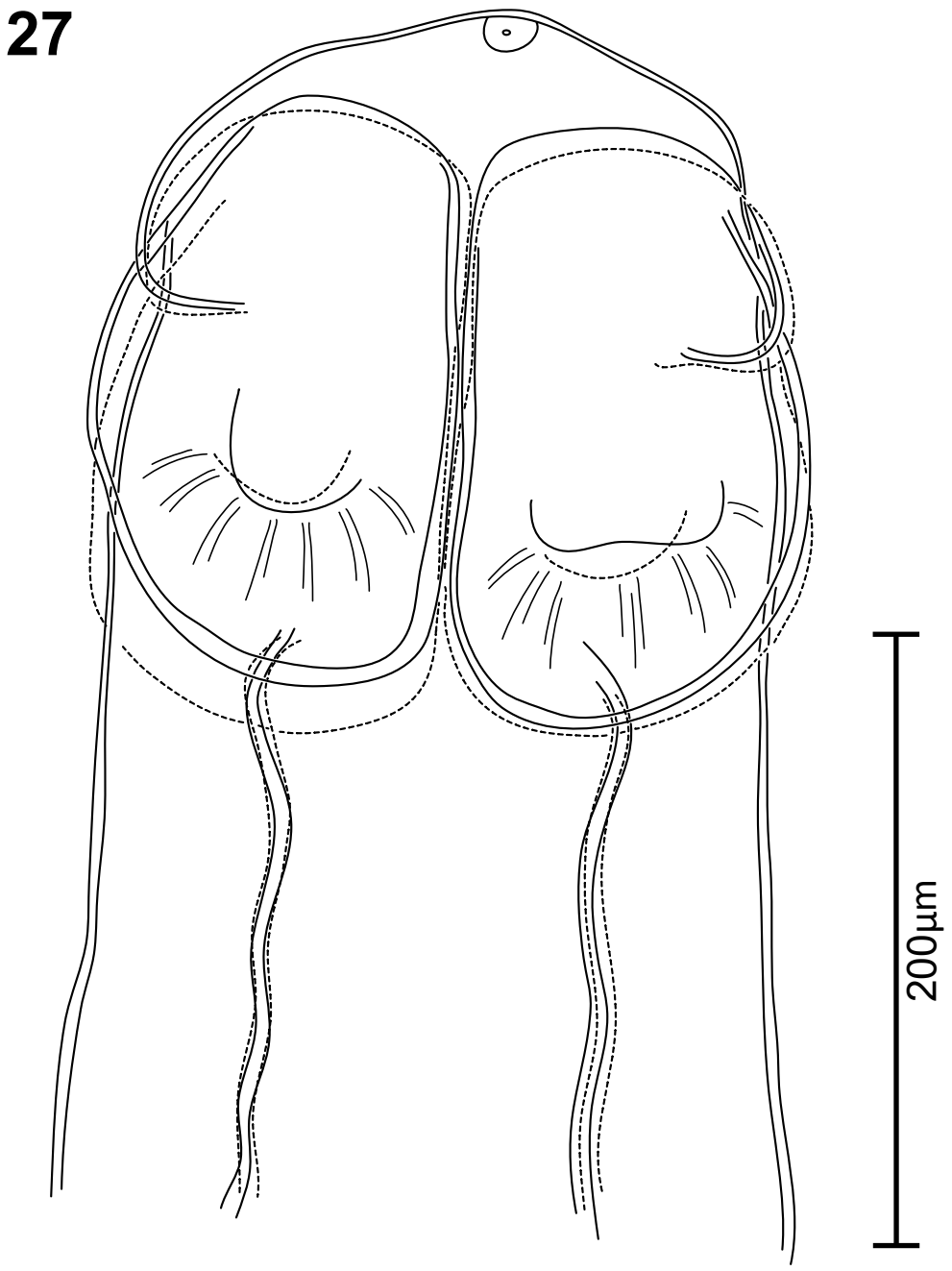

Figure 27. *Tetrabothrius aithuia* n. sp., scolex in dorsoventral view from holotype specimen (2926-1A) in *Aethia cristatella* from Talan Island, Sea of Okhotsk (scale bar in micrometers). The scolex is longer than wide with elongate bothridia and well-developed auricular appendages. Note rounded domelike apical region and vestigial apical organ at apex.

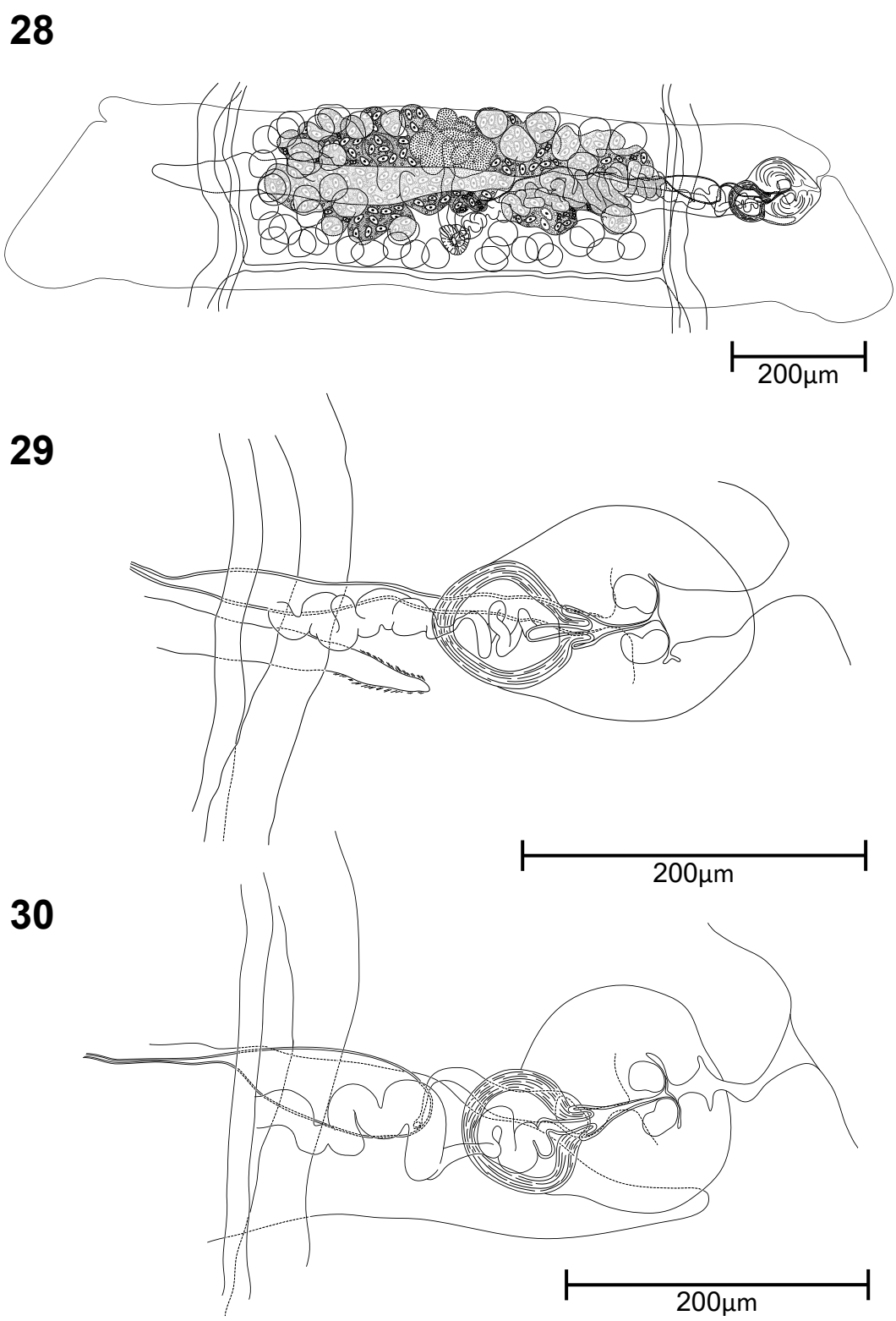

Figures 28–30. *Tetrabothrius aithuia* n. sp., with details of the genital atrium and terminal genital ducts in progressive stages of ontogeny based on the holotype (2926) in *Aethia cristatella* from Talan Island, Sea of Okhotsk (scale bars in micrometers). **Fig. 28.** Dorsal view of complete proglottid in maturity from whole mount in holotype specimen (2926-1A). **Fig. 29.** Genital atrium, dorsal view in maturity from whole mount (2926-1A). **Fig. 30.** Genital atrium, dorsal view in late maturity from whole mount (2926-1A). Note genital ducts passing between and uterus passing ventral to osmoregulatory canals and expansion of elongate, expanded vaginal seminal receptacle.

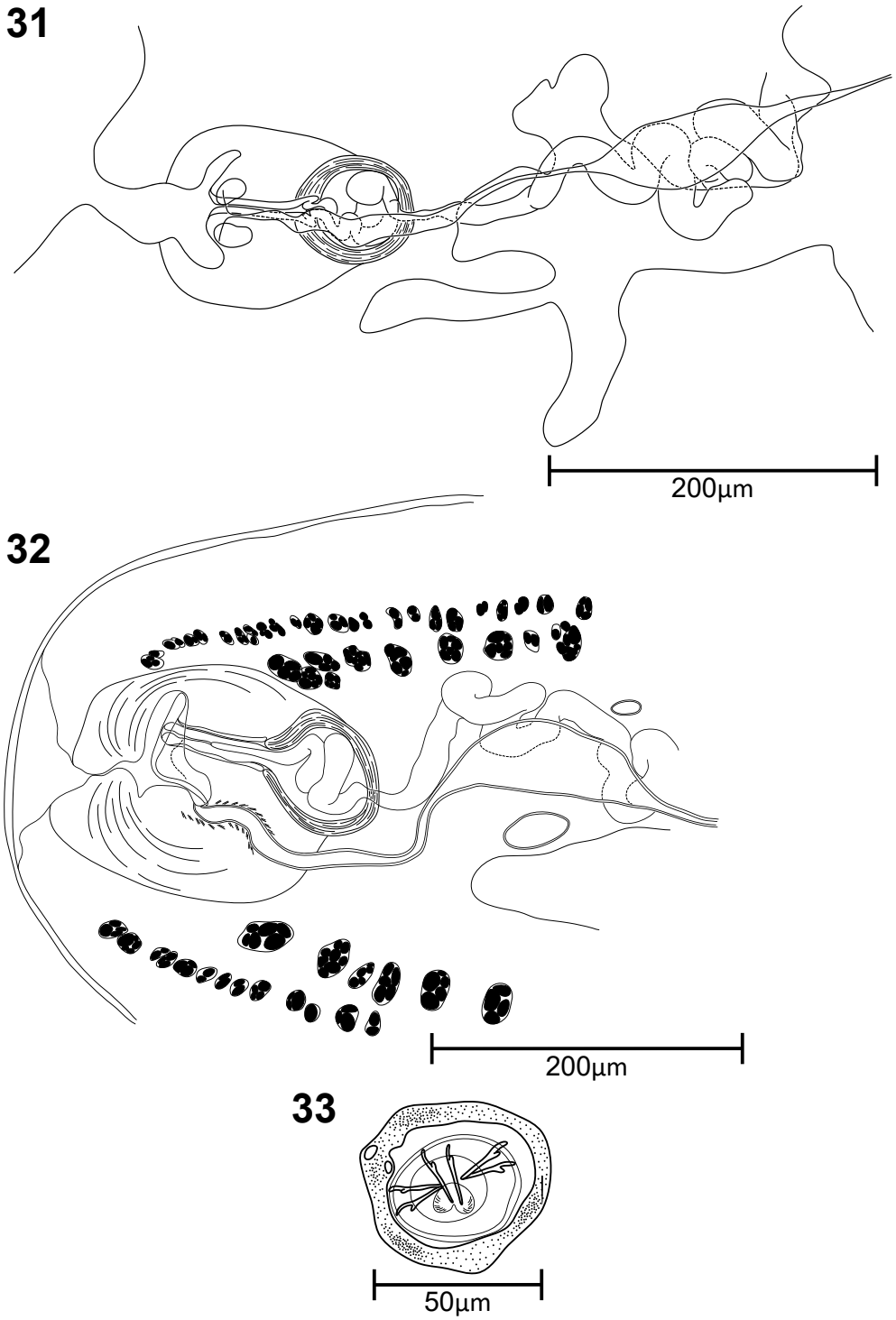

Figures 31–33. *Tetrabothrius aithuia* n. sp., showing details of genital atrium in ventral and view from anterior in transverse section and structure of the egg and embryophore (scale bars in micrometers). **Fig. 31.** Genital atrium, ventral view in pregravid condition from whole mount of paratype (11340) in *Aethia cristatella* from Amchitka Island, Aleutian Islands. Note expanding uterus with lobate extensions, dorsal to the convoluted vas deferens and spindle-shaped vaginal seminal receptacle. **Fig. 32.** Genital atrium in late maturity in transverse section viewed from anterior in holotype (2926-1B), dorsal to top. Note, complex structure of atrial systems with asymmetrical, paired male papillae and ventral aperture of female canal opening directly into atrial lumen. Genital ducts pass between the osmoregulatory canals and expanding uterus is ventral in position; note expansion of spindle-shaped vaginal seminal receptacle and developing atrial seminal receptacle. Note mediad shift in position of dorsal osmoregulatory canal and position and number of inner and outer longitudinal muscle bundles. **Fig. 33.** Oncosphere, embryophore, and egg envelopes from whole mount of gravid proglottid in holotype 2926-1A.

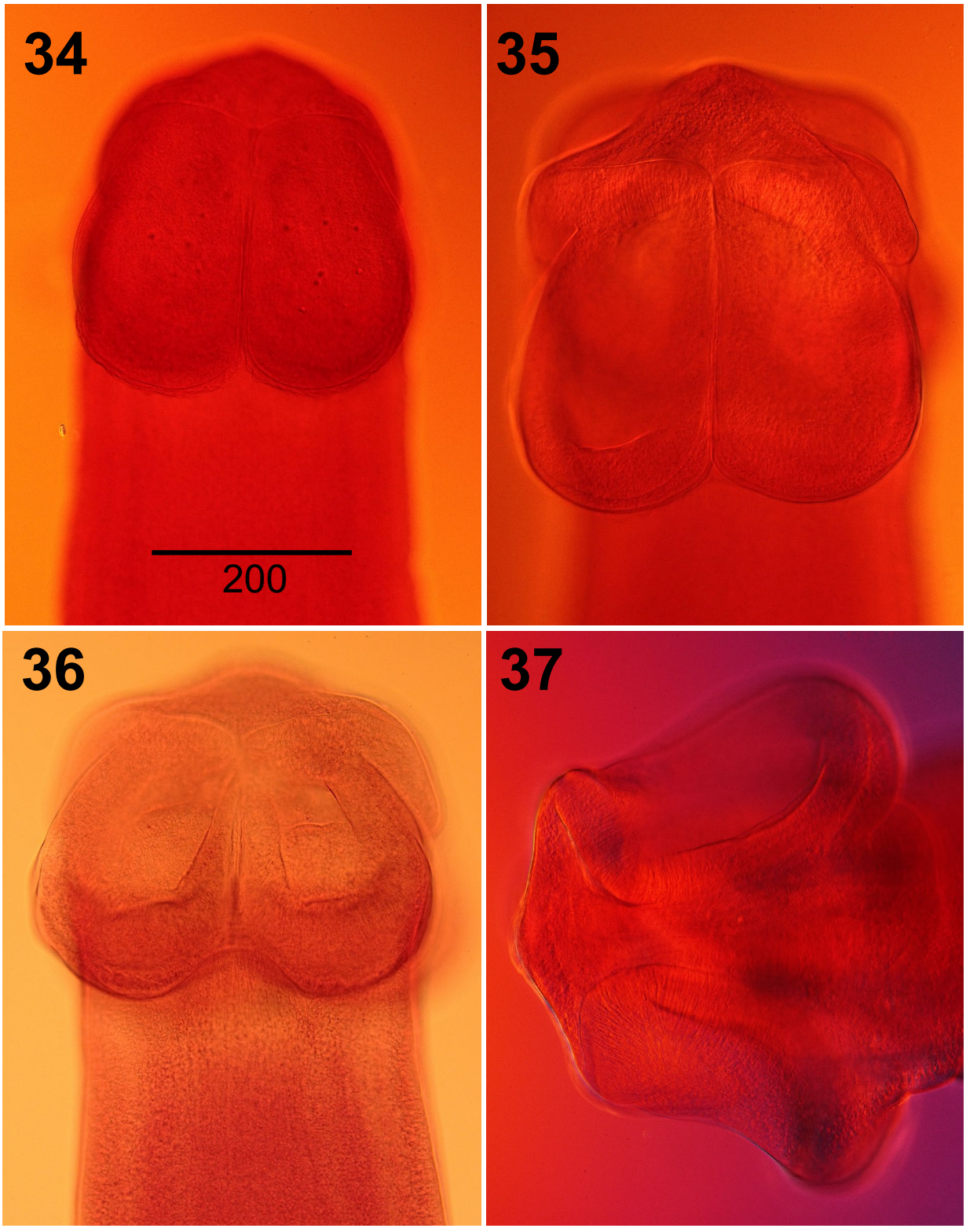

Figures 34–37. *Tetrabothrius aithuia* n. sp., structure and dimensions of adult scolex in dorsoventral and lateral views (scale bar in micrometers; all same scale). **Fig. 34.** Scolex, dorsoventral, showing elongate dimensions consistently longer than wide, with well-developed auricular appendages and rounded apical region from holotype specimen (2926-1A) in *Aethia cristatella* from Talan Island, Sea of Okhotsk. **Fig. 35.** Scolex in paratype specimen (2879-1A) in *A. cristatella* from Talan Island. **Fig. 36.** Scolex in paratype specimen (2879-3) in *A. cristatella* from Talan Island. **Fig. 37.** Scolex, lateral orientation, in paratype specimen (2879-2A) in *A. cristatella* from Talan Island.

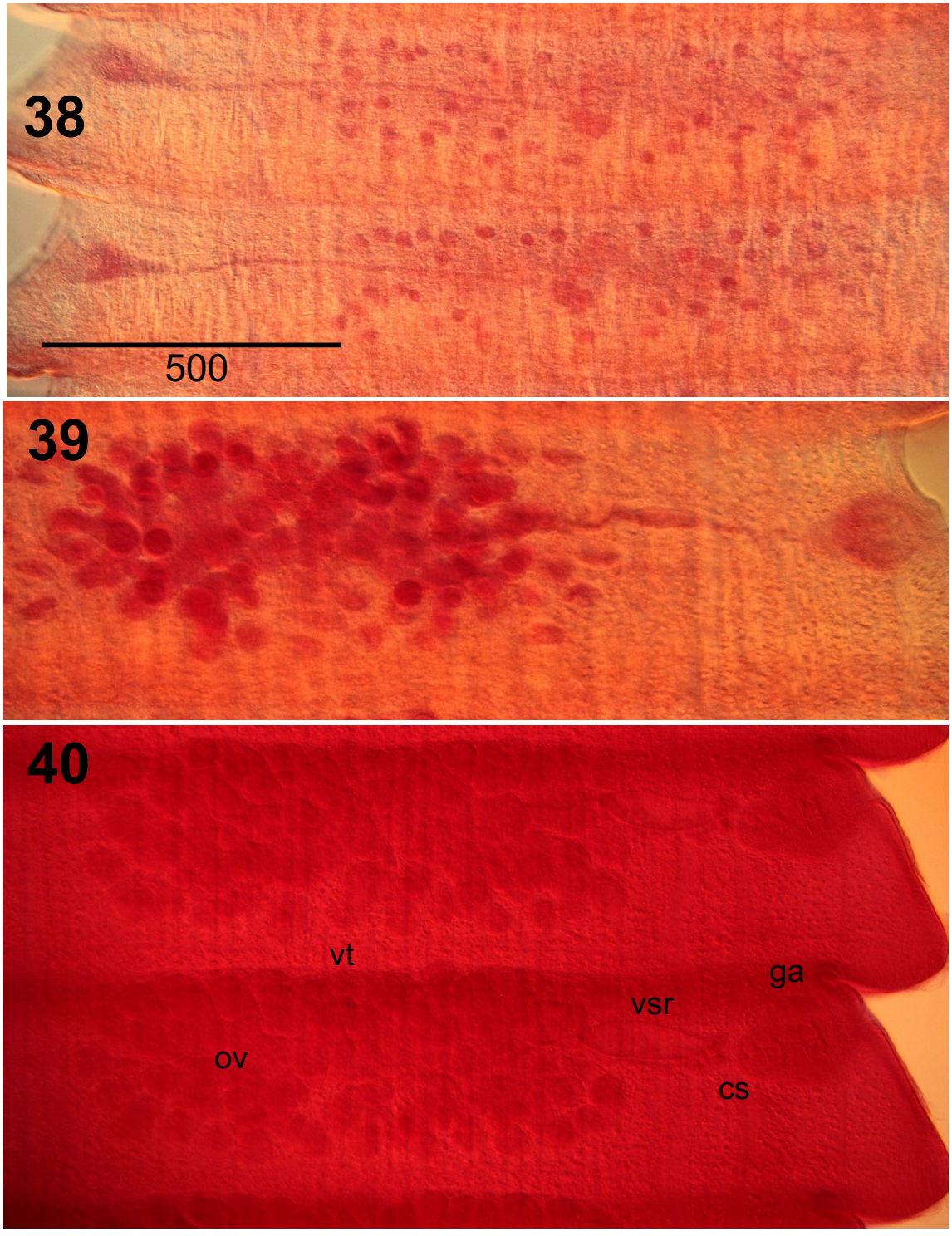

Figures 38–40. *Tetrabothrius aithuia* n. sp., showing structure of developing proglottids and distribution of male and female organ systems (scale bars in micrometers). **Fig. 38.** Immature proglottids in ventral view in paratype specimen (2323-1) in *Ptychoramphus aleuticus* from Grays Marine Canyon, showing number and arrangement of testes relative to initial development of ovary and vitelline gland; note position of the female organs on midline; dextral, marginal genital pore. **Fig. 39.** Early mature proglottid in dorsal view in paratype specimen (2323-1) in *Ptychoramphus aleuticus* from Grays Marine Canyon, showing distribution of testes with gap anterior to female organs; developing vaginal seminal receptacle. **Fig. 40.** Mature proglottid, dorsal view, in holotype specimen (2926-1A) in *Aethia cristatella* from Talan Island, showing structure of multilobate ovary (ov) and globular, compact vitelline gland (vt) on midline, expanded vaginal seminal receptacle (vsr), genital atrium (ga), and cirrus sac (cs).

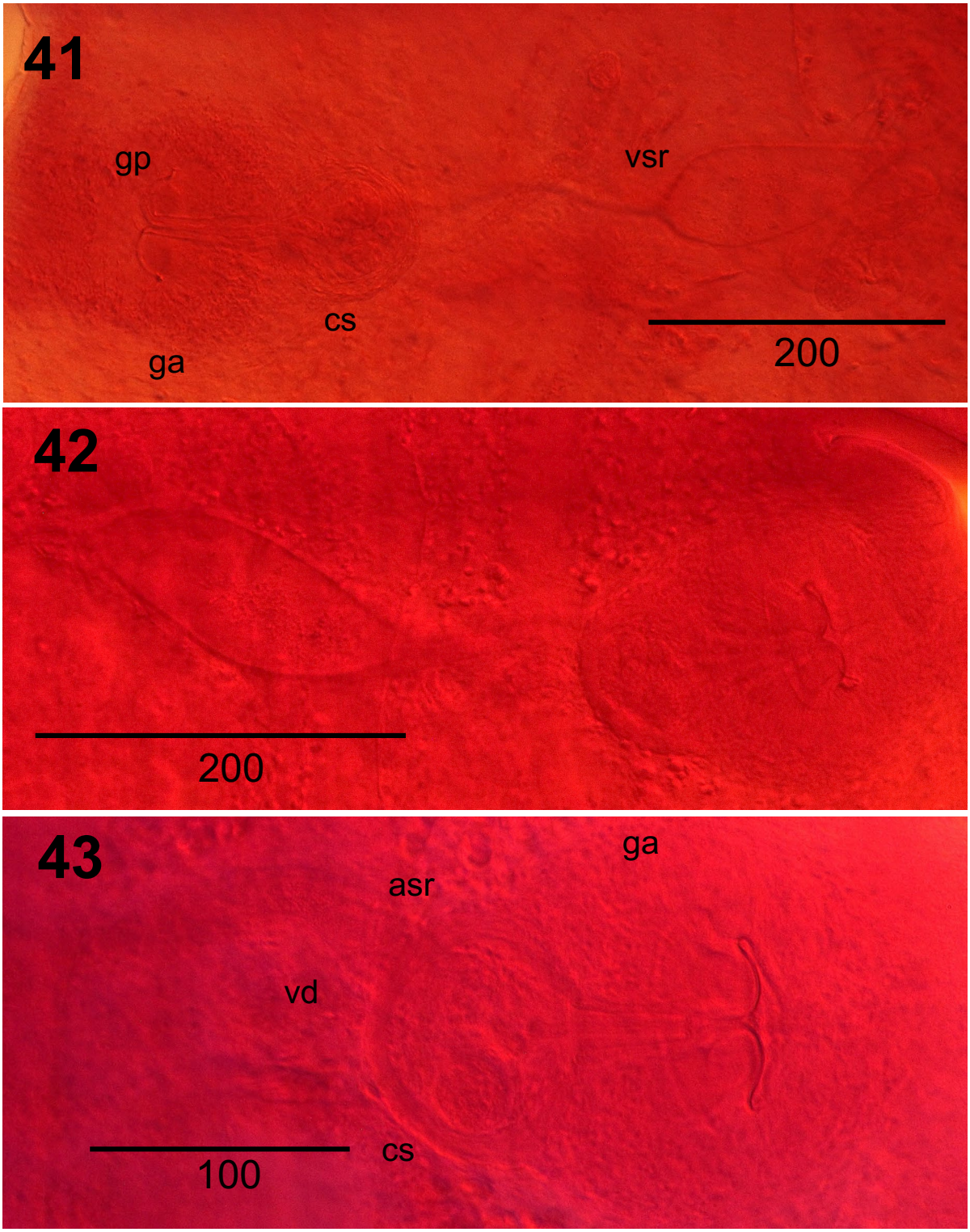

Figures 41–43. *Tetrabothrius aithuia* n. sp., showing genital atrium and associated structures in marginal views from whole mounts (scale bars in micrometers). **Fig. 41.** Proglottid in maturity, ventral view, paratype specimen (11340) in *Aethia cristatella* from Amchitka Island. Note genital atrium (ga), genital papillae (gp), cirrus sac (cs), and vaginal seminal receptacle (vsr). **Fig. 42.** Proglottid in maturity, dorsal view from holotype (2926-1A) in *A. cristatella* from Talan Island. **Figure 43.** Proglottid, fully developed, gravid, dorsal view in holotype (2926-1A), showing genital atrium (ga), genital papillae and male atrial canal, cirrus sac (cs), convoluted vas deferens (vd), and expansion of atrial seminal receptacle (asr).

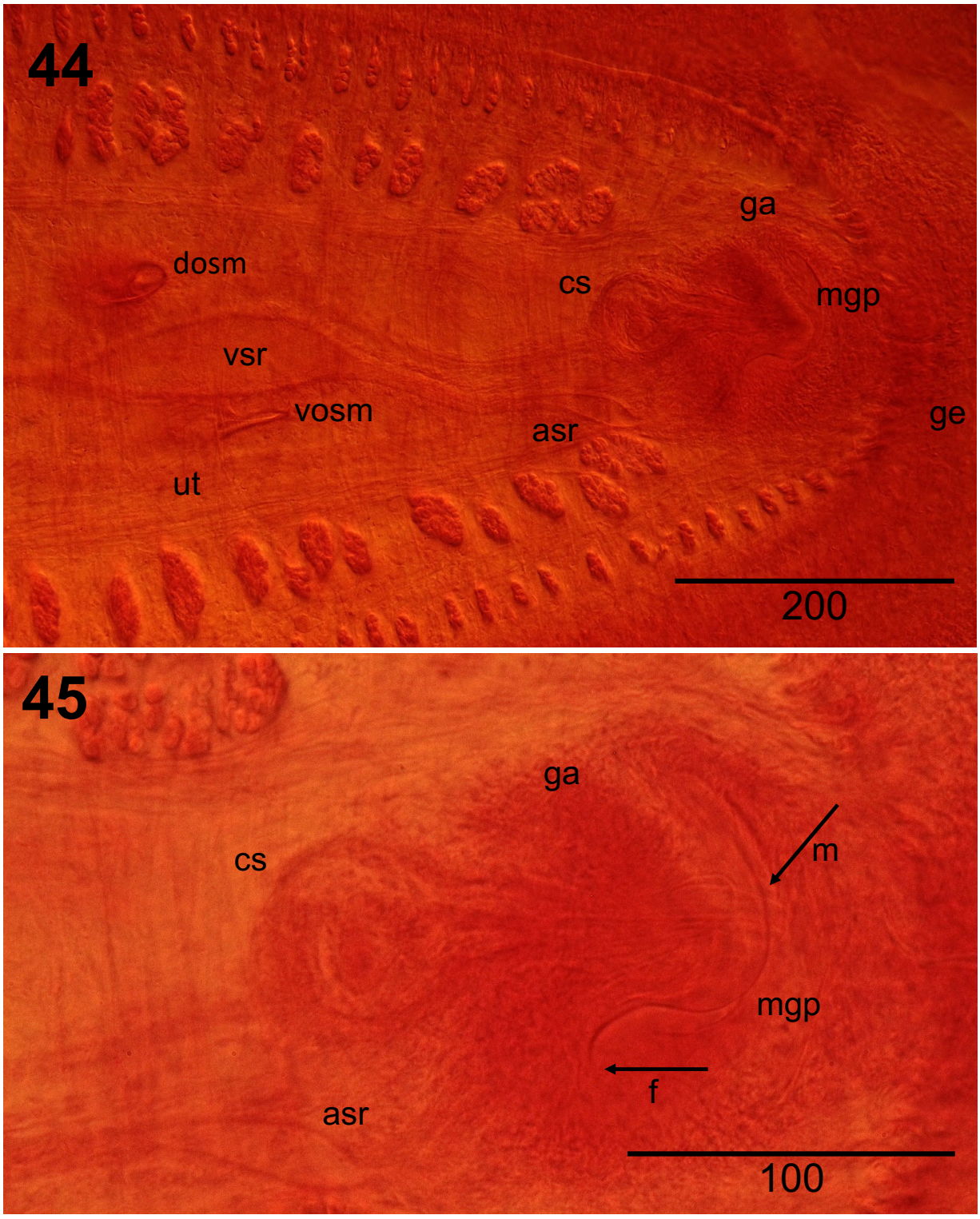

Figures 44–45. *Tetrabothrius aithuia* n. sp., showing genital atrium, in transverse section of mature proglottid, viewed from posterior, dorsal to top, from paratype specimen (2880-1B) in *Aethia cristatella* from Talan Island (scale bars in micrometers). **Fig. 44.** Poral region of proglottid showing lateral genital pore (ge), genital atrium (ga), and asymmetrical male genital papillae (mgp), cirrus sac (cs) with atrial (asr), and vaginal seminal receptacles (vsr). Note genital ducts passing between ventral (vosm) and dorsal (dosm) osmoregulatory canals, transverse uterine stem (ut) passing ventrally. **Fig. 45.** Genital atrium (ga), male genital papillae (mgp), cirrus sac (cs), and sinuous atrial seminal receptacle (asr). Note apertures of male (m) and female (f) atrial genital canals (*arrows*); straight male canal and evaginated cirrus.

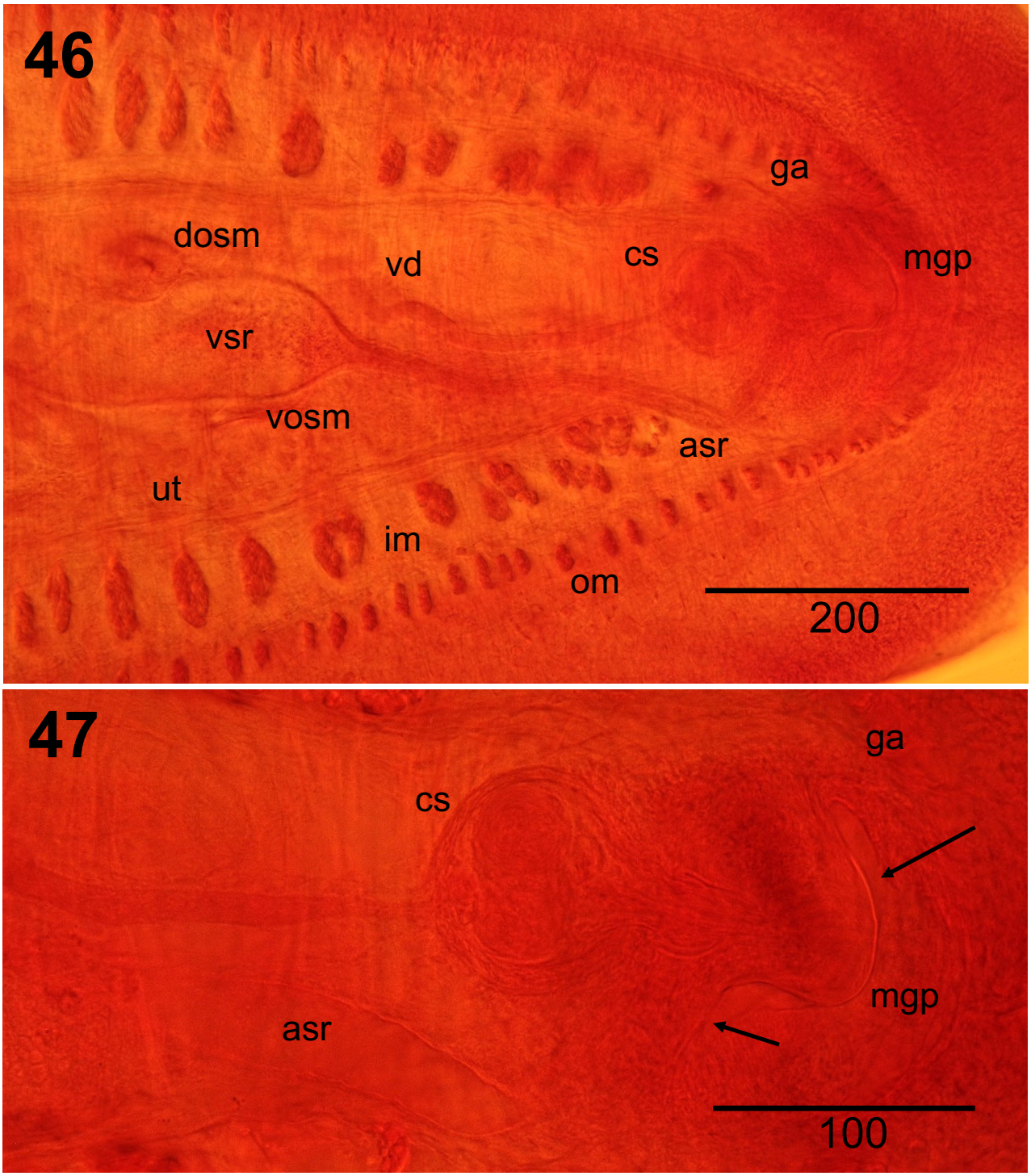

Figures 46–47. *Tetrabothrius aithuia* n. sp., showing structure of genital atrium, genital ducts, and relative positions of osmoregulatory canals in transverse sections of postmature proglottids, viewed from posterior, dorsal to top, from paratype specimen (2880-1C) in *Aethia cristatella* from Talan Island (scale bars in micrometers). **Fig. 46.** Poral region of proglottid showing distribution of inner (im) and outer (om) longitudinal muscle bundles, positions of genital atrium (ga), male genital papillae (mgp), cirrus sac (cs), vas deferens (vd), bipartite seminal receptacle system with atrial (asr) and vaginal (vsr) expansions, genital ducts passing between ventral (vosm) and dorsal (dosm) osmoregulatory canals. Note expanding uterus (ut) passing ventral to the vosm and extending porad to near base of cirrus sac. **Fig. 47.** Genital atrium (ga), position and asymmetry of male genital papillae (mgp), position of the cirrus sac (cs), apertures of male and sinuous female atrial genital canals (*arrows*), and expansion of atrial seminal receptacle (asr).

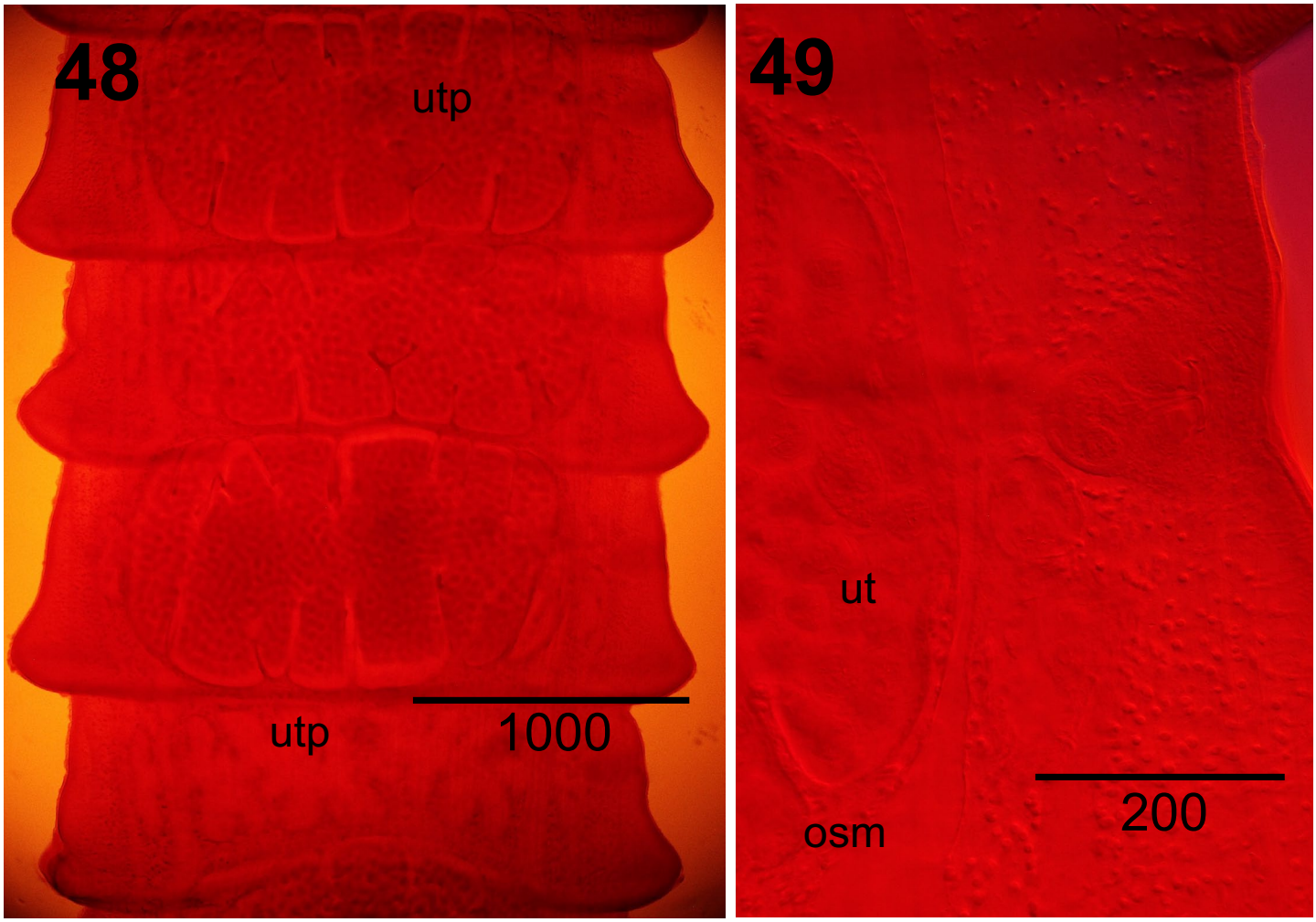

Figures 48–49. *Tetrabothrius aithuia* n. sp., gravid uterus, terminal proglottids from whole mount in holotype specimen (2926-1A) from *Aethia cristatella* at Talan Island (scale bars in micrometers). **Fig. 48.** Gravid proglottids dorsal view; note lobate, sacculate structure of uterus extending beyond the osmoregulatory canals, position of middorsal uterine pore (utp), and emptied uterus in near-terminal segment. **Fig. 49.** Poral margin of gravid proglottid, dorsal view; note position of genital atrium, cirrus sac, and extension of uterus (ut) ventral to osmoregulatory canals (osm).

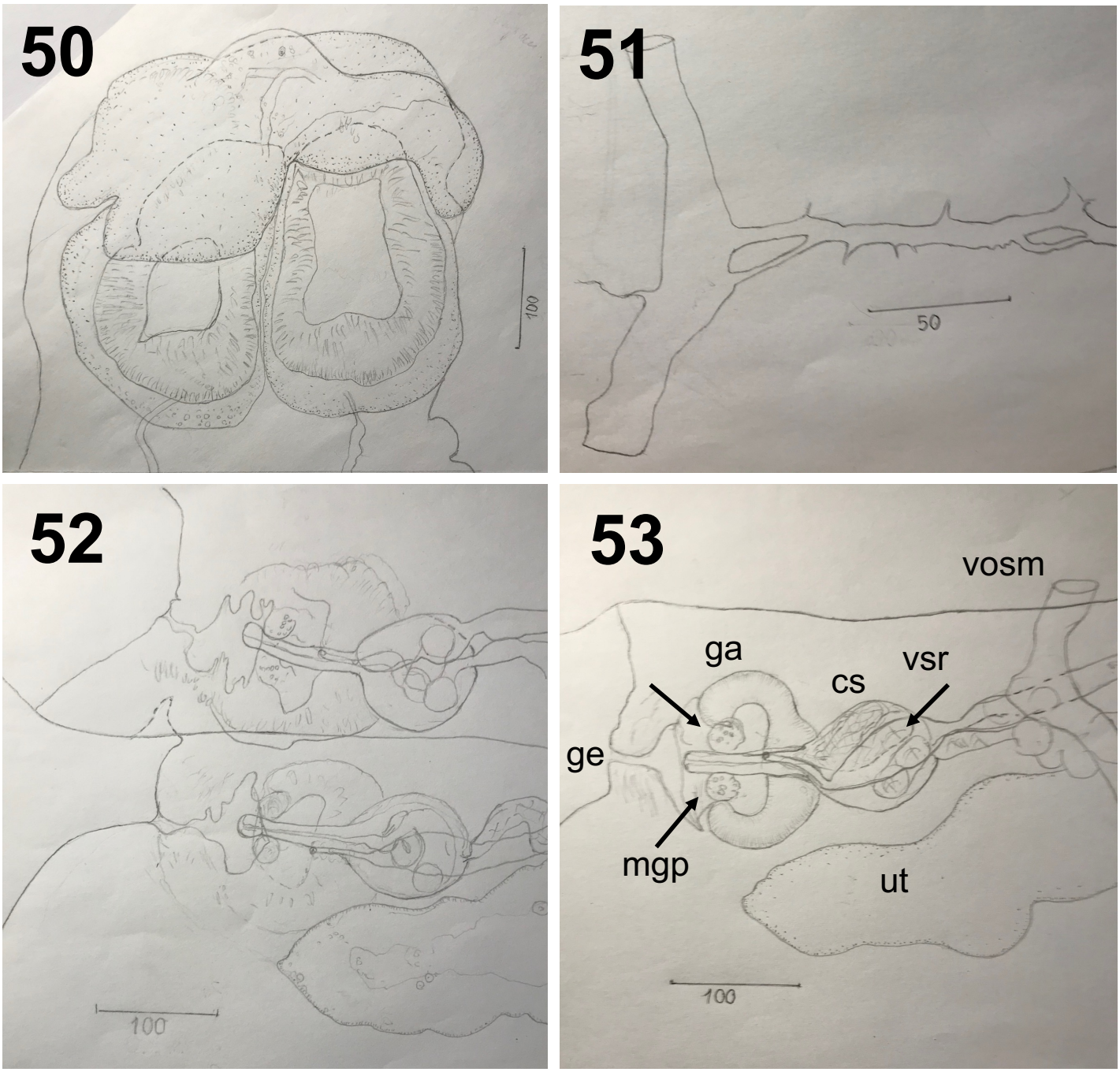

Figures 50–53. *Tetrabothrius aithuia* n. sp., preliminary line drawings, in ventral orientation, from whole-mounted paratype specimen (EKOI-HELMI 1163) in *Aethia cristatella* from Talan Island collected by S.K. Bondarenko and O. Orlovskaya on 8 August 1997. Figures prepared by SKB. These specimens morphologically substantiate the 1997 record at Talan Island. **Fig. 50.** Scolex. **Fig. 51.** Ventral osmoregulatory system showing anastomoses in transverse canal. **Fig. 52.** Genital pore, genital atrium, cirrus sac, and expanded atrial seminal receptacle and transverse uterine stem in late maturity. **Fig. 53.** Detail of genital pore (ge), genital atrium (ga) with paired male papillae (mgp, *arrows*), cirrus sac (cs), cirrus and vaginal seminal receptacle (vsr), showing genital ducts passing dorsally to the ventral osmoregulatory canal (vosm) and expanding transverse uterus (ut).

ovarian duct slightly dorsolateral to Mehlis' gland. Vagina extends porad from ISR as thin tube dorsal to ovary, ventral to testes. Seminal receptacle system distally bipartite. VSR voluminous, elongate, spindle-shaped dilatation of vagina with thin, membranous wall, extending between poral OSM; expansion defines onset of maturity; maximum diameter attained at level of OSM in mature to gravid proglottids, (n = 105) 140–350 (197) long × 25–105 (58) wide, not attaining ovarian margin; becoming variable, diminishing in dimensions in pregravid to gravid proglottids. Distal vagina with prominent expansion of ASR in pregravid to gravid proglottids, entering genital atrium in sinuous curve, ascending and at about 90° ventral to cirrus sac. ASR with dilatation near distal base of cirrus sac extending into atrial wall, mediad nearly confluent with VSR, separated by short tubular region of vagina. Female genital canal opening ventrally, directly into atrial lumen, near base of weakly bilobed male papillae; orifice ventral to aperture of male canal, not immediately adjacent. Ascending uterus extends anteriad from dorsal aspect of Mehlis' gland; transverse tubular uterine stem initially visible coinciding with ovarian development, dorsal to ovary, ventral to testes. Mature uterus, a broad sacculate, lobate, structure lined with prominent epithelium, situated dorsally in proglottid, extending ventrally beyond OSM; gravid by 212th to 340th segment. Uterus extends to level of cirrus sac and genital atrium and beyond antiporal OSM when fully gravid. Uterine pore median, dorsal, patent in pregravid strobilae; segments anapolytic. Mature eggs contained within capsule with granular membrane, (n = 50) 50–80 (62.5) in diameter. Hyaline embryophore (n = 50) 32.5–45 (41) wide × 30–42.5 (36) long, containing oncosphere (n = 50) 25–37.5 (30) wide × 22.5–27.5 (24.5) long. Embryonic hooks (n = 25) 13.7–17.5 (15) in length for medial pairs, (n = 50) 15–18.7 (17) for lateral groups.

Taxonomic Summary

Hosts: Type host—crested auklet, *Aethia cristatella* (Pallas, 1789). Other known hosts—whiskered auklet, *Aethia pygmaea* (Gmelin, 1789); least auklet, *Aethia pusilla* (Pallas, 1811); parakeet auklet, *Aethia psittacula* (Pallas, 1769); Cassin's auklet, *Ptychoramphus aleuticus* (Cassin, 1811) [*P. aleuticus aleuticus* (Pallas, 1811)]; and rhinoceros auklet, *Cerorhinca monocerata* (Pallas, 1811). Not currently observed in other Alcidae nor in an assemblage of sympatric northern seabirds.

Localities: Type locality—Talan Island, northern Sea of Okhotsk, Russia, ca. 59°19′N, 149°06′E in type host (breeding adult) on 13 July 1988. Other known localities—St. Lawrence Island, AK; St. Matthew Island, Bering Sea, AK; St. Paul Island, Bering Sea, AK; Buldir Island, western Aleutian Islands, AK; Amchitka Island, central Aleutian Islands, AK; pelagic waters over Grays Marine Canyon, eastern North Pacific, WA. (Table 2; Supplementary Data Tables 2, 3, and 4).

Specimens: Holotype—in type host, from type locality collected by E.P. Hoberg, A.Ya. Kondratiev, L. Kondratieva and S.K. Bondarenko (field number 2926 1-A through 2926 1B), single specimen on 2 slides including scolex, strobila, and hand-cut thick sections; identification by EPH, Museum of Southwestern Biology, MSB Collection No. 32035. Paratype and voucher series, along with georeferenced collection data, are archived in the Museum of Southwestern Biology, Division of Parasitology (Supplementary Data Table 4). A single paratype specimen from the type locality, subsequently collected in 1997 and identified by SKB, is archived in the collections of the Museum of the Institute of Ecology, Vilnius, Lithuania (EKOI-HELMI 1163).

Zoobank Name Registration for *Tetrabothrius aithuia*: LSID urn:lsid:zoobank.org:pub:0768AC62-B4C1-4737-8113-6DB413A241BE

Symbiotype: Host specimens or tissues not generally retained and archived. Some specimens of *Ptychoramphus aleuticus* and *Cerorhinca monocerata* are held in avian collections of the Burke Memorial Washington State Museum among an assemblage of seabirds from Grays Marine Canyon, eastern North Pacific during 1982, 1985, and 1987 (Supplementary Data Tables 3 and 4).

Etymology: *Tetrabothrius aithuia* n. sp. is based on "aíthuia" for a diving bird in New Latin, from Ancient Greek, and is proposed as the 5th species recognized in the *T. jagerskioeldi*–complex. The species taxon name further reflects the tribe Aethiini and generic nomenclature for 4 of 5 species of auklets, *Aethia* Merrem, 1788, including the type host *Aethia cristatella*.

Remarks and Diagnosis

Tetrabothrius aithuia n. sp. is the 5th cestode attributed to the *T. jagerskioeldi*–complex. We consider these descriptions to resolve the known limits for diversity within the *T. jagerskioeldi*–complex, with delineation of 5 distinct species. Further inventory among marine birds, especially species of Alcidae, that have not received attention (Table 2) and from localities in the North Pacific, greater Arctic Basin, and North Atlantic may broaden the current limits for species richness in this fauna (Hoberg and Soudachanh, 2020, 2021). It is essential that future considerations of diversity in this fauna contribute to an expanding body of archived specimens and data. Descriptions should incorporate an integrated perspective combining comparative morphology with sequence and genomic-based data streams from individual cestode specimens. Age of specimens and methods

of fixation in original field collections, spanning more than 100 years since Nybelin (1916) and Baylis (1919), among the 5 species currently preclude molecular-based analyses of this assemblage. Diversity of *Tetrabothrius* now includes 56 species, with 46 nominal taxa among avian hosts in addition to 10 distributed among Cetacea (see also Mariaux et al., 2017). Comparisons outlined farther along involve data from the redescription of *T. jagerskioeldi* s. str. as defined by Hoberg and Soudachanh (2020, 2021).

Morphologically, specimens attributed to *T. aithuia* are most similar to those of *T. jagerskioeldi* s. str., *T. alcae*, *T. sinistralis*, and *T. fraterculus*, principally among alcid seabirds and *T. erostris* Lönnberg, 1896 among larids and alcids (Hoberg and Soudachanh, 2020, 2021). Differentiation among this assemblage of species depends on structural and meristic comparisons of the scolex and genital complex (Table 1) (Figures 27–53). Overall dimensions of gravid strobilae among specimens of *T. aithuia* are considerably smaller relative to congeners in the *T. jagerskioeldi*–complex. Additionally, smaller dimensions for the cirrus sac and muscular genital atrium at progressive stages of development are typical for *T. aithuia.* Specimens of *T. aithuia* have fewer testes than all species of the complex, except *T. jagerskioeldi* and *T. sinistralis*. A distinct gap in distribution of the testes, anterior to the vitelline gland and ovary, is observed in *T. aithuia*, *T. alcae*, and *T. sinistralis*, contrasting with a continuous field in *T. fraterculus* and *T. jagerskioeldi*.

Specimens of *T. aithuia* are immediately distinguished from all congeners in the complex and other species of *Tetrabothrius* by the structure of the genital atrium, genital papillae, and terminal ducts of the male and female systems (Table 1) (Hoberg and Soudachanh, 2020, 2021) (Figures 28–32, 43, 44). Prominent, paired, male genital papillae, viewed in whole mounts and in transverse sections, are diagnostic for *T. aithuia* (Baer, 1954; Temirova and Skrjabin, 1978). In the male system, a bulbous and apparently weakly bilobed papilla, in dorsoventral view, is formed by paired terminal papillae which are parallel and in apposition (single papilla = 20–30 in width); in antero-postero orientation as viewed in sections, the male papillae are asymmetrical (Figures 29, 30, 32, 44–47). The male canal is straight, with a subterminal opening, between the apices of these paired papillae; a curved male atrial canal distinguishes *T. alcae* and *T. sinistralis* from *T. aithuia.* The distal region of the female canal expands as a prominent ASR, passing through the atrial wall in a 90° turn, with the aperture opening directly to the atrial lumen, not immediately adjacent to and at the base of the male papillae. The expansion of the ASR in *T. aithuia* with a tubular connection to the elongate spindle-shaped VSR constitutes a unique bipartite configuration in the distal vagina which is prominently developed relative to congeners in the complex (Figures 30, 32, 41–43, 46). In contrast, paired male genital papillae, characteristic of *T. fraterculus*, are laterally divergent, massive in dorsoventral view (single papilla = 55–75 in width) and with symmetry in antero-postero orientation. The expansion of the ASR is less substantial in *T. fraterculus*, with the terminal female canal opening ventrally in the atrial lumen through the apex of a single, rounded, triangular papilla, and the apertures of the male and female ducts are distant, not adjacent; a female papilla is absent in *T. aithuia*, *T. jagerskioeldi*, *T. sinistralis*, and *T. alcae*. A sinuous course for the terminal female atrial canal is typical in specimens of *T. aithuia, T. fraterculus, T. alcae*, and *T. sinistralis*. Structurally the genital complex appears distinct among cestodes in Fraterculini versus those in Aethiini.

Tetrabothrius aithuia and *T. fraterculus* share a range of attributes, contrasting with other species in the complex (Table 1), including a scolex that is consistently longer than wide (Figures 27, 34–37) (smaller dimensions in *T. aithuia*), a straight male canal (also in *T. jagerskioeldi*; straight in *T. fraterculus* and deflected dorsally), position and structure of the VSR (relatively narrow in *T. aithuia*), and a mediad shift in the dorsal OSM (also in *T. alcae*) (Figures 28, 32, 44). These species differ in the placement of the center of the female organs [midline in *T. aithuia* (+ *T. jagerskioeldi* and *T. sinistralis*) (Figures 28, 38–40), antiporal of the midline with the center of the vitelline gland shifted under the anitporal wing of the ovary (*T. alcae* and *T. fraterculus*)], numbers of testes (40–74 in *T. aithuia*, 50–96 in *T. fraterculus*) and smaller dimensions of the globular vitelline gland in *T. aithuia*, in addition to the characters of the genital atrium previously outlined.

Specimens of *T. aithuia* are distinguished from those of *T. jagerskioeldi* s. str. based on the structure of the genital atrium, position of the testes, and attributes of the VSR (Table 1). A broad, triangular male genital papilla and dorsoventrally directed muscular bars in the atrium, typical of *T. jagerskioeldi*, are absent in *T. aithuia* (Hoberg and Soudachanh, 2020, 2021). A prominent gap in the distribution of the testes occurs anterior to the vitelline gland, extending over the poral wing of the ovary in *T. aithuia* (Figures 28 and 38) whereas the field of testes is continuous in *T. jagerskioeldi*. The VSR crosses between the poral OSM in both species but lacks a thickened epithelium and is substantially elongate and greater in overall dimensions in specimens of *T. aithuia* (Table 1).

Specimens of *T. aithuia* further differ from those of *T. alcae* in overall dimensions of the strobila (smaller); larger scolex with typical, flattened bothridia and auricles; position of the genital ducts between the OSM; substantially fewer testes; smaller cirrus sac and genital atrium at all stages of development; smaller compact vitelline gland

with single descending duct; and smaller spindle-shaped VSR (Table 1). The ventral OSM have multiple anastomoses in *T. aithuia* and *T. alcae*, contrasting with congeners in the complex. Relative to *T. sinistralis*, cestodes attributed to *T. aithuia* have a dextral genital pore in dorsal view of the strobila, smaller dimensions of the strobila in gravid specimens, paired genital papillae in apposition, a straight male genital canal, compact-globular vitelline gland on the midline, and a smaller VSR that crosses the poral OSM (Table 1) (Hoberg and Soudachanh, 2021).

Comparisons between *T. aithuia* and *T. erostris* reveal similarities and differences for multiple structural and meristic attributes (Baer, 1954; Temirova and Skrjabin, 1978; Ryzhikov et al., 1985). In contrast to *T. aithuia*, the scolex in *T. erostris* is consistently wider than long and of greater dimensions (260–490 long and 280–600 wide); there is a smaller genital atrium (140 × 120), vitelline gland (125–170 wide), and ISR (about 38 in diameter). The testes are fewer in number in *T. erostris* (37–40, maximum 50), although similar to *T. aithuia* these are in a discontinuous field anterior to the vitelline gland and ovary. The configuration of the genital atrium in *T. aithuia*, paired male papillae with apices bordering the subterminal aperture of the male canal differs from *T. erostris*. In the latter, there is a single, weakly developed, male genital papilla, the male canal is straight and the aperture of the female genital canal is basal and separate (according to Baer, 1954) or is adjacent to the orifice of the male canal (according to Temirova and Skrjabin, 1978).

Other Species of *Tetrabothrius* in the Alcid and North Pacific Fauna

Other species of *Tetrabothrius* occurred infrequently among alcids, including specimens attributed to *T.* cf. *cylindraceus* Rudolphi, 1819, *T.* cf. *erostris*, and *T.* cf. *morschtini* Murav'eva, 1968 (Tables 3 and 4; Supplementary Data Table 5; Figures 54–67). Specimens representing these taxa were observed in 10 hosts among 6 of 17 alcid species from 6 of 44 localities. Unidentifiable immature or incomplete fragmented tapeworms were collected overall in 26 of 1,347 alcids (2%) and 7 of 17 species from 11 of 44 localities where alcids were examined (see also Hoberg and Soudachanh, 2020) (Tables 3 and 4; Supplementary Data Table 3). Specimens of *T.* cf. *cylindraceus* were revealed in 1 adult *Uria aalge* from Grays Marine Canyon (field number 2447-3, -4) and in 1 *F. corniculata* from the pelagic zone of the southwestern Aleutians (898-1, 3–6). Specimens of *T.* cf. *erostris* occurred in 1 adult *F. corniculata* from Buldir Island (041A), 1 adult *F. cirrhata* from Kodiak Island (296), 1 adult *B. marmoratus* from Pt. Roberts (755), 1 adult and 1 subadult *C. monocerata* from Grays Marine Canyon (2516-2, -11, and 2457-3, -4), and 1 *P. aleuticus* from Grays Marine Canyon. Cestodes identified as *T.* cf. *morschtini* occurred in 1 young of the year, *U. aalge* from Humboldt Bay (1111).

Cestodes attributed to *T.* cf. *cylindraceus* and *T.* cf. *erostris* occurred in multiple alcid species and hosts spanning the North Pacific basin. Among 6 specimens attributed to *T.* cf. *erostris*, cestodes were characterized by a scolex 300–420 long × 470–450 wide, testes numbering 30–44 surrounding the female organs (mean = 36; n = 43, 6 strobilae, 4 hosts) and cirrus sac 53–75 in diameter (mean = 62; n = 23, 5 strobilae, 5 hosts) (Figures 54–60). Among 8 specimens attributed to *T.* cf. *cylindraceus*, tapeworms were characterized by a scolex 270–330 long × 220–270 wide, testes numbering 11–25 surrounding the female organs (mean = 18; n = 35, 8 strobilae, 2 hosts), and cirrus sac 50–75 in diameter (mean = 63; n = 18, 4 strobilae, 2 hosts) (Figures 61 and 62). Yamaguti (1935, 1940) outlined morphological characters defining *T. cylindraceus* and *T. erostris* based on specimens in a North Pacific larid (*Larus argentatus* Pontoppidan, 1763). In the former, the scolex was 260–400 wide, testes numbered 21–25 (exceptionally 19 or 27), and the cirrus sac was 42–66 in diameter; among specimens of the latter species, the scolex was 480–520 wide, testes numbered 27–34, and the cirrus sac was 75–100 in diameter. Baer (1954) redescribed *T. cylindraceus* with a scolex 400 long × 250–350 wide, testes 22 in number, and cirrus sac 45–65 in diameter and *T. erostris* with a scolex measuring 200–350 long × 250–450 wide, testes 35–50 in number, and cirrus sac 59–80 in diameter. Temirova and Skrjabin (1978) and Ryzhikov et al. (1985) reported similar attributes for *T. cylindraceus* with a scolex 250–340 long × 240–340 wide, 19–27 testes, and cirrus sac 43–56 in diameter, and for *T. erostris*, a scolex 260–490 long × 280–600 wide, testes 37–50, and cirrus sac 80–106 in diameter.

Specimens of *Tetrabothrius* cf. *morschtini*, numbering 14 cestodes, were collected in a single *U. aalge* from Humboldt Bay, CA. These cestodes were characterized by a scolex 450–460 long × 630–670 wide; testes 24–38 in number, surrounding the female organs (mean = 29; n = 9, 2 strobilae); cirrus sac 63–98 in diameter (mean = 73; n = 12, 2 strobilae); and strongly decurved male genital papilla (Figures 63–67). Murav'eva (1968) provided the original description for cestodes attributed to *T. morschtini* in a glaucous gull, *Larus hyperboreus* Gunnerus, 1767, from the Kanin Peninsula, White Sea, Russia. Among 4 specimens in the type series, the scolex measured 500–780 long × 580–840 wide; testes were 32–34 in number; with cirrus sac 75–93 in diameter; and a muscular, decurved male genital papilla. This tetrabothriid has apparently not been reported since the original description (Ryzhikov et al., 1985). Our

Table 3. Diversity and Specimens for Species of *Tetrabothrius* among Alcid Hosts in the North Pacific Inventory and from Other High Latitude Sites

Species[1,2]	Locality[1,2]	Number[1,2]	Archived
Tetrabothrius cf. *cylindraceus*			
Fratercula corniculata	SW Aleutian Pelagic	1	X
Uria aalge	Grays Marine Canyon	1	X
Other Oceanographic Localities/Absence of Vouchers			
Uria aalge	Northwestern North Atlantic (Threlfall, 1971)		
Uria lomvia	Greenland (Ditlevsen, 1914)		
Tetrabothrius cf. *erostris*			
Brachyramphus marmoratus	Pt. Roberts, WA	1	X
Cerorhinca monocerata	Grays Marine Canyon	2	X
Fratercula cirrhata	Kodiak Island	1	X
Fratercula corniculata	Buldir Island	1	X
	SW Aleutian Pelagic	1	X
Ptychoramphus aleuticus	Grays Marine Canyon	1	—
Other Oceanographic Localities			
Alca torda	West Greenland (Baer, 1956) (Hoberg and Soudachanh, 2020, redetermination)		
Uria aalge	Cardiganshire, Wales (Hoberg and Soudachanh, 2020, redetermination)		
	Concarneau, France (Hoberg and Soudachanh, 2020, redetermination)		
	North Sea, Netherlands (Hoberg and Soudachanh, 2020, redetermination)		
Other Oceanographic Localities/Absence of Vouchers			
Uria aalge	Northwestern North Atlantic (Threlfall, 1971)		
Cepphus grylle	Greenland (Ditlevsen, 1914)		
Tetrabothrius macrocephalus			
Absence of Vouchers			
Brachyramphus marmoratus	Sakhalin Island, Western Pacific (Krotov and Deliamure, 1952)		
Tetrabothrius cf. *morschtini*			
Uria aalge	Humboldt Bay	1	X
Tetrabothrius sp.[3]			
Synthliboramphus scrippsi	Santa Barbara Island	1	X
Tetrabothrius sp./fragments, unidentified			
Aethia cristatella	Talan Island	1	—
Cepphus carbo	Khmotiyevskogo Peninsula	1	—
Fratercula cirrhata	Kodiak Island	3	X
	SW Aleutian Pelagic	5	X
	Sitkalidak Island	1	—
Fratercula corniculata	Buldir Island	1	—
	Kodiak Island	1	—
	SW Aleutian Pelagic	2	X
	Ugaiushak Island	1	—
Ptychoramphus aleuticus	Grays Marine Canyon	1	—
Uria aalge	Cape Thompson	1	—
	Grays Marine Canyon	1	X
	Humboldt Bay	1	X
	Kodiak Island	5	X
Other Oceanographic Localities/Absence of Vouchers			
Uria aalge	Northwestern North Atlantic (Threlfall, 1971)		
Uria lomvia	Northwestern North Atlantic (Muzzafar, 2009)		

Notes:

[1] See Supplementary Data Tables 2, 3, and 5. Species of *Tetrabothrius* and alcid hosts; general locality; number of hosts.

[2] Hoberg and Soudachanh (2020, 2021).

[3] Immature early strobilate specimens, putative undescribed species not associated with *T. jagerskioeldi*–complex (Hoberg and Soudachanh, 2000, 2001).

Table 4. Mixed Species Infections in Single Hosts

Western Aleutian pelagic zone
Cerorhinca monocerata subadult / 2 spp.
T. jagerskioeldi s. str. (1142-1)[1]; *T. fraterculus* (1142-2, 1142-3)
Fratercula corniculata adult / 2 spp.
T. cf. *cylindraceus* (898-1, 898-3 to 898-6); *T.* cf. *erostris* (898-2)
Kodiak Island, Chiniak Bay
Fratercula cirrhata adult / 2 spp.
T. cf. *erostris* (296); *Tetrabothrius* spp., unidentified (296-A, 296-B, 296-C)
Grays Marine Canyon
Uria aalge subadult / 2 spp.
T. alcae (2440-1–4, 6–7); *Tetrabothrius* spp. unidentified (2440-5)
Uria aalge adult / 2 spp.
T. alcae (2447-2, 5–7); *T.* cf. *cylindraceus* (2447-3, 2447-4, 2447)
Cerorhinca monocerata subadult / 2 spp.
T. fraterculus (2457-2, 5, 6); *T.* cf. *erostris* (2457-3, 2457-4)
Cerorhinca monocerata adult / 3 spp.
T. fraterculus (2516-1, 3, 5–10); *T. aithuia* (2516-4); *T.* cf. *erostris* (2516-2, 2516-11)

Note:
[1]Specimen field collection number. See Supplementary Data Tables 2, 3, 4, and 5; Hoberg and Soudachanh (2020, 2021).

specimens from the eastern North Pacific may constitute the first reported record outside of the Arctic Basin and in an alcid host.

Although North Pacific specimens are referred to these nominal species of *Tetrabothrius*, the range of diagnostic attributes for respective taxa are not entirely consistent relative to historical reports and most of these cestodes were in less than optimum condition. For example, variation in the numbers of testes for specimens of *T.* cf. *cylindraceus*, with a minimum of 11 in some strobila, has not been observed previously and may indicate the occurrence of a currently unrecognized species. We noted additional unidentified *Tetrabothrius*, fragments of mature and early mature cestode strobilae (not included with *T.* cf. *cylindraceus*), with 10–12 testes in adult *F. cirrhata* from Kodiak Island (No. 361-A) and from pelagic waters south of the Aleutian Islands (No. 1047) (Supplementary Data Table 5). Among congeners in avian hosts, only two nominal species, *T. filiformis* Nybelin, 1916 [in *Procellaria aequinoctialis* Linnaeus, 1758 from the Southern Ocean and *Ardenna gravis* (O'Reilly, 1818) from the Atlantic basin] and *T. minor* Loennberg,1893 [among procellariiforms including *Fulmarus glacialis* (Linnaeus, 1761) at high latitudes of the northern hemisphere and *Oceanodroma furcatus* (Gmelin, 1789) from the North Pacific basin, along with *Phoebastria irrorata* (Salvin, 1883) and *Thalassoica antarctica* (Gmelin, 1789) from the southern hemisphere] have been described with testes in the range of 9–12 (Temirova and Skrjabin, 1978; Hoberg and Ryan, 1989). Both of these species in procellariiforms are otherwise morphologically inconsistent with the specimens in alcids (Baer, 1954; Temirova and Skrjabin, 1978). Additionally, discordance in the dimensions of the cirrus sac in our specimens of *T.* cf. *cylindraceus* and *T.* cf. *erostris* with those redescribed in the literature may reflect variation in measurements across ontogenetic stages. The structure of the genital atrium, papillae, and ducts in transverse sections and anterior-posterior orientation could not be assessed in our North Pacific specimens.

Mixed Species Infections among Alcid Hosts

Multiple species of *Tetrabothrius* were infrequently observed in single hosts, involving 7 records for infections among alcids, in the North Pacific inventory (Table 4). Mixed species infections, irrespective of host age or breeding status, were documented in puffins, 3 of 39 *C. monocerata* (8%), 1 of 149 *F. corniculata* (< 1%), 1 of 286 *F. cirrhata* (< 1%), and murres 2 of 276 *U. aalge* (< 1%). Although rare, instances of these multispecies infections were most often observed from oceanic transition zones over Grays Marine Canyon from the Eastern Pacific and from pelagic waters south of the western Aleutian Islands (Supplementary Data

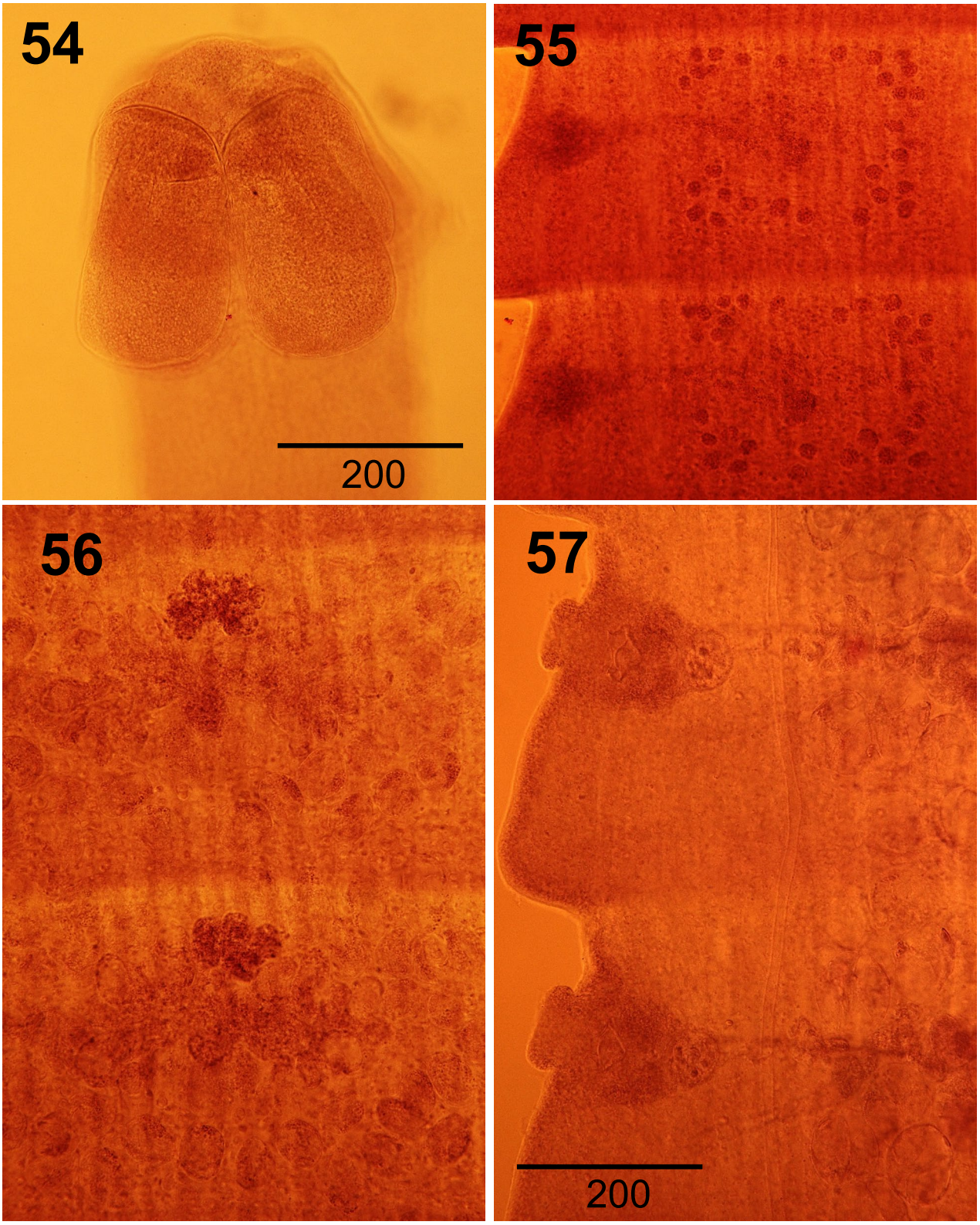

Figures 54–57. *Tetrabothrius* cf. *erostris* from voucher specimen 041A in *Fratercula corniculata* from Buldir Island (scale bars in micrometers; same scale throughout). **Fig. 54.** Scolex in dorsoventral view. **Fig. 55.** Proglottid, ventral view in early maturity, showing distribution and numbers of testes. **Fig. 56.** Proglottid, ventral view in maturity, showing globular vitelline gland, lobate ovary, surrounded by testicular fields. **Fig. 57.** Proglottid, ventral view in maturity, showing position of genital pore and atrium, ovoid cirrus sac, and narrow transverse uterine stem.

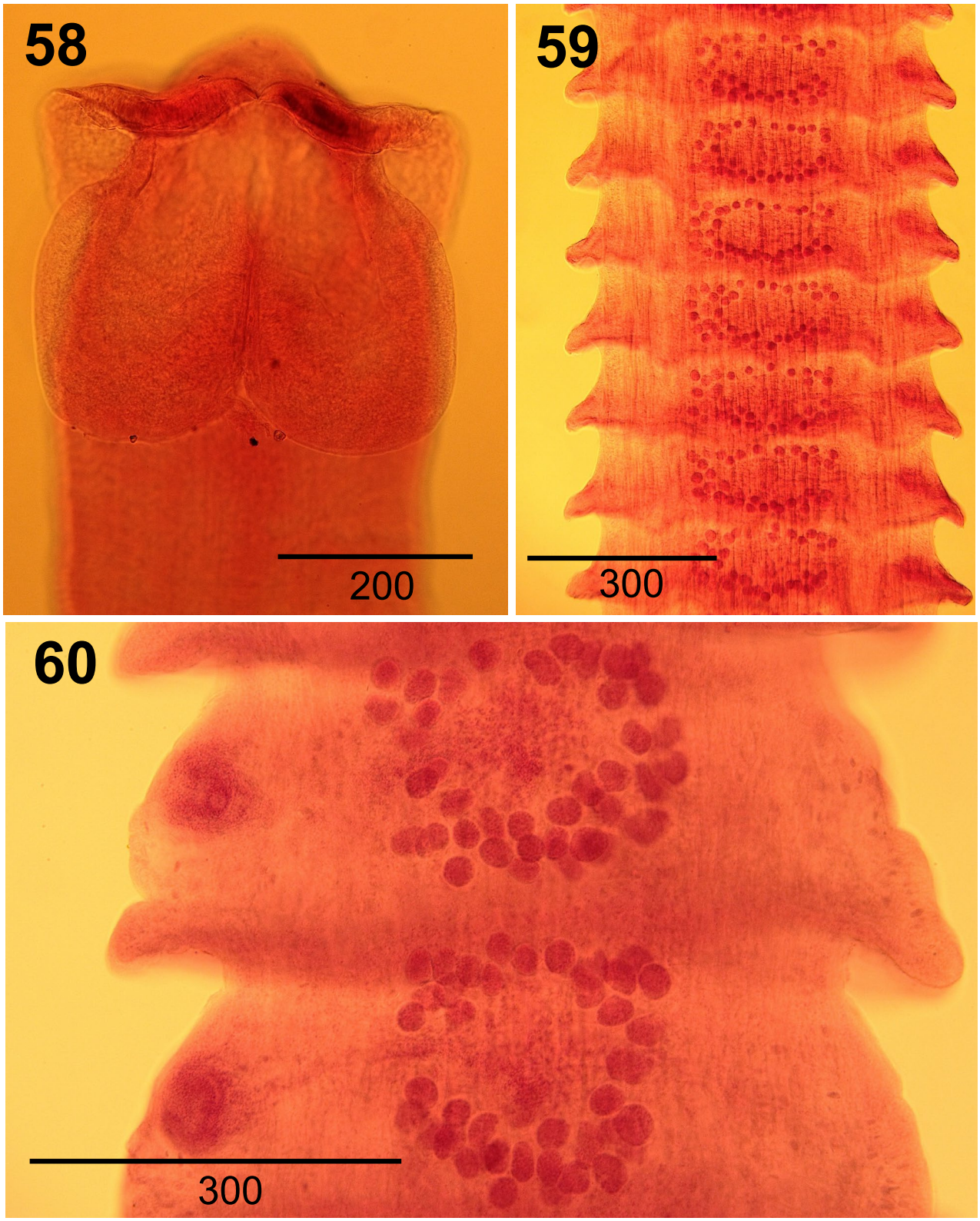

Figures 58–60. *Tetrabothrius* cf. *erostris* from voucher specimens 2457-3 in *Cerorhinca monocerata* from Grays Marine Canyon and 898-2 in *Fratercula corniculata* from pelagic waters south of Western Aleutian Islands (scale bars in micrometers). **Fig. 58.** Scolex in dorsoventral view from 2457-3. **Fig. 59.** Strobila, showing early mature proglottids in dorsal view and distribution of testes in 2457-3. **Fig. 60.** Proglottids in ventral view, early maturity, showing position of genital pore, genital atrium and distribution of testes surrounding female organs in 898-2.

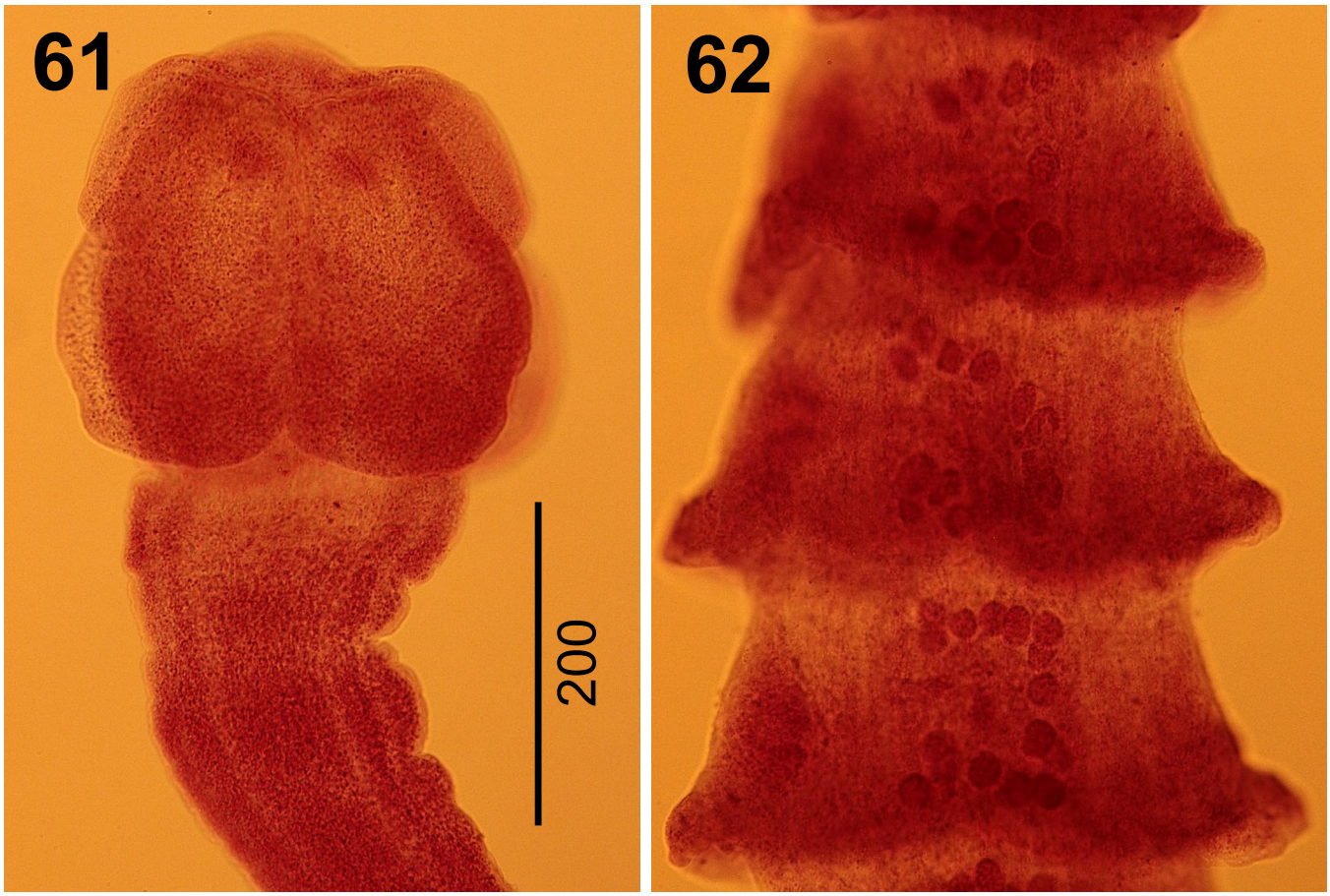

Figures 61–62. *Tetrabothrius* cf. *cylindraceus* from voucher specimens 898 in *Fratercula corniculata* from pelagic waters south of the western Aleutian Islands (scale bars in micrometers; same scale throughout). **Fig. 61.** Scolex in dorsoventral view in 898-5. **Fig. 62.** Proglottids in ventral view in early maturity showing distribution of testes in 898-4.

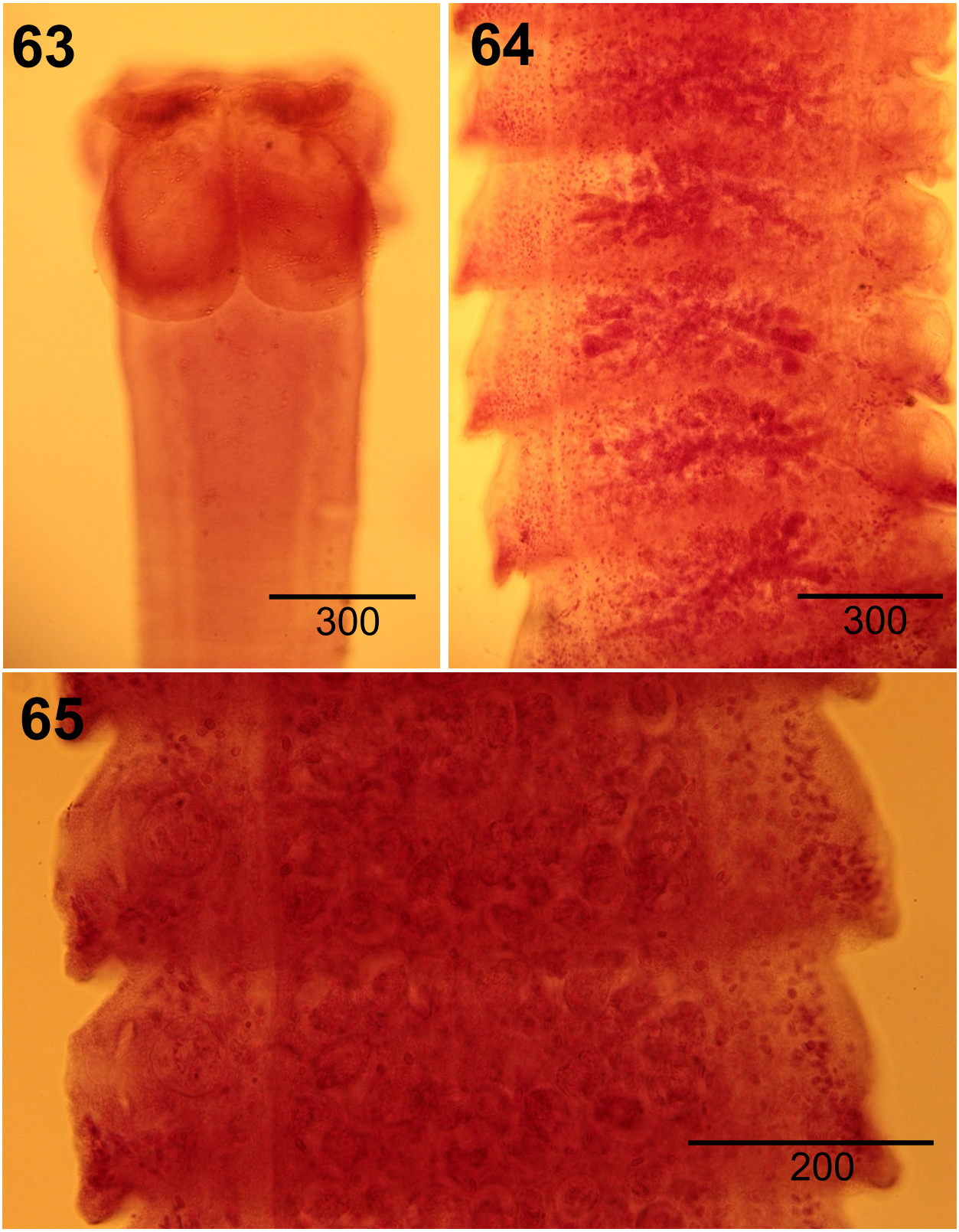

Figures 63–65. *Tetrabothrius* cf. *morschtini* from voucher specimens 1111 in *Uria aalge* from Humboldt Bay, California (scale bars in micrometers). **Fig. 63.** Scolex in dorsoventral view in 1111-1. **Fig. 64.** Strobila showing late mature proglottids in dorsal view in 1111-1. **Fig. 65.** Proglottids in ventral view in maturity showing structure of genital atrium, ovoid cirrus sac, distribution of testes and female genital organs in 1111-2.

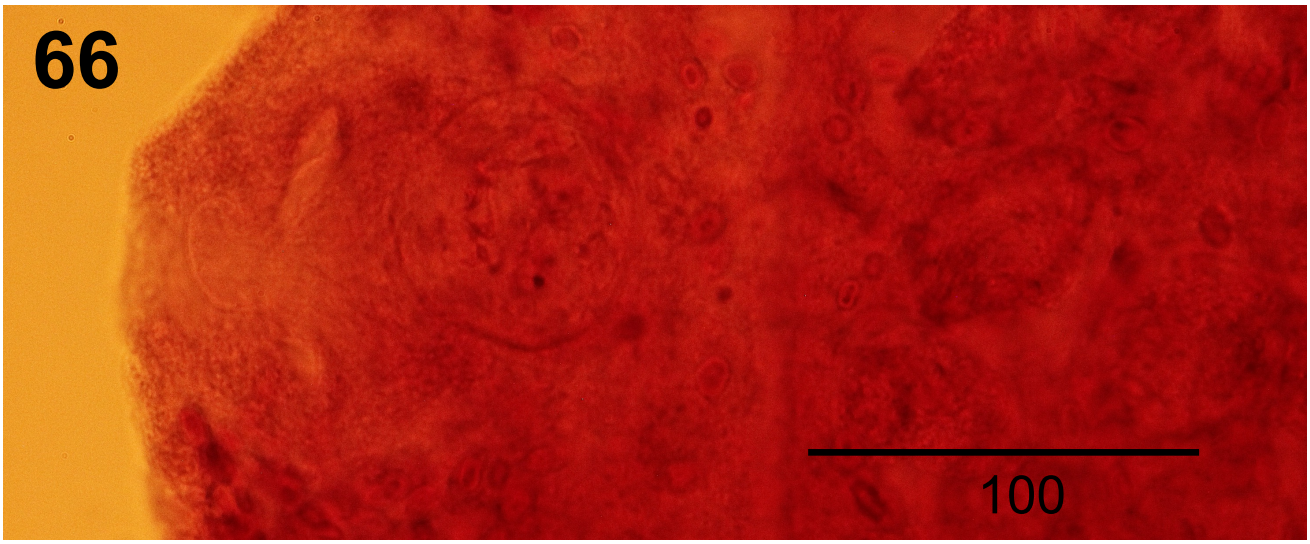

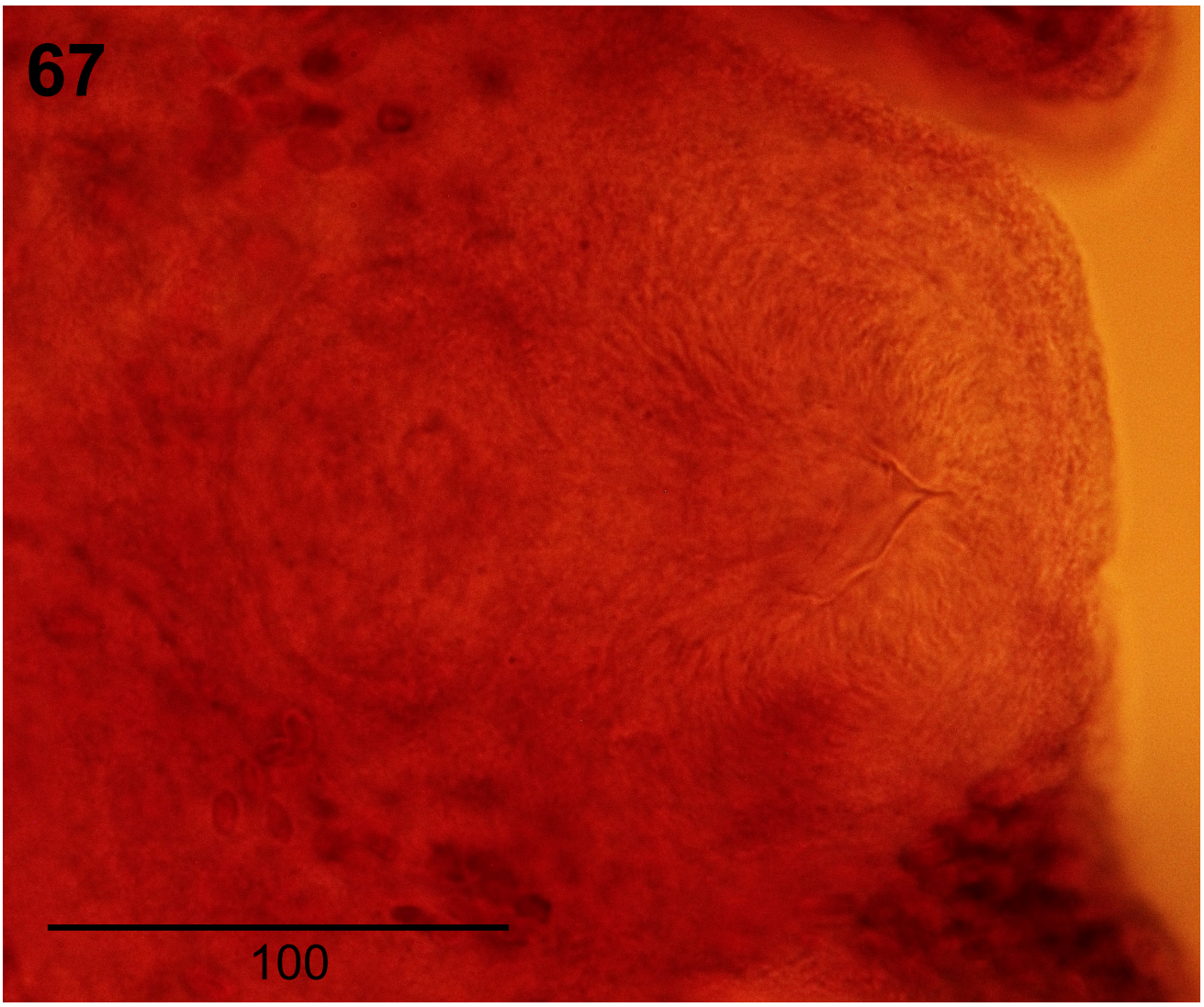

Figures 66–67. *Tetrabothrius* cf. *morschtini* from voucher specimens 1111 in *Uria aalge* from Humboldt Bay, California (scale bars in micrometers). **Fig. 66.** Genital atrium and cirrus sac in maturity in ventral view in 1111-2. **Fig. 67.** Genital atrium and cirrus sac in late maturity in dorsal view in 1111-1.

Tables 3, 4, 5). Overall, extensive sympatry across localities and oceanographic domains spanning the greater North Pacific basin, including the Bering Sea and Sea of Okhotsk, is evident for 4 of 5 widespread species in the *T. jagerskioeldi*–complex (Figures 68 and 69). Further, abundant tetrabothriid faunas, multispecies assemblages primarily circulating among larids or procellariiforms, which are broadly synchronic and sympatric but ecologically segregated, remain largely distinct from that observed among the alcids (Hoberg and Soudachanh, 2021) (Supplementary Data Table 3).

Discussion

Resolving the Species Complex

Resolution of the *T. jagerskioeldi*–complex, with inclusion of *T. fraterculus* n. sp. and *T. aithuia* n. sp., contributes to recognition of 46 nominal species of *Tetrabothrius* among marine avian hosts (Mariaxux et al., 2017; Hoberg and Soudachanh, 2020, 2021). Cryptic diversity revealed within *T. jagerskioeldi* sensu lato may be an exception, or is representative of the potential for considerable species richness effectively hiding within a component of the 56 nominal congeneric taxa referred to *Tetrabothrius* among marine homeotherms (Hoberg et al., 2015; Mariaux et al., 2017). The need for synoptic revision among the tetrabothriids has been apparent for more than 40 years (Temirova and Skrjabin, 1978; Mariaux et al., 2017), a process that can be achieved only through targeted collections and accumulation of archival specimens from avian and mammalian hosts across global oceanic systems (Hoberg, 1996; Hoberg and Soudachanh, 2020, 2021; Hoberg et al., 2022). Increasing logistical challenges for large-scale collections in marine environments suggests an understanding and documentation of the limits and extent of historical diversity in ecological time may no longer be achievable.

Cestodes we attribute to the complex are superficially similar, for example, with relatively large, robust, strobilae and wide terminal proglottids. Historically, over a century, absence of voucher specimens, uncritical redescriptions, and perpetuation of largely unverified records of occurrence became the source of confusion for a speciose complex of cestodes attributed to a single taxon (e.g., Baer, 1954; Temirova and Skrjabin, 1978; Muzzafar and Jones, 2004). Detailed comparative morphology, however, provides a window on species differentiation, and the structural limits defined in the case of the *T. jagerskioeldi*–complex appear unequivocal (e.g., Hoberg and Soudachanh, 2020, 2021). Anatomical attributes revealed among morphospecies remain a gateway and backdrop for broadening recognition and characterization of cryptic diversity. Revision with the possibility of integrated genomic, sequence-based, and morphological comparisons from single specimens (e.g., Makarikov et al., 2013; Haukisalmi et al., 2014; Haas et al., 2020; Galbreath et al., 2023) would be expected to provide insights about the extent and limits for generic and species diversity among tetrabothriids.

Archival specimens assembled from the North Pacific inventory and a limited number of cestodes in global collections served as a basis for characterization of the 5 species in the complex, although none were amenable to explorations of molecular and genetic diversity. Overlapping variation for some meristic characters is apparent within the assemblage with mean values that are often distinct (e.g., testes number, dimensions of cirrus sac, genital atrium, vitelline gland, vaginal seminal receptacle; Table 1). Structural attributes are diagnostic providing clear morphological partitions defining limits for the 5 species in the *T. jagerskioeldi*–complex and among the diverse assemblage of congeners in marine avian hosts (Table 1) (Hoberg and Soudachanh, 2020, 2021). The configuration of the genital atrium and genital papillae (both male and female), atrial and vaginal seminal receptacle, position of the female organs within the proglottid, structure of the vitelline gland, distribution of the testes and position of the uterus and genital ducts are fundamental in discrimination. Assessment of attributes revealed in transverse sections remain essential, consistent with a century of comparative morphology within the Tetrabothriidae (e.g., Nybelin, 1916; Baer, 1954; Temirova and Skrjabin, 1978; Hoberg, 1994).

Other species we tentatively document in alcids, *T.* c.f. *cylindraceus*, *T.* c.f. *erostris* and *T.* c.f. *morschtini*, from the North Pacific inventory were not entirely consistent morphologically with published descriptions and redescriptions (Figures 54–67). Apparently discordant meristic data may be attributed to stages of development in early mature and mature strobilae, or possibly to polymorphism associated with these hosts. Ontogenetic progression, reflected in differentiation in the male and female genital systems, may lead to measurements that are not from developmentally comparable regions of strobila as reported in different published re-descriptions; meristic data attributed to particular species of tetrabothriids generally do not specify the relative age of the strobila nor the position and number of proglottids which have been examined. Equivocal taxonomic resolution among this limited series of specimens highlights the necessity for a standardized series of observations which document the range of morphological variation to establish a comparative basis for discrimination among species assemblages in sympatry.

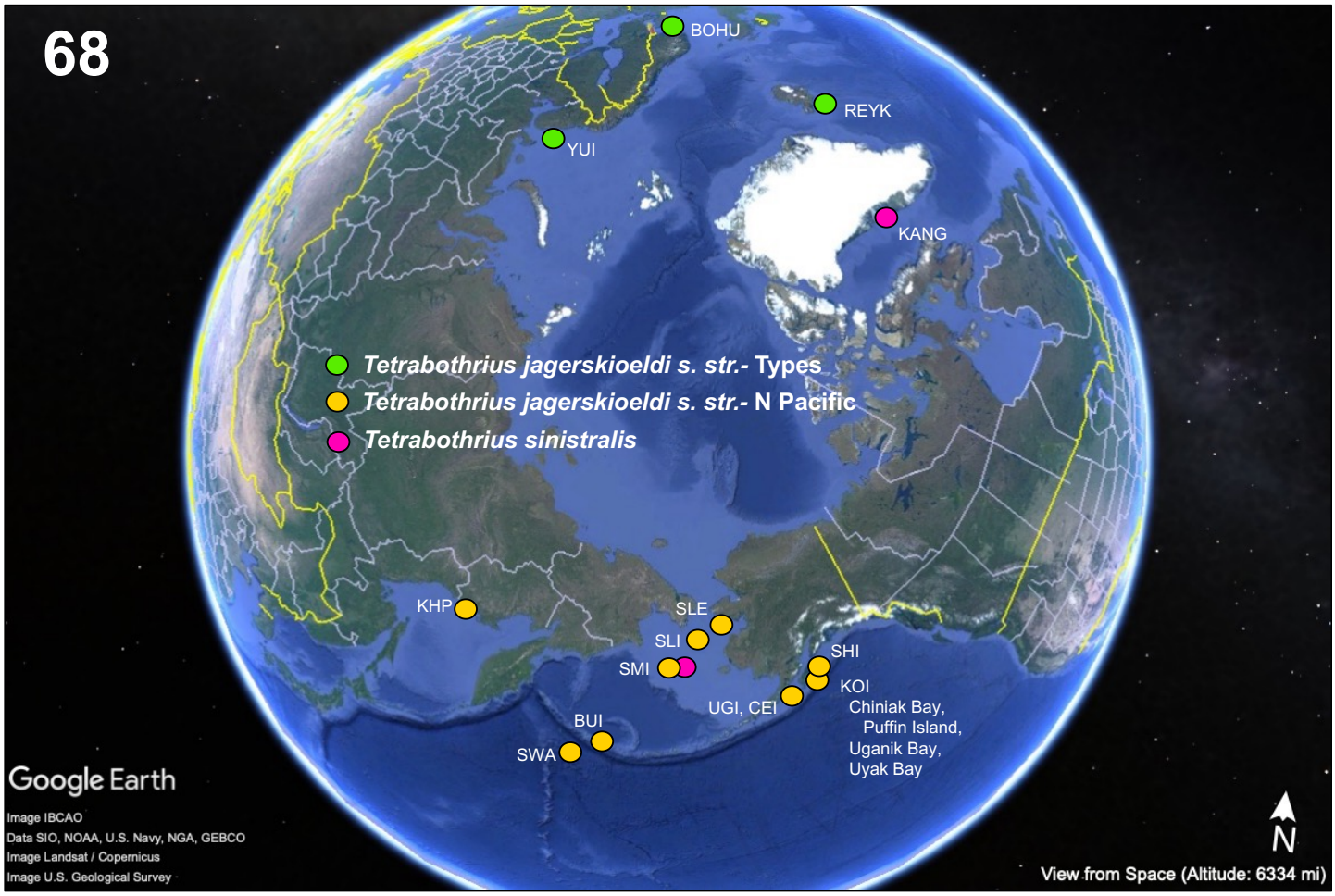

Figure 68. The circumpolar region depicting the localities of occurrence and Holarctic ranges, based on specimens, of *Tetrabothrius jagerskioeldi* s. str. and *T. sinistralis*. Shown are distributions for cestodes primarily among species of guillemots (Hoberg and Soudachanh, 2020, 2021). Specimens of the type series and other validated specimens of *T. jagerskioeldi* are known in black guillemots at Bohuslän, Kristineberg, Sweden (Type) and Väderöarna (Weather Islands Archipelago) = BOHU. Types for *T. intrepidus*, a junior synonym, are known in black guillemots from the Yukanski Islands, Barents Sea = YUI (Baylis, 1919); later voucher specimens in this guillemot are known from Reykjavik, Iceland = REYK (Hoberg and Soudachanh, 2020). Across high latitudes of the North Pacific basin, *T. jagerskioeldi* s. str. is documented among species of *Cepphus*, including spectacled guillemot from the Khmotiyevskogo Peninsula, Russia = KHP; pigeon guillemot from St. Matthew Island = SMI, Sledge Island = SLE, Ugaiushak Island = UGI, Uyak Bay and Uganik Bay, Kodiak Island = KOI; and pigeon and black guillemot from St. Lawrence Island = SLI. Among other alcids, records also encompass specimens in marbled murrelet from Chiniak Bay, Kodiak Island = KOI, in common murre from Shuyak Island = SHI, and rhinoceros auklet from the pelagic zone of the southwestern Aleutian Islands = SWA. Validated host species among other seabird groups include the pelagic shag from Buldir Island = BUI and glaucous-winged gulls from Central Island = CEI and Puffin Island = PUI. Holarctic ranges, derived from records linked to archived specimens, are currently demonstrated for *T. jagerskioeldi* s. str. and *T. sinistralis* but not among other species of the complex (Hoberg and Soudachanh, 2020, 2021). Also, among guillemots, *T. sinistralis* is known in pigeon guillemot from St. Matthew Island, Bering Sea, and in black guillemot from Kangerluk, Greenland = KANG.

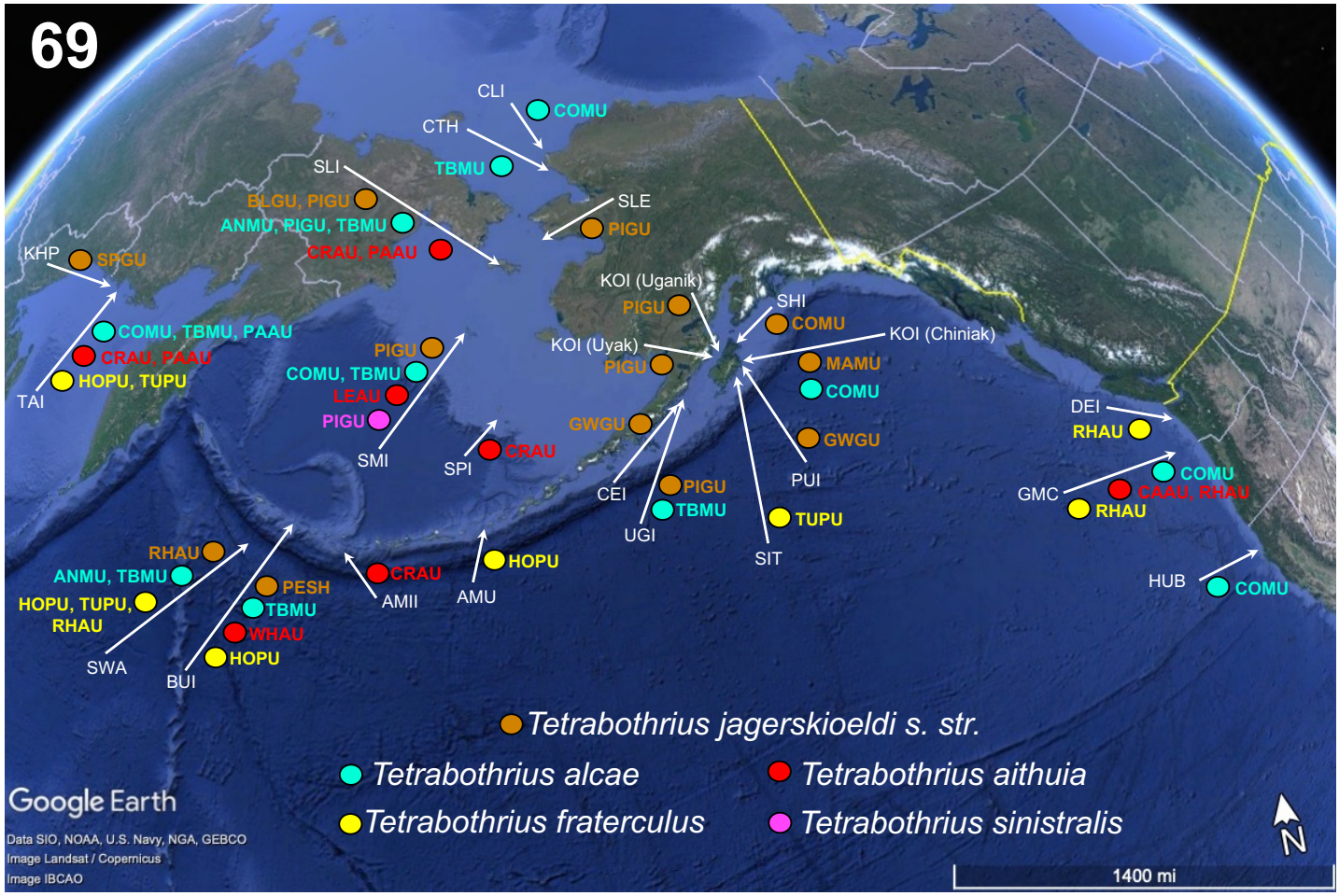

Figure 69. Localities of occurrence for species of the *Tetrabothrius jagerskioeldi*–complex among an assemblage of known seabird hosts from the greater North Pacific basin. Shown are the distributions for *T. jagerskioeldi* s. str., *T. alcae*, *T. aithuia*, *T. sinistralis*, and *T. fraterculus* based on specimens from the North Pacific inventory. Localities spanning the North Pacific, from west to east, are denoted (*in white*) as follows: Okhotsk Sea–KHP = Khmotiyevskogo Peninsula, Russia; TAI = Talan Island, Russia; Aleutian Islands–SWA = southwestern Aleutians, pelagic zone; BUI = Buldir Island; AMI = Amchitka Island; AMU = Amukta Island; Bering Sea and Chukchi Sea–SPI = St. Paul Island; SMI = St. Matthew Island; SLI = St. Lawrence Island; CLI = Cape Lisburne; CTH = Cape Thompson; SLE = Sledge Island; Gulf of Alaska–CEI = Central Island; UGI = Ugaiushak Island; KOI (Uyak) = Kodiak Island, Uyak Bay; KOI (Uganik) = Kodiak Island, Uganik Bay; KOI (Chiniak) = Kodiak Island, Chiniak Bay; SHI = Shuyak Island; PUI = Puffin Island; SIT = Sitkalidak Island; Eastern Pacific–DEI = Destruction Island; GMC = Grays Marine Canyon; HUB = Humboldt Bay. Host species are denoted by their four-letter acronyms and color-coded relative to respective species of cestodes within the complex: ANMU = ancient murrelet; BLGU = black guillemot; CAAU = Cassin's auklet; COMU = common murre; CRAU = crested auklet; GWGU = glaucous-winged gull; horned puffin = HOPU; least auklet = LEAU; marbled murrelet = MAMU; parakeet auklet = PAAU; pelagic shag = PESH; pigeon guillemot = PIGU; rhinoceros auklet= RHAU; spectacled guillemot (SPGU); thick-billed murre = TBMU; tufted puffin = TUPU; whiskered auklet = WHAU. Note the extensive geographic/oceanographic distributions for all cestode species of the complex except *T. sinistralis*. Complete georeferenced locality, host data, and prevalence of infections are summarized in Table 2, Supplementary Data Tables 1–3, and Hoberg and Soudachanh (2020, 2021). These supplementary summary tables reflect the broader context (presence and absence) for host and geographic distribution for species of the *T. jagerskioeldi*–complex relative to a diverse assemblage of marine avian species examined (Hoberg and Soudachanh, 2021).

Ghosts of Cospeciation and Host Specificity

Distribution for species of *Tetrabothrius* among alcid seabirds reflects ecological rather than phylogenetic limits on host range, emphasizing complex interactions that include oceanographic and trophic (foodweb) drivers with apparently minimal coevolutionary context, consistent with complexity in faunal assembly and dynamics under the Stockholm Paradigm (SP) (Brooks et al., 2019, 2023; Hoberg and Soudachanh, 2021; Agosta, 2022). Concerning avian cestodes, Fuhrmann (1908, 1932), based in part on Krabbe (1869), had proposed the idea of strict coevolutionary associations (what would be regarded in a contemporary sense as phylogenetic association by descent, represented by congruence in tree topology) to explain the distribution and evolution of assemblages of avian parasites (what became Fuhrmann's Law and Fahrenholz's Rule) (also see Gustafsson and Najer, 2022). A linkage of strict cospeciation and specificity had origins in the observations of parasite and host distributions and the idea that cestode species were historically bound to particular avian groups by association through evolutionary descent. Under these constraints, events of colonization were not possible nor were seldom recognized but secondarily (when observed) became explained as incidental aberrations or occurrences attributed to accidental or remarkable infection. By the 1950s, phylogenetic branching patterns were explicitly discussed across many assemblages of parasites and hosts, including tetrabothriids, and a continuum from higher taxa to species relationships (e.g., Baer, 1954; Mayr, 1957; Szidat,1964). Only later in 1979 was a robust methodology available to develop insights about parasite phylogeny (Hennig, 1966; Brooks, 1979). Subsequently, explicit and direct comparisons became possible for exploring tree topology, evolutionary connectivity, and biogeography among assemblages of parasites and hosts (Brooks, 1981; reviewed in Brooks and McLennan, 2002; Brooks et al., 2019; Trivellone and Pannasiti, 2022).

Terminology for "cospeciation" was originally proposed by Brooks (1979, 1981), leading to expansion of essential comparative (tree-based) methods in coevolution, biogeography, and historical ecology (see historical summaries in Brooks, 1985; Brooks and McLennan, 1993, 2002; Hoberg and Klassen, 2002; Hoberg and Brooks, 2008; Brooks et al., 2019). By the middle 1980s, substantial empirical and phylogenetic evidence was accumulating, which was sufficient to reject a history of strict cospeciation in diversification and to decouple the expectation of host specificity from cospeciation (e.g., Hoberg, 1986, 1992). Relative simplicity and constraints posed by formal assumptions of cospeciation (e.g., summarized in Paterson and Banks, 2001; Page, 2003) were increasingly replaced with a picture of complexity in descriptions of the biosphere (Brooks and McLennan, 2002; Brooks et al., 2015, 2019; Hoberg and Brooks, 2008, 2010; Agosta et al., 2010; Nylin et al., 2018; Trivellone and Panassiti, 2022).

A view of complexity and a rejection of pervasive coevolutionary histories was summarized by Mikhail Yakovlevich Ass (1939) in what appears to have been the first critical exploration of Fuhrmann's Law. Ass had substantial insights (across animal and plant associations)—and like other Russian works, this early synthesis seems to have remained hidden in obscurity. Ass concluded that cospeciation was not a generality and served as a limited, incomplete, and flawed foundation in understanding the nuanced and complex association of parasite evolution, host range, and faunal assembly (see Trivellone, 2022; Trivellone and Panassiti, 2022). Complexity is in accordance with what we now consider to represent the origin and assembly of diversity as outlined in the SP and the current models of colonization (e.g., Hoberg and Brooks, 2008, 2010; Agosta et al., 2010; Araujo et al., 2015; Braga et al. 2018; Nylin et al., 2018; Brooks et al., 2019, 2023). Despite contrary empirical evidence, the cospeciation school came to dominate thinking in parasitology for most of the last century (some of this history is outlined in Hoberg and Brooks, 2008; Brooks et al., 2019; Gustafsson and Najer, 2022; Trviellone, 2022; Trivellone and Panassiti, 2022). It appears that the synthesis developed by Ass, although lacking a clear and robust phylogenetic context, was an initial commentary refuting the generality of cospeciation processes, discarding the original historical paradigm for a more powerful and complete picture of complexity in the biosphere.

Elsewhere (Brooks et al., 2023), we have discarded the terminology for host specificity, replacing this conceptually with "host range" established in the context of fundamental and realized fitness space, sloppy fitness space, and ecological fitting with opportunity and capacity (compatibility) as determinants of host associations (Agosta et al., 2010; Brooks et al., 2019; Agosta, 2022). As Brooks et al. (2023) have noted with respect to colonization and faunal assembly for emergent pathogens, establishing a broader generality for parasite-host assemblages—"Host fitness space has been traditionally called *host specificity*. Fundamental host fitness space is a matter of the phylogenetic distribution of the essential resources needed for the pathogen to survive at least minimally. Realized host fitness space is a matter of how much of the fundamental host fitness space is accessible to the pathogen at any given place and time. The SP therefore predicts that both realized and fundamental host fitness space will be variable (see Matthews et al., 2023, for an excellent recent example). Traditional views of pathogen-host associations assume that there is a tight fit between fundamental and realized host fitness space,

thus the cospeciation-based concept of host specificity. As noted, the SP assumes that fundamental host fitness space is more extensive than realized host fitness space, the difference being a manifestation of how "sloppy" the host fitness space is and, therefore, what potential there might be for host range expansion, given the opportunity" (Agosta, 2022). These insights provide an explanation for the structure of marine tapeworm faunas and more generally diverse assemblages in evolutionary and ecological time involving the complex connectivity for parasites and hosts under oscillating climate and environmental change (e.g., Hoberg et al., 2017; Brooks et al., 2019, 2023; Hoberg and Soudachanh, 2021).

Tetrabothrius *diversity in avian hosts*

Among the Alcidae, 21 of 25 recently extant species have been examined from localities across Holarctic seas (Table 2). In the greater North Pacific basin 16 host species for *Tetrabothrius* spp. (among 21 alcid species considered endemic in the region) are recognized. Species attributed to the *T. jagerskioeldi*–complex are distributed minimally among 15 species of Alcidae based on archived specimens (Table 2); unrelated to the complex, an undescribed species of *Tetrabothrius* may occur in *S. scrippsi* (Hoberg and Soudachanh, 2020, 2021). Occurrence of *Tetrabothrius* or other cestodes has not been evaluated in species of *Synthliboramphus* (*S. craveri*, *S. hypoleucus*, and *S. wumizuzume*) and *Brachyramphus* (*B. perdix*) from the North Pacific.

Unsubstantiated records, originally designated as *T. jagerskioeldi* s. lato in the absence of voucher specimens, may include species of *Tetrabothrius* now attributable to the complex, potentially expanding the number of known hosts to 18 species of alcids (with *Alca torda*, *Alle alle*, and *Fratercula arctica* from the North Atlantic and Arctic Basin). Included are reports in the literature known from 10 putative host species across the Holarctic—razorbill, dovekie, common and thick-billed murres, black and spectacled guillemots, ancient murrelet, Atlantic puffin, tufted puffin, and rhinoceros auklet (summarized in Muzzafar and Jones, 2004; Hoberg and Soudachanh, 2020) (Table 2). Label identifications of *T. jagerskioeldi* s. lato and other congeners for a limited series of specimens in alcid hosts held in various museum archives have either been confirmed (as *T. jagerskioeldi* s. str.) or redetermined as *T. erostris* (Hoberg and Soudachanh, 2020, 2021) (Table 3). Previously we incorrectly reported *C. grylle* as a host for *T. erostris* based on redetermination of specimens collected and originally identified as *T. jagerskioeldi* by Baer (1956) from West Greenland; the correct host attribution is *Alca torda* for these specimens of *T. erostris* (see Hoberg and Soudachanh, 2020). Concurrently, other specimens designated as *T. jagerskioeldi* by Baer (1956) in black guillemot from West Greenland were also redetermined and attributed to the type series for *T. sinistralis* (see Hoberg and Soudachanh, 2021).

Limits for cestode diversity among alcids (and other seabirds) are confounded by ambiguity in the actual identity and distribution of *T. jagerskioeldi* s. str. and any of 4 nominal species in the complex associated with oceanographic or insular localities from the Russian Far East (Belopol'skaia, 1963a, 1963b; Temirova and Skrjabin, 1978; Smetanina, 1979, 1981; Smetanina and Leonov, 1984), Barents Sea (Belopol'skaia, 1952; Kuklin and Kuklina, 2005), western North Atlantic (Threlfall, 1971; Muzzafar, 2009), and Greenland (Baer, 1956). Putative reports of *T. jagerskioeldi* s. lato in *Stercorarius parasiticus* from the Barents Sea and from Chukotka (Belopol'skaia, 1952; Temirova and Skrjabin, 1978) cannot be substantiated. Although, if attributed to the complex, along with confirmed specimens of *T. jagerskioeldi* s. str. in *L. glaucescens* and *U. pelagicus* from the North Pacific would suggest a broad capacity for these cestodes to infect alcid, larid, stercorariid, and phalacrocoracid hosts in marine environments assuming compatibility and ecological opportunity (Table 2) (Hoberg and Soudachanh, 2020, 2021).

Overall, based on current sampling, species of the complex describe a Pan-Pacific to Holarctic distribution, with extensive sympatry (Figures 68 and 69; Table 2; Supplementary Data Table 3). *Tetrabothrius jagerskioleldi* s. str. and *T. sinistralis* have demonstrated Holarctic distributions linking the North Pacific and North Atlantic through the Arctic Basin. Determination of widespread ranges for *T. alcae*, *T. fraterculus*, or *T. aithuia* across high-latitude marine systems requires validated specimens at sites in the Arctic Basin and North Atlantic. Within an extensive oceanographic range, species occurrences are infrequent and geographically heterogeneous, having distributions circumscribed by an already rare and cryptic complex. Heterogeneity can reflect real differences in distribution among host assemblages and/or outcomes of uneven and minimal sampling among some genera and species of alcids compounded by rare occurrence. *Tetrabothrius alcae* has been recognized across all regions that have been sampled extending from the eastern Pacific through the Gulf of Alaska, Aleutian Islands, Bering and Chukchi Seas, and Sea of Okhotsk (Hoberg and Soudachanh, 2021). Specimens and records for *T. jagerskioeldi* s. str. are absent from the eastern Pacific, for *T. fraterculus* from the Bering Sea and *T. aithuia* from the Gulf of Alaska. *Tetrabothrius sinistralis* is Holarctic, but in the North Pacific basin there are no records outside of the Bering Sea; such may reflect that *T. sinistralis* is currently known from 3 complete specimens in 2 hosts. Multiple species within the assemblage minimally occur in sympatry in the northern Sea

of Okhotsk (4 species, Talan Island), Aleutian Island arc (3, southwestern Aleutian pelagic; 4, Buldir Island), Bering Sea (3, St. Lawrence Island; 4, St. Matthew Island), Gulf of Alaska (3, Kodiak Island region), and eastern Pacific (3, Grays Marine Canyon). Transmission is demonstrated to be focused oceanographically associated with dispersed foraging zones around specific insular sites and is temporally constrained during the breeding cycles for respective alcid species. Pan-Pacific ranges crossing marine transition zones and domains for all species in the complex are apparent (Hoberg, 1995; Hoberg and Soudachanh, 2021).

Congeneric species, exclusive of the complex, that may be expected or which also occur in alcids are those observed among larids, including species of *Rissa* and *Larus* in sympatry (e.g., Talan Island; Buldir Island; southwestern Aleutian pelagic zone; Kodiak Island region; Grays Marine Canyon; Humboldt Bay) (Hoberg and Soudachanh, 2020). Based on specimens in the North Pacific inventory these are *T. erostris*, *T. cylindraceus*, and *T. morschtini*. In the North Pacific basin, such infections were generally rare, demonstrated by cestodes in 10 alcid hosts (< 1% of 1,347) of 6 species from 6 localities (Table 3; Supplementary Data Tables 3 and 5). Immature and some fragmented specimens that were ultimately unidentified occurred in 26 alcid hosts (2%) of 7 species from 11 localities. Congeneric species and unidentified *Tetrabothrius* represented specimens occurring in young of the year, subadult, and adult breeding birds (Supplementary Data Tables 3 and 5). Unsubstantiated records of *T. cylindraceus* and *T. erostris* in murres and black guillemot from the region of the northwestern Atlantic and *T. macrocephalus* in marbled murrelet from Sakhalin Island (Krotov and Deliamure, 1952) were summarized by Muzzafar and Jones (2004) and Muzzafar (2009) (Table 3).

Mixed species infections involving the *T. jagerskioeldi*–complex and congeneric species such as *T. cylindraceus* and *T. erostris* in single alcid hosts at a locality are rare and have been most often observed at oceanic transitions including pelagic zones of Grays Marine Canyon and south of the Western Aleutian Islands (Table 4). In contrast, mixed species infections with *T. jagerskioeldi* s. str., *T. erostris*, and *T. cylindraceus* were abundant in *Larus glaucescens* at Central Island and Puffin Island from the northwestern Gulf of Alaska (Hoberg and Soudachanh, 2020); the sole records of *T. jagerskioeldi* in larid hosts were from the Holarctic. Specimens of *Tetrabothrius* in *S. longicaudus* and *S. pomarinus* from Grays Marine Canyon in our study are not attributed to *T. jagerskioeldi* or other species in the complex (Supplementary Data Table 3). Characterization of *T. fraterculus* and *T. aithuia* and other species within the complex continues to emphasize the disparity in prevalence and abundance among largely segregated *Tetrabothrius* faunas circulating among Alcidae, Laridae, and Procellariiformes in the North Pacific and more broadly across northern seas (see Hoberg and Soudachanh, 2020, 2021).

Foraging, Oceanography, and *Tetrabothrius*

Alcid cestodes circulate under the dynamics of capacity (potential observed for broad multispecies host assemblages), within limits imposed by ecological opportunity. Relative ecological isolation among murres, guillemots, puffins, zooplanktivorous auklets, and their respective prey assemblages, or factors that determine opportunity through foodwebs and spatial distribution, may have explanatory power for understanding the host ranges for *T. jagerskioeldi*, *T. alcae, T. sinistralis*, *T. fraterculus*, and *T. aithuia* with parasites secondarily revealing insights about the structure of the North Pacific marine ecosystem.

As we have observed for this assemblage, transmission for species of the complex occurs across the extent of the greater North Pacific basin (Sea of Okhotsk, Bering Sea, Chukchi Sea, Aleutian Arc, Gulf of Alaska, and California Current systems) (Figures 68 and 69). *Tetrabothrius* faunas among alcids are not partitioned regionally.

Pan-Pacific circulation for respective species of *Tetrabothrius* transcends oceanographically definable domains or provinces (characterized by water mass, advection, and upwelling), each distinguished by distinct, diverse, but ecologically equivalent assemblages of micro- and macro-zooplankters (including copepods, amphipods, euphausiids, ctenophores, and pteropods), cephalopods, and fishes. Foundations for prey selection and resource use by particular seabirds are restricted by provincial-level foodwebs (e.g., Ainley and Sanger, 1979; Piatt and Springer, 2003; Iverson et al., 2007; Sydeman et al., 2017; Piatt et al., 2018). Relatively few specific prey species occur consistently across all marine domains. There is broad capacity, however, for completion of life cycles for cestodes across all domains, with transmission circumscribed by breeding cycles and oceanographic location of colonies as indicated by the distribution of infections across age classes.

Transmission appears limited by opportunity in the context of partitions in the distribution of tapeworms among particular marine birds (e.g., murres, murrelets and guillemots; puffins and auklets), which are to a degree ecologically segregated relative to spatial range, foraging, and trophic linkages (e.g., Ainley and Sanger, 1979; Ainley et al.,1990; Iverson et al., 2007; Springer et al., 2007; Woo et al., 2008; Sydeman et al., 2017). Persistence for respective species of *Tetrabothrius* among diverse alcids is

driven by a discrete host genus, with broad fundamental fitness space (capacity) relative to a conserved host-based resource indicated by sporadic infection of multiple host genera and species in relative sympatry (Figures 68–70). These interactions describe the dimensions of host range and the relationship of fundamental fitness space (potential host range), realized fitness space (actual host range temporally and spatially) and outcomes for opportunity and ecological fitting in sloppy fitness space as a basis for faunal assembly and diversification over time as predicted under the SP (Agosta et al., 2010; Brooks et al., 2019, 2023; Agosta and Brooks, 2020; Agosta, 2022). We suggest that colonization processes have historically and continue to be a critical dynamic in structuring this assemblage (Araujo et al., 2015; Nylin et al., 2018; Brooks et al., 2019), consistent with episodic faunal assembly and diversification in evolutionary and ecological time for other marine tapeworm groups in alcids and pinnipeds, respectively (Hoberg, 1992, 1995, 1996; Hoberg and Adams, 2000; Hoberg and Brooks, 2008).

Host range and cophylogeny for species of the *T. jagerskioeldi*–complex

A robust estimate of phylogeny is lacking among the 56 species of *Tetrabothrius* in marine homeotherms, including 10 species in Cetartiodactyla (Odontocetes and Mysticetes) and 46 species distributed across 8 orders of marine avian hosts (Hoberg, 1996; Jarvis et al., 2014; Mariaux et al., 2017). Consequently, there is currently no basis for postulating age of associations, whether 5 species of the *T. jagerskioeldi*–complex are a monophyletic assemblage or have broader independent phylogenetic connections (patterns of colonization) across an array of congeners (Figure 70). This challenge is unlikely to be easily resolved because of a history of incomplete descriptions, a need for extensive taxonomic revision, recognition of sufficient and diagnostic structural attributes, and the general paucity of molecular sequence and genomic data for any species of *Tetrabothrius* or more generally among the tetrabothriideans (Hoberg, 1989, 1994; Mariaux et al., 2017).

Alcidae has an extended history in the Pacific basin with connectivity to the North Atlantic (Friesen et al., 1996; Moum et al., 2002; Pereira and Baker, 2008; Smith, 2011). Pan-Alcidae within Charadriiformes is sister of Stercorariidae + Laridae with a deep history of diversification extending from origins in the Eocene-Paleocene (Smith, 2011; Pereira and Baker, 2008; Jarvis et al., 2014). Current phylogenetic inference is consistent with origins in the Pacific basin and a rapid radiation during the history of the basal and now extinct Mancalline auks (Smith, 2011). Multiple episodes of oceanographic expansion are apparent into the North Atlantic among the assemblages of genera and species during the Cenozoic following Pacific origins (Friesen et al., 1996; Moum et al., 2002).

The contemporary *Tetrabothrius* fauna, and particularly the *T. jagerskioeldi*–complex, has no clear affinities (based on structural attributes that could be postulated as synapomorphic) with species in either Laridae or Stercorariidae. Extinction of the basal Mancalline auks and faunal turnover for alcids during cooling of the North Pacific and North Atlantic following the Miocene could have influenced the distribution and diversity of a *Tetrabothrius* fauna that historically may have been of greater diversity. Declining marine temperatures and ecological disruption differentially influenced alcid lineages in the North Pacific and North Atlantic, with substantial reduction in diversity in the latter oceanic region (Smith, 2011). In this regard, the *T. jagerskioeldi*–complex may represent a relictual monophyletic fauna, or was assembled through independent episodes of colonization with links to other seabird taxa, or among related alcid genera and species; these are not mutually exclusive. Thus, it is essential to establish a phylogenetic context for the 46 species of *Tetrabothrius* relative to the Aequornithae (core water birds—Gaviiformes, Procellariiformes + Sphenisciformes, Suliformes [Phalacrocoracidae, Sulidae, Fregatidae, Anhingidae] + Pelecaniformes [Pelecanidae and others]), Phaethontiformes, Podicipediformes, and other Charadriiformes, in addition to cetaceans and pinnipeds (e.g., Hoberg, 1996; see Jarvis et al. [2014] for entry to current higher avian phylogeny and taxonomy).

A snapshot of host range is apparent from mapping species of the complex onto a robust phylogeny for the Alcidae (Figure 70). Incomplete as a cophylogenetic analysis (combining and potentially revealing colonization and cospeciation), this mapping process may provide initial insights about fundamental and realized host range within the complex and for individual species (Brooks et al., 2023). Consistent with considerations of broader diversity for *Tetrabothrius* spp. in alcids and larids (e.g., Table 3), colonization dynamics within the complex and for congeners such as *T. cylindraceus* and *T. erostris* are apparent. As mentioned, these associations and demonstrated host range reflect the interaction of capacity and opportunity in this slice of ecological time. All species attributed to the *T. jagerskioeldi*–complex indicate a considerable host range within the Alcidae; only *T. fraterculus* appears limited to a host group, the puffins or Fraterculini, based on cumulative sampling from the North Pacific. Increasingly detailed comparative phylogenetic explorations of *Tetrabothrius* spp. among respective alcid clades (Alcinae—Alcini, Cepphini, Brachyrampnini,

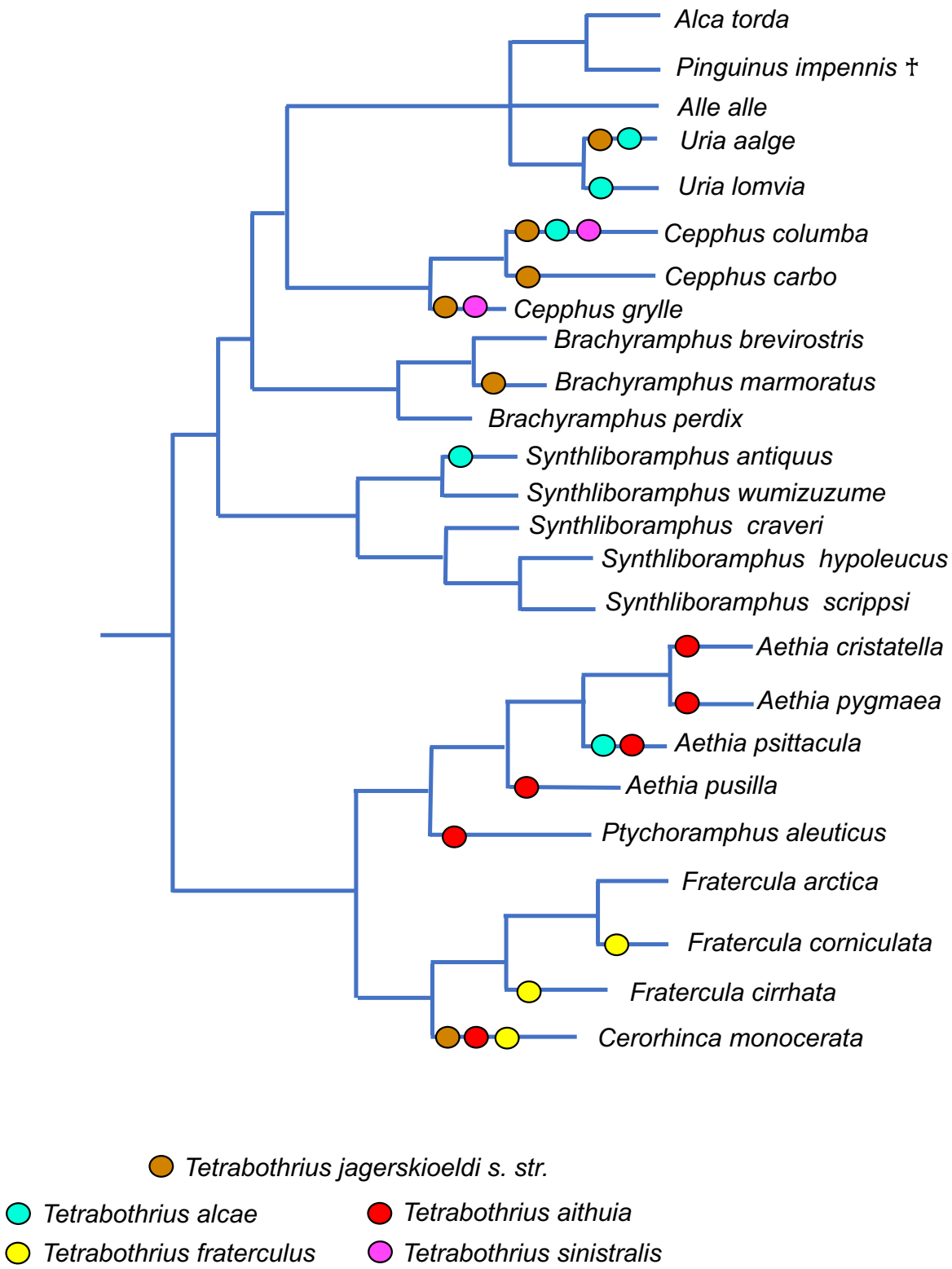

Figure 70. Phylogeny for genera and species of contemporary Alcidae showing host range for species of the *Tetrabothrius jagerskioeldi*–complex. Records for putative host range of *T. jagerskioeldi* sensu lato, which cannot be substantiated based on archived vouchers, are excluded (see Hoberg and Soudachanh, 2020, 2021). Specimens and records in *Larus glaucescens* and *Urile pelagicus* (see Hoberg and Soudachanh, 2020) are not shown. Host phylogeny based on Friesen et al. (1996) and Smith (2011).

Synthliboramphini; Fraterculinae—Aethiini, Fraterculini) in a broader context for *Tetrabothrius* among diverse host groups among an assemblage of seabirds are necessary to resolve a complex history of colonization and cospeciation (Hoberg, 1996).

Marine Diversity and Ecological Perturbation

Changing conditions, especially ecological perturbations driven by climate oscillations, have been the active force in oceanic community dynamics extending to and providing a direct nexus across evolutionary to ecological time (e.g., Hoberg, 1995, 1996; Hoberg and Brooks, 2008; Smith, 2011). As in terrestrial systems, environmental sloshing and fluctuating temperature influence ecosystem and community structure (Hoberg and Brooks, 2015; Kafle et al., 2020). In marine systems, these factors—under climate forcing—directly and indirectly determine production cycles and distributions of micro- and macro-zooplankton, forage fishes, cephalopods, and trophic structure in high-latitude marine ecosystems (Springer et al., 1996, 2007; Sydeman et al., 2015). In ecological time, ocean-atmosphere oscillations, or regime shifts from cold to warm cycles, such as the El Niño Southern Oscillation, Pacific Decadal Oscillation, and the North Atlantic Oscillation, drive one scale of episodic ecological reorganization that will influence foodwebs and the potential for persistence and transmission of marine parasites (e.g., Piatt et al., 1998; Anderson and Piatt, 1999; Hurrell et al., 2003; Chavez et al., 2003; Sydeman et al., 2012; Hoberg et al., 2017; Hoberg and Soudachanh, 2020). Climate, ocean warming, and the broadening occurrence of persistent marine heatwaves attributed to anthropogenic forcing can drive the potential for local to regional reorganization and tipping points in the North Pacific ecosystem (e.g., Springer et al., 2007; Di Lorenzo and Mantua, 2016; Jones et al., 2018; Piatt et al., 2020; Suryan et al., 2021). Coincidental shifts in the host and geographic distribution of tetrabothriideans and a diverse parasite fauna are predicted, where ecological opportunity meets capacity, compatibility, and altered patterns of resilience (Hoberg and Soudachanh, 2020, 2021, and references therein). It is possible to anticipate that fluctuating conditions could alter opportunity space (breakdown in ecological isolation), leading to broadening host range, with the possibility that even if the original host(s) becomes extinct, the parasite(s) will persist (e.g., Hoberg and Brooks, 2008; Stigall et al., 2017; Brooks et al., 2019; Hoberg and Soudachanh, 2021).

Environmental oscillation is characteristic of the oceanic systems where alcids originated, radiated, and underwent episodic expansion and isolation leading to persistence of the contemporary fauna (Pereira and Baker, 2008; Smith, 2011). High species turnover and dramatic fluctuations in species diversity have accompanied changes in oceanic circulation, temperature profiles, water-mass structure, atmosphere-ocean dynamics, and sea-level cycling related to episodes of isolation and connectivity of the North Atlantic and Pacific basins since the Miocene and through the Quaternary (Pereira and Baker, 2008). Interactions within the dynamics of the SP are essential in defining outcomes of opportunity, capacity, and compatibility across this persistent assemblage of alcid hosts and cestodes under historical and trophic connectivity in complex marine environments (Brooks et al., 2019; Agosta and Brooks, 2020).

Alternating episodes of stability and perturbation are the source for oscillating modes of host range reduction (exploitation) and host range expansion (exploration) (Agosta and Brooks, 2020). In periods of relative stability, exploitation modes occur, leading to specialization and limited or narrowing host range. In contrast, disruption or disturbance (often driven by climate) are sources of movement and ecological breakdown as a precursor of exploration modes leading to broadening host range. These mechanisms of oscillation are subsumed within the SP in an episodic-refugial model that provides a view of the biosphere through cumulative slices of time. The SP is central in understanding the outcomes of wobbling climate and environmental sloshing in evolutionary and ecological time (e.g., Hoberg 1992, 1995; Hoberg and Brooks, 2015; Hoberg et al., 2017; Kafle, 2020; Marko et al., 2009).

Seabirds, marine mammals, and parasites are indicators of changing conditions over space and time. Oceanic regime shifts, prey cascades, and diversity for birds and parasites serve as proxies for revealing accelerating perturbation in marine foodwebs (e.g., Springer and Piatt, 1996; Andersen and Piatt, 1999; Hoberg et al., 2013; Hoberg and Soudachanh, 2020, 2021). As proxies, specimens and data describing diversity lead to cumulative snapshots of systems in dynamic and accelerating change (Dunnum et al., 2018; Cook et al., 2020; Hoberg et al., 2022). Marine baselines result from site intensive and geographically extensive sampling (field collections) across multispecies assemblages circumscribed in a broad temporal and spatial arena with representative species within larger assemblages linked to discrete foodweb dynamics and oceanographic partitions. Integrated pictures of diversity are derived from specimens, as the source of comparative and molecular data streams and validated information held in biorepositories (Hoberg et al., 2013; Colella et al., 2020, 2021; Hoberg et al., 2022). These are the strategic and focused geographic/oceanographic benchmarks, against which change is revealed and assessed over specific intervals and time frames.

Acknowledgments – Joseph and Nella Cook, Felipe Cook, Soledad, Remy, Kitty, and Moqui on the Cook Estancia, in the shade of the cottonwoods and shadow of Sandia Mountain, contributed immeasurably to completion of our explorations of *Tetrabothrius* diversity among marine birds. Appreciation to Daniel Brooks, Walter Boeger, Salvatore Agosta, and Valeria Trivellone for the continuing and expanding synthesis that is the Stockholm Paradigm. Specimens from the North Pacific inventory were archived, database, and curated in the Museum of Southwestern Biology (MSB), Parasitology Division, University of New Mexico, by collections manager Sara Brant. Further, the MSB provided laboratory facilities, instrumentation, and general support. Scott Gardner and Gabor Racz from the Harold W. Manter Laboratory of Parasitology, University of Nebraska–Lincoln, provided access to their extensive research library and literature for the Tetrabothriidae and other helminths. Specimens from field collections spanning decades in Alaskan marine waters, assembled by Robert and Virginia Rausch, are curated in the R.L. and V.R. Rausch Helminthological Collections at the MSB. Field collections by EPH (1975–1988) spanned the North Pacific basin with logistical support from the US Geological Survey (under the former US Fish and Wildlife Service [USFWS]) and were ancillary to the Aleutian Canada Goose Recovery Program and the Outer Continental Shelf Environmental Assessment Program. Collections in the Russian Arctic and the northern Sea of Okhotsk were advanced by support to EPH through the Interacademy Exchange Program between the National Academy of Sciences (USA) and Russian Academy of Sciences, with field logistics from the Institute for Biological Problems of the North, Magadan (IBPN) in 1981 and 1988. Diversity assessments and collections were centered at Chaun Biological Station, Chukotka, in 1981 with SKB, Vitus Kontrimavichus, Gennady Atrashkevich, Alexander Ya. Kondratiev, and Luba Kondratieva. Components of the type series for 3 species of the complex were based on collections at Talan Island, Magadanskaya Oblast, in 1988 through collaborations and fieldwork with A.Ya. Kondratiev, L. Kondratieva, Alexander Kitaysky, Alexi Pinchuck, and SKB. Specimens and data from subsequent collections by SKB and Olga Orlovskaya at Talan Island in 1997 were facilitated by the IBPN; tetrabothriid and other cestodes from these later biodiversity assessments are held in the Helminthological Collection of the Institute of Ecology, Lithuanian Academy of Sciences, Vilnius, curated by Rasa Binkiene. A substantial number of cestodes in auklets and puffins, pertinent here, were derived from marine collections over the oceanic shelf-break and continental shelf of Washington State (1982, 1985, 1987), organized by Sievert Rohwer and staff of the Burke Memorial Washington State Museum, University of Washington, Seattle, and supported in part by Garett Eddy. Diversity assessments were further augmented by specimens provided through a considerable network of field biologists, including Richard Fitzner (Destruction Island and Protection Island, Washington, 1981); Charles Drost (Channel Islands, California, 1987, 1988); Mark Phillips (Humboldt Bay, California, 1977, 1979); Patrick Gearin (western Aleutians, 1981, 1982); Douglas Causey (western Aleutians, 1991, 1992, 2002); Jane Homan (Utqiagvik, Alaska, and St. Paul Island, Alaska, 1979); and Jean Bédard, John Piatt, Alan Springer, and David Roseneau (St. Lawrence Island, Alaska). Cestodes in avian specimens collected adjacent to Sarichev Island, Shishmaref, Alaska, by USFWS personnel during the marine heat-wave and mortality event for shearwaters and other seabirds in the Chukchi Sea during 2019 were provided by Gary E. Shugart from the Slater Museum, University of Puget Sound. Our current studies continue to benefit from discussions with Kirill Galaktionov, from the Zoological Institute, Russian Academy of Sciences, St. Petersburg, about faunal diversity and historical biogeography across northern marine ecosystems. Lastly, Lori Hawkins provided technical assistance in the preparation of our manuscript.

Literature Cited

Agosta, S.J. 2022. The Stockholm Paradigm explains the dynamics of Darwin's entangled bank, including emerging infectious disease. MANTER: Journal of Parasite Biodiversity 27. https://doi.org/10.32873/unl.dc.manter27

Agosta, S.J.; Brooks, D.R. 2020. The Major Metaphors of Evolution: Darwinism Then and Now. Springer International Publishing, Cham, Switzerland. 273 pp. https://doi.org/10.1007/978-3-030-52086-1

Agosta, S.J.; Janz, N.; Brooks, D.R. 2010. How specialists can be generalists: resolving the "parasite paradox" and implications for emerging infectious disease. Zoologia (Curitiba) 27: 151–162. https://doi.org/10.1590/S1984-46702010000200001

Ainley, D.G.; Sanger, G.A. 1979. Trophic relations of seabirds in the northeastern Pacific Ocean and Bering Sea. In: Conservation of Marine Birds of Northern North America. J. Bartonek, D.N. Nettleship (eds.). United States Department of the Interior. Wildlife Research Report 11. Washington, DC. 95–122 p.

Ainley, D.G.; Strong, C.S.; Penniman, T.M.; Boekelheide, R.J. 1990. The feeding ecology of Farallon seabirds. In: Seabirds of the Farallon Islands: Ecology, Dynamics and Structure of an Upwelling-System Community. D.G. Ainley, R.J. Boekelheide (eds.). Stanford University Press, Stanford, CA. 51–127 p.

Anderson, P.J.; Piatt, J.F. 1999. Community reorganization in the Gulf of Alaska following ocean climate regime shift. Marine Ecology Progress Series 189: 117–123.

Araujo, S.B.L.; Braga, M.P.; Brooks, D.R.; Agosta, S.; Hoberg, E.P.; von Hathental, F.; Boeger, W.A. 2015. Understanding host-switching by ecological fitting. PLOS ONE 10: e0139225. https://doi.org/10.1371/journal.pone.0139225

Ass, M.Y. 1939. Pravilo Furmana (filogeneticheskie soot-nosheniya parasitov i khozyaev). Trudy Leningradskogo obshchestva estestvoispytateleî. Travaux de la Société des naturalists de Leningrad 67: 8–54.

Baer, J.G. 1954. Revision taxonomique et étude biologique des cestodes de la famille Tetrabothriidae, parasites d'oiseaux de haute mer et de mammifères marins. Mémoires de l'Université de Neuchâtel, série in-quarto Tome 1. 1–121 p.

Baer, J.G. 1956. Parasitic helminths collected in West Greenland. Meddelelser om Grønland, Bd. 124, Nr. 10. pp. 5–55.

Baylis, H.A. 1919. A collection of Entozoa, chiefly from birds, from the Murman coast. Annals and Magazine of Natural History 3: 501–514.

Belopol'skaia, M.M. 1952. Parazitofauna morskikh vodoplavaiushchikh ptits. Leningradskogo Universitet Uchenye Zapiski. Seria Biologicheskikh Nauk 141: 129–180.

Belopol'skaia, M.M. 1963a. Obzor parazitofauny ptits Sudzukhinskogo Zapovednika (Primor'e). Parazit Sbornik 21: 221–224.

Belopol'skaia, M.M. 1963b. Parazitofauna ptits Sudzukhinskogo Zapovednika (Primor'e) IV. Lentochnye chervii (Cestoidea). Trudy Gel'mintologicheskii Laboratoriia 13: 144–163.

Braga, M.P.; Araujo, S.B.L.; Agosta, S.; Brooks, D.; Hoberg, E.; Nylin, S.; Janz, N.; Boeger, W.A. 2018. Host use dynamics in a heterogeneous fitness landscape generates oscillations in host range and diversification. Evolution 72: 1773–1783. https://doi.org/10.1111/evo.13557

Brooks, D.R. 1979. Testing the context and extent of host-parasite coevolution. Systematic Zoology 28: 299–307.

Brooks, D.R. 1981. Hennig's parasitological method: a proposed solution. Systematic Biology 30: 229–249.

Brooks, D.R. 1985. Historical ecology: a new approach to studying the evolution of ecological associations. Annals of the Missouri Botanical Garden 72: 660–680.

Brooks, D.R.; Boeger, W.A.; Hoberg, E.P. 2023. The Stockholm Paradigm: the conceptual platform for coping with the emerging infectious disease crisis. In: An Evolutionary Pathway for Coping with Emerging Infectious Disease. S.L. Gardner, D.R. Brooks, W.A. Boeger, E.P. Hoberg (eds.). Zea Books, Lincoln, NE. 47–58 p.

Brooks, D.R.; Hoberg, E.P. 2000. Triage for the biosphere: the need and rationale for taxonomic inventories and phylogenetic studies of parasites. Comparative Parasitology 67: 1–25.

Brooks, D.R.; Hoberg, E.P.; Boeger, W.A. 2015. In the eye of the Cyclops: the classic case of cospeciation and why paradigms are important. Comparative Parasitology 82: 1–8.

Brooks, D.R.; Hoberg, E.P.; Boeger, W.A. 2019. The Stockholm Paradigm: Climate Change and Emerging Disease. University of Chicago Press, Chicago. 423 pp.

Brooks, D.R.; Hoberg, E.P.; Gardner, S.L.; Boeger, W.; Galbreath, K.E.; Herczeg, D.; Mejía-Madrid, H.H.; Racz, E.; Tsogtsaikhan Dursahinhan, A. 2014. Finding them before they find us: informatics, parasites, and environments in accelerating climate change. Comparative Parasitology 81: 155–164.

Brooks, D.R.; McLennan, D.A. 1993. Parascript: Parasites and the Language of Evolution. Smithsonian Institution Press, Washington, DC.

Brooks, D.R.; McLennan, D.A. 2002. The Nature of Diversity: An Evolutionary Voyage of Discovery. University of Chicago Press, Chicago.

Chavez, F.P.; Ryan, J.; Lluch-Cota, S.E.; Miguel Ñiquen, C. 2003. From anchovies to sardines and back: multidecadal change in the Pacific Ocean. Science 299: 217–221.

Chesser, R.T.; Billerman, S.M.; Burns, K.J.; Cicero, C.; Dunn, J.L.; Kratter, A.W.; et al. 2020. Check-list of North American Birds (online). American Ornithological Society. http://checklist.aou.org/taxa

Colella, J.P.; Bates, J.; Burneo, S.F.; Camacho, M.A.; Bonilla, C.C.; Constable, I.; et al. 2021. Leveraging natural history biorepositories as a global, decentralized, pathogen surveillance network. PLOS Pathogens 17: e1009583. https://doi.org/10.1371/journal.ppat.1009583

Colella, J.P.; Talbot, S.L.; Brochmann, C.; Taylor, E.B.; Hoberg, E.P.; Cook, J.A. 2020. Conservation genomics in a changing Arctic. Trends in Ecology and Evolution 35: 149–162. https://doi.org/10.1016/j.tree.2019.09.008

Cook, J.A.; Arai, S.; Armién, B.; Bates, J.; Carrion Bonilla, C.A.; de Souza Cortez, M.B.; et al. 2020. Integrating biodiversity infrastructure into pathogen discovery and mitigation of epidemic infectious diseases. Bioscience 70: 531–534. https://doi.org/10.1093/biosci/biaa064

Di Lorenzo, E.; Mantua, N. 2016. Multi-year persistence of the 2014/15 North Pacific marine heatwave. Nature Climate Change 6: 1042–1047.

Dunnum, J.L.; Yanagihara, R.; Johnson, K.M.; Armien, B.; Batsaikhan, N.; Morgan, L.; Cook, J.A. 2017. Biospecimen repositories and integrated databases as critical infrastructure for pathogen discovery and pathobiology research. PLOS Neglected Tropical Diseases 11: e0005133. https://doi.org/10.1371/journal.pntd.0005133

Friesen, V.L.; Baker, A.J.; Piatt, J.F. 1996. Phylogenetic relationships within the Alcidae (Charadriiformes: Aves) inferred from total molecular evidence. Molecular Biology Evolution 13: 359–367.

Fuhrmann, O. 1908. Die Cestoden der Vogel. Zoolgische *Jahrbücher* (Supplement) 10: 1–232.

Fuhrmann, O. 1932. Les Ténias des Oiseaux. Mémoires de l'Université de Neuchâtel 8: 1–381.

Galbreath, K.E.; Makarikov, A.; Bell, K.; Greiman, S.; Allen, J.; Haas, G.; et al. 2023. Late Cenozoic history and the role of Beringia in assembling a Holarctic cestode species complex. Molecular Phylogenetics and Evolution 183: 107775. https://doi.org/10.1016/j.ympev.2023.107775

Gustafsson, D.R.; Najer, T. 2022. Fahrenholz's Rule is not a valid methodology for determining species limits in chewing lice (Psocodea, Phthiraptera). Bionomina 29: 1–73. https://doi.org/10.11 646/bionomina.29.1.1

Haas, G.M.S.; Hoberg, E.P.; Cook, J.A.; Henttonen, H.; Makarikov, A.A.; Gallagher, S.R.; et al. 2020. Taxon pulse dynamics, episodic dispersal and host colonization across Beringia drive diversification of a Holarctic tapeworm assemblage. Journal of Biogeography 47: 2457–2471. https://doi.org/10.1111/jbi.13949

Haukisalmi, V.; Hardman, L.M.; Hoberg, E.P.; Henttonen, H. 2014. Phylogenetic relationships and taxonomic revision of *Paranoplocephala* Lühe, 1910 sensu lato (Cestoda, Cyclophyllidea, Anoplocephalidae). Zootaxa 3873: 371–415.

Hennig, W. 1966. Phylogenetic Systematics. University of Illinois Press, Urbana.

Hoberg, E.; Ryan, P. 1989. Ecology of helminth parasitism in *Puffinus gravis* (Procellariiformes) on the breeding grounds at Gough Island. Canadian Journal of Zoology 67: 220–225. https://doi.org/10.1139/z89-030

Hoberg, E.P. 1986. Evolution and historical biogeography of a parasite-host assemblage: *Alcataenia* spp. (Cyclophyllidea:Dilepididae) and Alcidae (Charadriiformes). Canadian Journal of Zoology 64: 2576–2589.

Hoberg, E.P. 1987. *Tetrabothrius shinni* sp. n. (Eucestoda), from *Phalacrocorax atriceps bransfieldensis* (Pelecaniformes) in Antarctica, with comments on morphological variation and host-parasite biogeography and evolution. Canadian Journal of Zoology 65: 2969–2975.

Hoberg, E.P. 1989. Phylogenetic relationships among genera of the Tetrabothriidae (Eucestoda). Journal of Parasitology 75: 617–626.

Hoberg, E.P. 1992. Congruent and synchronic patterns in biogeography and speciation among seabirds, pinnipeds and cestodes. Von Ihering Centenary Symposium in Biogeography and Coevolution. Journal of Parasitology 78: 601–615.

Hoberg, E.P. 1994. Order Tetrabothriidea. In: CIP Keys to the Cestode Parasites of Vertebrates. L.F. Kahlil, A. Jones, R. Bray (eds.). CAB International Institute of Parasitology and British Museum (Natural History), London. 295–304 p.

Hoberg, E.P. 1995. Historical biogeography and modes of speciation across high latitude seas of the Holarctic: concepts for host-parasite coevolution among the Phocini (Phocidae) and Tetrabothriidae (Eucestoda). Canadian Journal of Zoology 73: 45–57.

Hoberg, E.P. 1996. Faunal diversity among avian parasite assemblages: the interaction of history, ecology and biogeography. Bulletin of the Scandinavian Society of Parasitology 6: 65–89.

Hoberg, E.P.; Adams, A.M. 2000. Phylogeny, history and biodiversity: understanding faunal structure and biogeography in the marine realm. Bulletin of the Scandinavian Society of Parasitology 10: 19–37.

Hoberg, E.P.; Adams, A.M.; Rausch, R.L. 1991. Revision of the genus *Anophryocephalus* Baylis, 1922 from pinnipeds in the Holarctic with descriptions of *Anophryocephalus nunivakensis* sp. n. and *A. eumetopii* sp. n. (Tetrabothriidae) and evaluation of host records from the Phocidae. Canadian Journal of Zoology 69: 1653–1668.

Hoberg, E.P.; Agosta, S.J.; Boeger, W.A.; Brooks, D.R. 2015. An integrated parasitology: revealing the elephant through tradition and invention. Trends in Parasitology 31: 128–133.

Hoberg, E.P.; Boeger, W.A.; Molnár, O.; Földvári, G.; Gardner, S.L.; Juarrero, A.; et al. 2023. The DAMA protocol: anticipating to prevent and mitigate emerging infectious diseases. In: An Evolutionary Pathway for Coping with Emerging Infectious Disease. S.L. Gardner, D.R. Brooks, W.A. Boeger, E.P. Hoberg (eds.). Zea Books, Lincoln, NE. 112–121 p.

Hoberg, E.P.; Brooks, D.R. 2008. A macroevolutionary mosaic: episodic host-switching, geographic colonization, and diversification in complex host-parasite systems. Journal of Biogeography 35: 1533–1550.

Hoberg, E.P.; Brooks, D.R. 2010. Beyond vicariance: integrating taxon pulses, ecological fitting and oscillation in historical biogeography and evolution. In: The Geography of Host-Parasite Interactions. S. Morand, B. Krasnov (eds.). Oxford University Press. 7–20 p.

Hoberg, E.P.; Brooks, D.R. 2015. Evolution in action: climate change, biodiversity dynamics and emerging infectious disease. Philosophical Transactions of the Royal Society B 370: 20130553. https://doi.org/10.1098/rstb.2013.0553

Hoberg, E.P.; Cook, J.A.; Agosta, S.J.; Boeger, W.; Galbreath, K.E.; Laaksonen, S.; Kutz, S.J.; Brooks, D.R. 2017. Arctic systems in the Quaternary: ecological collision, faunal mosaics and the consequences of a wobbling climate. Journal of Helminthology 91: 409–421. https://doi.org/10.1017/S0022149X17000347

Hoberg, E.P.; Klassen, G.J. 2002. Revealing the faunal tapestry: Coevolution and historical biogeography of hosts and parasites in marine systems. Parasitology 124 (Supplement): S3–S22.

Hoberg, E.P.; Kutz, S.J.; Cook, J.A.; Galaktionov, K.; Haukisalmi, V.; Henttonen, H.; et al. 2013. Parasites. In: Arctic Biodiversity Assessment: Status and Trends in Arctic Biodiversity. H. Meltofte (ed.). Conservation of Arctic Flora and Fauna, Arctic Council, Akureyi, Iceland. 421–449 p.

Hoberg, E.P.; Soudachanh, K.M. 2020. Insights about diversity of Tetrabothriidae (Eucestoda) among Holarctic Alcidae (Charadriiformes): what is *Tetrabothrius jagerskioeldi*? MANTER: Journal of Parasite Biodiversity 11. https://doi.org/10.32873/unl.dc.edu/manter11

Hoberg, E.P.; Soudachanh, K.M. 2021. Diversity of Tetrabothriidae (Eucestoda) among Holarctic Alcidae (Charadriiformes): resolution of the *Tetrabothrius jagerskioeldi* cryptic species complex: cestodes of Alcinae—provides insights on the dynamic nature of tapeworm and marine bird faunas under the Stockholm Paradigm. MANTER: Journal of Parasite Biodiversity 16. https://doi.org/10.32873/unl.dc.manter/16

Hoberg, E.P.; Trivellone, V.; Cook, J.A.; Dunnum, J.L.; Boeger, W.B.; Brooks, D.R.; et al. 2022. Knowing the biosphere: documentation, specimens, archives, and names reveal environmental change and emerging pathogens. MANTER: Journal of Parasite Biodiversity 26. https://doi.org/10.32873/unl.dc.manter26

Hurrell, J.W.; Kushnir, Y.; Otterson, G.; Visbeck, M. 2003. An overview of the North Atlantic Oscillation. Geophysical Monographs 134: 1–35.

Iverson, S.J.; Springer, A.M.; Kitaysky, A.S. 2007. Seabirds as indicators of food web structure and ecosystem variability: qualitative and quantitative diet analyses using fatty acids. Marine Ecology Progress Series 352: 235–244.

Jarvis, E.D.; Mirarab, S.; Aberer, A.J.; Li, B.; Houde, P.; Li, C.; et al. 2014. Whole-genome analyses resolve early branches in the tree of life of modern birds. Science 346: 1320–1331. https://doi.org/10.1126/science.1253451

Jones, T.; Parrish, J.K.; Peterson, W.T.; Bjorkstedt, E.P.; Bond, N.A.; Ballance, L.T.; et al. 2018. Massive mortality of a planktivorous seabird in response to a marine heatwave. Geophysical Research Letters 45: 3193–3202. https://doi.org/10.1002/2017GL076164

Kafle, P.; Peller, P.; Massolo, A.; Hoberg, E.P.; Leclerc, L-M.; Tomaselli, M.; Kutz, S. 2020. Range expansion of muskox lungworms track rapid Arctic warming: implications for geographic colonization under climate forcing. Scientific Reports 10:17323. https://doi.org/10.1038/s41598-020-74358-5

Kennedy, M.; Spencer, H.G. 2014. Classification of the cormorants of the world. Molecular Phylogenetics Evolution 79: 249–257.

Krabbe, H. 1869. Bidrag til Kundskab om Fuglenes Baendelorme. Videnskabernes Selskabs Skrifter, 5 Raekke, Naturvidensk og Matematisk 8: 251–363.

Krotov, A.I.; Deliamure, S.A. 1952. K faune paraziticheskikh chervei mlekopitaiushchikh i ptits SSSR. Trudy Gel'mintologicheskie Laboratoria 6: 278–292.

Kuklin, V.V.; Kuklina, M.M. 2005. Helminths of Birds of the Barents Sea: Fauna, Ecology and Influence on the Hosts. Kola Scientific Centre of the Russian Academy of Sciences Press, Apatity. [In Russian]

Makarikov, A.A.; Galbreath, K.E.; Hoberg, E.P. 2013. Parasite diversity at the Holarctic nexus: species of *Arostrilepis* (Eucestoda: Hymenolepididae) in voles and lemmings (Cricetidae: Arvicolinae) from greater Beringia. Zootaxa 3608: 401–439.

Mariaux, J.; Kuchta, R.; Hoberg, E.P. 2017. Tetrabothriidea Baer, 1954. In: Planetary Biodiversity Inventory (2008–2017): Tapeworms from Vertebrate Bowels of the Earth. J.N. Caira, K. Jensen (eds.). University of Kansas, Natural History Museum, Special Publication No. 25, Lawrence. 357–370 p.

Marko, P.B.; Hoffman, J.M.; Emme, S.A.; McGovern, T.M.; Keever, C.C.; Cox, L.N. 2009. The 'Expansion-Contraction' model of Pleistocene biogeography: rocky shores suffer a sea change? Molecular Ecology 19: 146–149. https://doi.org/10.1111/j.1365-294X.2009.04417.x

Matthews, A.E.; Wijeratne, A.J.; Sweet, A.D.; Hernandes, F.A.; Toews, D.P.L.; Boves, T.J. 2023. Dispersal-limited symbionts exhibit unexpectedly wide variation in host specificity. Systematic Biology 72: 802–819. https://doi.org/10.1093/sysbio/syad014

Mayr, E. 1957. Evolutionary aspects of host specificity among parasites of vertebrates. In: Premier Symposium sur la Spécificité Parasitaire des Parasites de Vertébrés. J.G. Baer (ed.). International Union of Biological Sciences and Université Neuchâtel, Paul Attinger, S.A., Neuchâtel, Switzerland. 7–14 p.

Moum, T.; Arnasson, U.; Arnasson, E. 2002. Mitochondrial DNA sequence evolution and phylogeny of the Atlantic Alcidae, including the extinct great auk (*Pinguinus impennis*). Molecular Biology Evolution 19: 1434–1439.

Murav'eva, S.I. 1968. New species of tetrabothriidae from the glaucous gull *Tetrabothrius morschtini* n. sp. Nauchnye Doklady Vysshei Shkoly Biologicheskie Nauki 11: 11–13.

Murav'eva, S.I. 1975. Morfologicheskie osnovi sistematiki tetrabotriid. Problemy Parazitologii. Materialy 8th nauch Konf. Parazitologov, YSSR. Naukova Dumka, Kiev, Ukraine. 49 pp.

Murav'eva, S.I.; Popov, V.N. 1976. Sistematicheskoe polozhenie i neketorye dannye ob ekologii *Anophryocephalus skrjabini* (Cestoda: Tetrabothriidae) parazita lastonogikh. Zoologicheskie Zhurnal 55: 1247–1250.

Muzzafar, S.B. 2009. Helminths of murres (Alcidae: *Uria* spp.) markers of ecological change in the marine environment. Journal of Wildlife Diseases 45: 672–683. https://doi.org/10.7589/0090-3558-45.3.672

Muzzafar, S.B.; Jones, I.A. 2004. Parasites and diseases of the auks (Alcidae) of the world and their ecology—a review. Marine Ornithology 32: 121–146.

Nybelin, O. 1916. Neue Tetrabothriiden aus Vogel. Zoologischen Anzeiger 47: 297–301.

Nylin, S.; Agosta, S.; Bensch, S.; Boeger, W.A.; Braga, M.P.; Brooks, D.R.; et al. 2018. Embracing colonizations: A new paradigm for species association dynamics. Trends in Ecology & Evolution 33: 4–14. https://doi.org/10.1016/j.tree.2017.10.005

Page, R.D.M. (ed.) 2003. Tangled Trees: Phylogeny, Cospeciation, and Coevolution. University of Chicago Press, Chicago.

Paterson, A.M.; Banks, J. 2001. Analytical approaches to measuring cospeciation of host and parasites: through a glass, darkly. International Journal for Parasitology 31: 1012–1022. https://doi.org/10.1016/s0020-7519(01)00199-0

Pereira, S.L.; Baker, A.J. 2008. DNA evidence for a Paleocene origin of the Alcidae (Aves: Charadriiformes) in the Pacific and multiple dispersal across northern oceans. Molecular Phylogenetics and Evolution 46: 430–445. https://doi.org/10.1016/j.ympev.2007.11.020

Piatt, J.F.; Arimitsu, M.L.; Sydeman, W.J.; Thompson, S.A.; Renner, H.; Zador, S.; et al. 2018. Biogeography of pelagic food webs in the North Pacific. Fisheries Oceanography 27: 366–380. https://doi.org/10.1111/fog.12258

Piatt, J.F.; Drew, G.; Van Pelt, T.; Abookire, A.; Nielsen, A.; Shuktz, M.; Kitaysky, A. 1998. Biological effects of the 1997/98 ENSO in Cook Inlet, Alaska. Sisyphus News 3: 1–3.

Piatt, J.F.; Parrish, J.K.; Renner, H.M.; Schoen, S.K.; Jones, T.T.; Arimitsu, M.L.; et al. 2020. Extreme mortality and reproductive failure of common murres resulting from the northeast Pacific marine heatwave of 2014–2016. PLOS ONE 15: e0226087. https://doi.org/10.1371/journal.pone.0226087

Piatt, J.F.; Springer, A.M. 2003. Advection, pelagic food webs and the biogeography of seabirds in Beringia. Marine Ornithology 31: 141–154.

Ryzhikov, K.M.; Rysavý, B.; Khokhlova, I.G.; Tolkatcheva, L.M.; Kornyushin, V.V. 1985. Helminths of Fish-Eating Birds of the Palearctic Region II. Cestoda and Acanthocephales. USSR Academy of Sciences, Helminthological Laboratory, Moscow.

Smetanina, Z.B. 1979. Tsestody ryboiadnykh ptits primorskogo kraia. Materialy nauchnoii konferentsii vsesoyznogo obshchestva gel'mintologov Vypusk 31. Tsestody i Tsestodzy. Akademii Nauk SSSR. Laboratoria Gel'mintologii, Moskva: Akademii Nauk USSR. 120–128 p.

Smetanina, Z.B. 1981. Gel'minty morskikh ryboiadnykh ptits Zaleva Petra Velikogo. Biologiia I Sistematika Gel'mintov Zhivotnykh Dal'nevo Vostoka. Akad Nauk SSSR., Dal' nevostochnyi Nauchnyi Tsentr, Vladivostok. 71–81 p.

Smetanina, Z.B.; Leonov, V.A. 1984. Gel'minty riboiadnykh ptits Kuril'skikh Ostrov. Biologiia I Taksonomiia Gel'mintov Zhivotnikh I Cheloveka. 34: 59–66.

Smith, N.A. 2011. Taxonomic revision and phylogenetic analysis of the flightless Mancallinae (Aves, Pan-Alcidae). ZooKeys 91: 1–116. https://doi.org/10.3897/zookeys.91.709

Springer, A.M.; Byrd, G.V.; Iverson, S.J. 2007. Hot oceanography: planktivorous seabirds reveal ecosystem responses to warming of the Bering Sea. Marine Ecology Progress Series 352: 289–297.

Springer, A.M.; Piatt, J.F.; Shuntov, V.P.; Van Vliet, G.B.; Vladimirov, V.L.; Kuzin, A.E.; Perlov, A.S. 1999. Marine birds and mammals of the Subarctic Gyres. Progress in Oceanography 43: 443–487.

Springer, A.M.; Piatt, J.F.; Van Vliet, G. 1996. Sea birds as proxies of marine habitats and food webs in the western Aleutian Arc. Fisheries Oceanography 5: 45–55.

Stigall, A.L.; Bauer, J.E.; Lam, A.R.; Adriane R.; Wright, D.F. 2017. Biotic immigration events, speciation, and the accumulation of biodiversity in the fossil record. Global and Planetary Change 148: 242–257.

Suryan, R.M.; Arimitsu, M.L.; Coletti, H.A.; Hopcroft, R.R.; Lindeberg, M.R.; Barbeaux, S.J.; et al. 2021. Ecosystem response persists after a prolonged marine heatwave. Scientific Reports 11: 6235. https://doi.org/10.1038/s41598-021-83818-5

Sydeman, W.J.; Piatt, J.F.; Thompson, S.A.; García-Reyes, M.; Hatch, S.A.; Arimitsu, M.L.; et al. 2017. Puffins reveal contrasting relationships between forage fish and ocean climate. Fisheries Oceanography 26: 379–395.

Sydeman, W.J.; Poloczanska, E.; Reed, T.E.; Thompson, S.A. 2015. Climate change and marine vertebrates. Science 350: 772–777.

Sydeman, W.J.; Thompson, S.A.; Kitaysky, A. 2012. Sea birds and climate change: roadmap for the future. Marine Ecology Progress Series 454: 107–117.

Szidat, L. 1964. Vergleichende helminthologische Untersuchungen an den argentinischen Grossmowen *Larus marinus dominicanus* Lichtenstein und *Larus ridibundus maculipennis* Lichtenstein nebst neuen Beobachtungen tiber die Artbildung bei Parasiten. Zeitschrift für Parasitenkunde 24: 351–414.

Temirova, S.I.; Skrjabin, A.S. 1978. Tetrabotriaty i mezotsestoidaty lentochnye gel'minty ptits i mlekopitaiushchikh. Osnovy Tsestodologii 9. Akademii Nauk SSR, Moscow.

Threlfall, W. 1971. Helminth parasites of alcids in the northwestern North Atlantic. Canadian Journal of Zoology 49: 461–466.

Trivellone, V. 2022. Let emerging plant diseases be predictable. MANTER: Journal of Parasite Biodiversity 30. https://doi.org/10.32873/unl.dc.manter30

Trivellone, V.; Panassiti, B. 2022. A systematic review and meta-analyses of cophylogenetic studies: what is affecting congruence between phylogenies? MANTER: Journal of Parasite Biodiversity 24. https://doi.org/10.32873/unl.dc.manter24

Woo, K.J.; Elliot, K.H.; Davidson, M.; Gaston, A.J.; Davoren, G.K. 2008. Individual specialization in diet by a generalist marine predator reflects specialization in foraging behavior. Journal of Animal Ecology 77: 1082–1091.

Yamaguti, S. 1935. Studies on the helminth fauna of Japan, Pt. 6. Cestodes of Birds, I. Japanese Journal of Zoology 6: 183–232.

Yamaguti, S. 1940. Studies on the helminth fauna of Japan, Pt. 30. Cestodes of birds, II. Japanese Journal of Medical Sciences 1: 176–211.

Supplementary files (attached to this document record):

Supplementary Data Table 1. Avian Specimens (Alcidae, Laridae, Stercorariidae, Phalacrocoracidae, Procellariidae, Hydrobatidae, Diomedeidae) from the Greater North Pacific Basin Examined for Helminth Parasites (1949–2019)

Supplementary Data Table 2. Field Data with Georeferencing, Dates, and Collectors for Specimens of Alcidae, Some Laridae, and Other Seabirds Examined for Helminth Parasites from the Greater North Pacific Basin (1949–2019)

Supplementary Data Table 3. Summary of Hosts and Geographic Range for Species of the *Tetrabothrius jagerskioeldi*–complex and *Tetrabothrius* Tapeworms among Alcidae and Other Seabirds from the North Pacific Basin

Supplementary Data Table 4. *Tetrabothrius fraterculus* n. sp. and *Tetrabothrius aithuius* n. sp. Type Series and Voucher Specimens Catalogued in the Museum of Southwestern Biology (MSB) and Museum of the Institute of Ecology (EKOI HELMI)

Supplementary Data Table 5. Additional Species and Unidentified Specimens of *Tetrabothrius* spp. among Alcidae Hosts Archived and Catalogued in the Museum of Southwestern Biology